A SEMI-CLASSICAL THEORY FOR DIFFERENTIAL AND TOTAL SCATTERING CROSS SECTIONS WITH APPLICATION TO ELECTRON-ATOM, ION-ATOM, AND ATOM-ATOM SCATTERING

A THESIS

Presented to

The Faculty of the Division of Graduate

Studies and Research

By

Kevin James McCann

In Partial Fulfillment

of the Requirements for the Degree

Doctor of Philosophy

in the

School of Physics

Georgia Institute of Technology

August, 1974

A SEMI-CLASSICAL THEORY

FOR DIFFERENTIAL AND TOTAL SCATTERING CROSS SECTIONS

WITH APPLICATION TO ELECTRON-ATOM, ION-ATOM, AND ATOM-ATOM SCATTERING

Approved:

M. R. Flannery, Chairman

E. W. McDaniel

T. F. Moran

Date approved by Chairman: 5/28/74

DEDICATION

It is with sincere appreciation and love that I dedicate this work to my wife, Louise. Without her love and understanding, the journey would have been far less pleasant.

ACKNOWLEDGEMENTS

It is with pleasure that I acknowledge the assistance and guidance of my advisor, Dr. M. R. Flannery, who not only suggested the topic of my research, but also provided the necessary motivation to complete the investigation.

I would also like to extend my thanks to my reading committee, especially Dr. E. W. McDaniel for his helpful criticism.

Most of all I thank my wife, Louise, and my son, Eric, for providing an atmosphere which made the endeavor possible, and who also put up with my neglect of my home life.

TABLE OF CONTENTS

TABLE OF CONTENTS (Continued)

LIST OF TABLES

LIST OF ILLUSTRATIONS

SUMMARY

A semiclassical theoretical treatment of elastic and inelastic collisions is developed. The relative motion of the colliding systems is described by a generalization of the eikonal approximation, and the internal electronic motion of the systems is treated by a multistate expansion.

The theory is applied to the calculation of differential and total cross sections for electron-atom, ion-atom, and atom-atom collisions, and the comparison with available experimental data is found to be excellent.

Further, it is shown that by adopting simplifying approximations, the present theory yields formulae presented by other investigators. The relationships between these various theories are examined and the inadequacies of the earlier theories are displayed.

CHAPTER I

INTRODUCTION

In recent years there has been great interest in obtaining cross sections for electron-atom, ion-atom, and atom-atom collisions, particularly in such areas of research as the investigation of the earth's atmosphere, planetary and stellar atmospheres, gas discharges, and controlled thermonuclear fusion reactions. A number of methods have been developed for the calculation of these cross sections, and these methods fall into three general categories: fully quantal treatments, semiclassical treatments, and classical treatments. A comprehensive survey of the application of these treatments to electron-atom cross section calculations has been given by Moiseiwitsch and Smith (1968). Some of the more important theories in the above three categories are briefly summarized below.

Perhaps the simplest quantal calculation is the Born approximation along with its modifications which include the second-Born approximation, the distorted-wave Born approximation (Bates 1961), and the Bethe approximation (Inokuti 1971). The Born approximation and its modifications are primarily high energy theories which are based on the assumptions that the only important coupling in the process is the direct coupling between the initial state and the final state of the scattering system, with back-coupling from the final to the initial state ignored, and that the system wave function is well described by the initial state function, which implies that the population of the initial state

of the system is not significantly depleted by the interaction. Because of its simplicity, the Born approximation has received wide application to electron-atom collisions (e.g. Bell et al. 1969) and to atom-atom collisions (e.g. Bates and Griffing 1953). In general, the Born approximation yields valid results at high energies, i.e. above 500 eV for electron-atom collisions and above 200 keV for heavy-particle collisions; however, the Born approximation usually overestimates the experimental cross sections for lower energies.

A second quantal treatment, which has received considerable attention for electron-atom collisions, is the close-coupling method (Burke et al. 1967). In the close-coupling approximation the system wave function is expanded in a symmetrized set of atomic wave functions, and upon substitution of this expansion into the Schrödinger equation, yields an infinite set of coupled integro-differential equations for each value of the total angular momentum L. Necessarily, the infinite summations over angular momentum and over the wave function expansion must be truncated, and herein lie the major problems of the close-coupling method. Although the close-coupling mehtod has achieved noteable success in the prediction of resonances in the total cross section of electron-hydorgen scattering (Burke et al. 1967), the slow convergence of the truncated summations makes the calculation intractable at high energies, for which more states are accessible and more angular momenta become important. Further, for the same reasons, it is almost impossible to apply the close-coupling method to scattering from excited states, since the closeness of the excited states requires that a large number of these states be included in the expansion of the system wave

function. The large number of angular momenta which occurs in heavy-particle collisions also makes the close-coupling method impractical for the treatment of atom-atom collisions.

The semiclassical approximations are distinguished from the fully quantal treatments of scattering theory by the fact that they treat the relative motion of the colliding systems by a semiclassical method such as the JWKB approximation or the eikonal approximation (Bransden 1970). Perhaps the first significant semiclassical theory to appear is that of Bates (1961), in this theory the system wave function Ψ is expanded as

$$\Psi(\vec{R},\vec{r}) = \sum_{k=1}^{N} a_k(\vec{\rho},Z)\ \psi_k(\vec{r})\ e^{i\epsilon_k Z/\hbar v} \qquad (1\text{-}1)$$

where $\vec{R} = \vec{\rho} + \vec{Z}$ is the relative separation of the colliding systems, $\vec{\rho}$ is the classical impact-parameter, $\vec{Z}$ is the distance along the assumed straight-line trajectory, the ψ_k are the products of the unperturbed wave functions of the collision partners, e.g. the product of a 1s hydrogen wave function and a $2\ ^1S$ wave function of helium for H-He collisions, the ϵ_k are the internal atomic energies of the system, and the a_k are coefficients to be determined. Upon substitution of (1-1) into the Schrödinger equation, a set of coupled first-order differential equations for the a_k is obtained, which is identical to the time-dependent perturbation theory equations (Merzbacher 1961) with the substitution $Z = vt$. Here v is the velocity of the incident particle in the center of mass system, and is assumed to remain constant through-

out the collision. in correspondence with the time-dependent theory, the $|a_k(\rho,\infty)|^2$ are identified with the probabilities for the transitions $i \to k$ at impact-parameter ρ. The resulting cross section is then obtained by integrating these transition probabilities over all space

$$\sigma_k(v) = 2\pi \int_0^\infty |a_k(\rho,\infty)|^2 \, \rho \, d\rho \qquad (1\text{-}2)$$

The impact-parameter treatment of Bates has achieved great success in the area of heavy-particle collisions (Flannery 1969a, 1969b, 1969c, 1970); however, no corresponding theory had been developed at this time for the calculation of differential cross sections. More refined treatments based on the JWKB approximation have been advanced by Bates and Holt (1966) and by Bates and Crothers (1970). Only recently (Byron 1971; Bransden and Coleman 1972a, 1972b; Flannery and McCann 1973) have differential cross sections been determined for the impact-parameter method. Further, it has been shown by Flannery and McCann (1973) that (1-2) is a valid expression for the total cross section only in the limit of high energies, and is not at all suitable for electron-atom collisions. The correct expression for the total cross section is obtained by integration over the differential cross sections, i.e.

$$\sigma_k(v) = \int \frac{d\sigma}{d\Omega}(\theta,\phi) \, d\Omega \qquad (1\text{-}3)$$

A different type of semiclassical treatment has been advanced by Flannery (1970b). This treatment, called the semiquantal treatment, treats the entire collision classically with an injection of quantum mechanics to determine the velocity distribution of the active electron, and to determine the correct projectile-electron cross section. This procedure, however, is designed primarily to treat ioniaztion processes.

The fully classical theories (Thomson 1912, 1924; Thomas 1927; Gryzinski 1959, 1965; Flannery 1970) are intended for the treatment of ionization processes. A detailed account of binary-encounter and classical collision theories has been given by Vriens (1969).

An examination of the existing theories indicates that for a wide range of applications the semiclassical theories seem to enjoy the greatest seccess. In the present work a semiclassical theoretical treatment of elastic and inelastic collisions is developed in which the relative motion of the colliding systems is described by the eikonal approximation, and the internal electronic motion of the systems is treated by a multistate expansion.

The theory is applied to the calculation of differential and total cross sections for electron-atom, ion-atom, and atom-atom collisions, and the comparison with available experimental data is found to be excellent. The present theory is found to be applicable to a wide range of collisions and to be valid over an energy range from near the excitation threshold on up to very high energies. Further, it is seen that the energy at which the Born approximation becomes valid is considerably higher than previously thought; this fact should be of consider-

able interest to experimentalists who frequently normalize their data to the Born cross section at "high" energies.

Finally, it is shown that by adopting simplifying approximations, the present treatment yields formulae presented by other investigators. The relationships between these various theories and the present theory are examined and the inadequacies of the earlier theories are displayed.

CHAPTER II

THE MULTICHANNEL EIKONAL THEORY

In this chapter a semiclassical theory for the description of scattering processes is developed. The semiclassical nature of the theory arises from the treatment of the relative motion of the colliding systems by the eikonal approximation rather than by a full quantal treatment, such as in the close-coupling approximation which does not separate the translational and electronic motions of the system.

Eikonal Approximation

Before developing the present theory, it is necessary to present the underlying approximation, the eikonal approximation. The eikonal theory is a high energy or weak interaction theory which represents the relative motion of two interacting systems by a distorted plane-wave, and may be considered to be a first order correction to the Born approximation, which represents the relative motion of the systems by a simple plane-wave.

In order to develop the eikonal theory, the wave function for the relative motion is written as

$$\psi(\vec{R}) = \exp\{i\, S(\vec{R})\} \tag{2-1}$$

which may be done formally for any wave function. Use of (2-1) in the Schrödinger equation,

$$-\frac{\hbar^2}{2m}\nabla^2\psi(\vec{R}) = \{E - V(\vec{R})\}\,\psi(\vec{R})$$

where E is the total translational energy of the system, yields the equation which $S(\vec{R})$ must satisfy,

$$-i\nabla^2 S(\vec{R}) + (\vec{\nabla}S)^2 = \frac{2m}{\hbar^2}\{E - V(\vec{R})\} \qquad (2\text{-}2)$$

If the wave function (2-1) is replaced by a plane-wave, i.e. $S(\vec{R}) = kZ$, then $\nabla^2 S(\vec{R}) = 0$. Based on the assumption that $S(\vec{R})$ is slowly varying for high energy or weak interaction collisions, (2-2) may be reasonably approximated by

$$(\vec{\nabla}S)^2 \simeq \frac{2m}{\hbar^2}\{E - V(\vec{R})\} \qquad (2\text{-}3)$$

which is just the Hamilton-Jacobi equation of classical mechanics. The approximation (2-3) is expected to be valid for collisional energies which are significantly greater than the interaction energy and the internal energy of the system. When these conditions are satisfied, the classical trajectory of the system will not deviate significantly from a straight line path. For convenience, the classical straight line trajectory is chosen to be parallel to the Z-axis. Use of the straight line trajectory allows (2-3) to be rewritten as

$$\left(\frac{\partial S}{\partial Z}\right)^2 = \frac{2m}{\hbar^2}\{E - V(\vec{R})\} \tag{2-4}$$

Integration of (2-4) yields

$$S(\vec{\rho},Z) = \int \frac{2m}{\hbar^2}\{E - V(\vec{R})\}\, dZ \tag{2-5}$$

In order to determine the constant of integration in (2-5), it is necessary to consider the asymptotic boundary condition

$$\lim_{Z\to-\infty} \psi(\vec{R}) = e^{ikZ} \tag{2-6}$$

The condition (2-6) states that before the colliding systems interact, the relative motion of the systems is described by a plane-wave. Use of (2-6) in (2-5) yields the desired equation for $S(\vec{R})$

$$S(\rho,Z,\phi) = kZ + \int_{-\infty}^{Z} \left\{\left[\frac{2m}{\hbar^2}(E - V)\right]^{1/2} - k\right\} dZ \tag{2-7}$$

where the vector $\vec{R}$ has been replaced by its cylindrical coordinates (ρ,Z,ϕ).

Hence, when the assumptions inherent in the eikonal approximation hold, the relative motion of a colliding system may be described by

a distorted plane-wave (2-1) where $S(\vec{R})$ is given by (2-7). It should also be noted that if the second term in (2-7) can be neglected, then the Born approximation is valid, so that a validity criterion for the applicability of the Born approximation is that the following inequality hold

$$\left| \frac{m}{\hbar^2} \int_{-\infty}^{\infty} V \, dZ \right| \ll 1$$

Multistate Scattering Theory

In the development of the present theory, the following type of reaction is considered

$$A + (B+e) \rightarrow A + (B+e)^*$$

where the asterisk denotes the possibility of excitation of the (B+e) system. For clarity, only one active electron is considered; however, the necessary generalization to many electrons is straightforward. Although the present treatment neglects both charge transfer and electron exchange effects, it can be modified to incorporate these effects. The inclusion of charge transfer channels and electron symmetry, however, introduces severe computational difficulties; further, these effects are important only at low energies in the reactions considered.

The coordinate system used to describe the collision process is represented in Figure 1. The origin, O, in Figure 1 is at rest in the laboratory (LAB) system. Use of the coordinate system in Figure 1 yields the LAB Hamiltonian

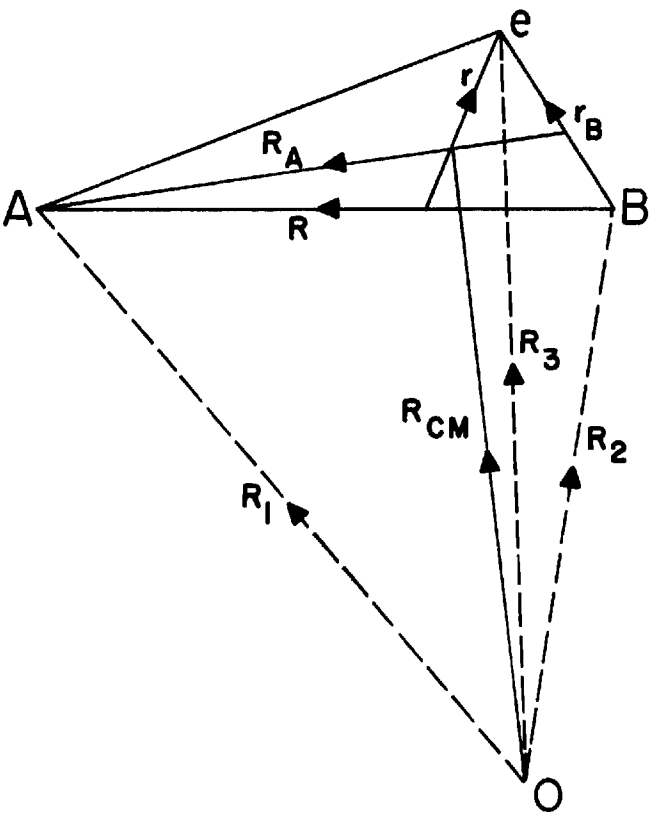

Figure 1. Coordinate System Used in the Description of the A + (B + e) Collision.

$$H_{LAB} = -\frac{\hbar^2}{2M_A}\nabla_1^2 - \frac{\hbar^2}{2M_B}\nabla_2^2 - \frac{\hbar^2}{2m}\nabla_3^2 + V_{Ae} + V_{Be} + V_{AB} \qquad (2\text{-}9)$$

where M_A, M_B, and m are the masses of particles A, B, and the active electron, respectively; the $\vec{\nabla}_i (i = 1,2,3)$ represent differentiation with respect to the coordinates $\vec{R}_i$; and V_{Ae}, V_{Be}, and V_{AB} are the two-body interaction potentials between the indicated particles. Generally, it is more convenient to work in the center-of-mass (CM) coordinate system. In order to represent (2-9) in this system, the following transformations are made

$$\vec{R} = \vec{R}_1 - \vec{R}_2 \qquad (2\text{-}10a)$$

$$\vec{r} = \vec{R}_3 - \frac{M_A\vec{R}_1 + M_B\vec{R}_2}{M_A + M_B} \qquad (2\text{-}10b)$$

$$\vec{R}_{CM} = \frac{M_A\vec{R}_1 + M_B\vec{R}_2 + m\vec{R}_3}{M_A + M_B + m} \qquad (2\text{-}10c)$$

Coordinate $\vec{R}$ is the relative internuclear coordinate; coordinate $\vec{r}$ is the coordinate of the active electron with respect to the nuclear center of mass; and $\vec{R}_{CM}$ is the coordinate of the center of mass of the system with respect to the LAB origin. The coordinates $\vec{R}$, $\vec{r}$, and $\vec{R}_{CM}$ are shown in Figure 1.

Use of the transformations (2-10a,b,c) allows the derivatives

appearing in the LAB Hamiltonian to be rewritten as

$$\vec{\nabla}_1 = \frac{M_A}{M_{tot}} \vec{\nabla}_{CM} + \vec{\nabla}_R - \frac{M_A}{M_A+M_B} \vec{\nabla}_r \tag{2-11a}$$

$$\vec{\nabla}_2 = \frac{M_B}{M_{tot}} \vec{\nabla}_{CM} - \vec{\nabla}_R - \frac{M_B}{M_A+M_B} \vec{\nabla}_r \tag{2-11b}$$

$$\vec{\nabla}_3 = \frac{m}{M_{tot}} \vec{\nabla}_{CM} + \vec{\nabla}_r \tag{2-11c}$$

By using (2-11a,b,c) in (2-9) the LAB Hamiltonian may be reexpressed as

$$H_{LAB} = - \frac{\hbar^2}{2M_{tot}} \nabla^2_{CM} - \frac{\hbar^2}{2\mu} \nabla^2_R - \frac{\hbar^2}{2m'} \nabla^2_r + V_{Ae} + V_{Be} + V_{AB} \tag{2-12}$$

where

$$M_{tot} = M_A + M_B + m \tag{2-13a}$$

$$\mu = \frac{M_A M_B}{M_A + M_B} \tag{2-13b}$$

$$m' = \frac{m(M_A + M_B)}{M_A + M_B + m} \tag{2-13c}$$

M_{tot} is the total mass of the system; μ is the reduced mass of the nuclei; and m' is the reduced mass of the electron, which, in practice, may be replaced by the mass of the electron, since $M_A+M_B \sim O(10^3\ m)$.

The interactions V_{Ae}, V_{Be}, V_{AB} are independent of the location of the center of mass, and thus the motion of the system's center of mass may be described by a plane-wave. Since the translational motion of the system's center of mass is not relevant to the problem, it is more convenient to deal with the center-of-mass Hamiltonian

$$H \equiv -\frac{\hbar^2}{2\mu}\nabla_R^2 - \frac{\hbar^2}{2m}\nabla_r^2 + V_{Ae} + V_{Be} + V_{AB} \tag{2-14}$$

The wave equation describing the complete system in the CM frame is

$$(H - E)\,\Psi(\vec{R},\vec{r}) = 0 \tag{2-15}$$

where H is given by (2-14) and the coordinates $\vec{R}$ and $\vec{r}$ are given by (2-10a,b). The wave equation must be solved subject to the asymptotic boundary condition

$$\Psi(\vec{R},\vec{r}) \xrightarrow[R_A\to\infty]{} \sum_n \delta_{n0} e^{i\vec{k}_o\cdot\vec{R}_A} + f_{n0}(\theta)\,\frac{e^{ik_nR_A}}{R_A}\,\psi_n(\vec{r}) \tag{2-16}$$

where $\vec{k}_n$ is the wave vector of the relative motion in the n^{th} channel, ψ_n is the product of the unperturbed wave functions in the n^{th} channel (e.g. $\psi_n = \phi_{1s}\phi_{2'S}$ for hydrogen-helium collisions), and $f_{n0}(\theta)$

is the scattering amplitude for scattering through the angle θ.

In order to separate the relative motion of the system from the internal motion, the system wave function is expanded as

$$\Psi(\vec{R},\vec{r}) = \sum_n F_n(\vec{R})\ \chi_n(\vec{R},\vec{r}) \tag{2-17}$$

where $F_n(\vec{R})$ is the channel eigenfunction which represents the relative motion of the system, and $\chi_n(\vec{R},\vec{r})$ is the internal wave function of the system which depends, however, on the relative separation of the colliding particles. The expansion (2-17) could be symmetrized and taken to include charge transfer channels; however, as previously mentioned, the computational difficulties involved are great.

The functions $F_n(\vec{R})$ in (2-17) are required to satisfy the following asymptotic boundary conditions

$$F_n(\vec{R})\ \underset{R\to\infty}{} \sum_n \left[\delta_{no} e^{i\vec{k}_o\cdot\vec{R}} + f_{no}(\theta_R)\frac{e^{ik_nR}}{R}\right] \tag{2-18}$$

where θ_R is the angle through which the relative separation vector $\vec{R}$ changes, rather than the angle through which $\vec{R}_A$ is changed; asymptotically both θ_R and θ are the same. The channel eigenfunctions $F_n(\vec{R})$ are assumed to provide most of the description of the relative motion.

It is now necessary to find the asymptotic boundary conditions for the $\chi_n(\vec{R},\vec{r})$, such that the conditions (2-16) are satisfied. From Figure 2, which is a detail of part of Figure 1, it is seen that $\vec{R}_A$ is

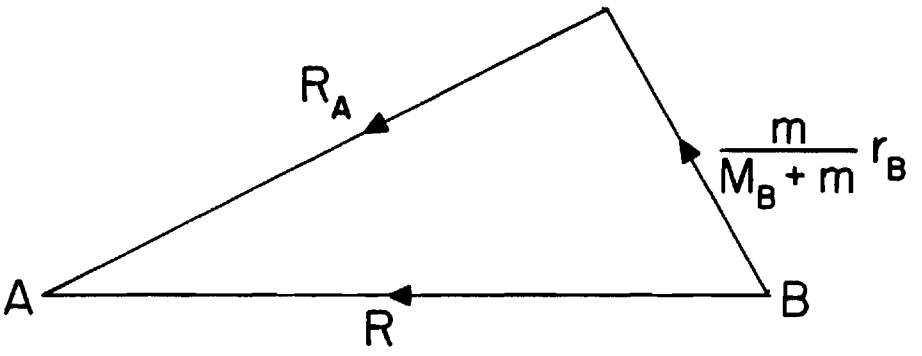

Figure 2. A Detail of the Coordinate System Shown in Figure 1.

a vector which joins the center of mass of the (B+e)-system to the projectile A. Hence, we may write the exponential factor $\vec{k}_0 \cdot \vec{R}_A$ as

$$\vec{k}_0 \cdot \vec{R}_A = \vec{k}_0 \cdot \left(\vec{R} - \frac{m}{M_B + m} \vec{r}_B \right)$$

which may be rewritten as

$$\vec{k}_o \cdot \vec{R}_A = \vec{k}_0 \cdot \vec{R} + \beta \vec{k}_0 \cdot \vec{r}_B \tag{2-19}$$

where

$$\beta = - \frac{m}{M_B + m} \tag{2-20}$$

Further, with the aid of the law of cosines

$$R_A = \left[R^2 - \frac{2m}{M_B + m} \vec{r}_B \cdot \vec{R} + \left(\frac{m}{M_B + m} \right)^2 r_B^2 \right]^{1/2}$$

When $R >> r_B$, i.e. in the asymptotic limit, the above equation may be approximated by

$$R_A \simeq \left[R^2 - \frac{2m}{M_B + m} \vec{r}_B \cdot \vec{R} \right]^{1/2}$$

or

$$R_A \simeq R - \frac{m}{M_B + m} \vec{r}_B \cdot \vec{R} \tag{2-21}$$

where terms of order $O(r_B^2/R^2)$ have been neglected. When R and R_A are large, $\vec{k}_n$ lies along the direction of $\vec{R}$; therefore

$$k_n R_A \xrightarrow[R, R_A \to \infty]{} k_n R + \beta \vec{k}_n \cdot \vec{r}_B \tag{2-22}$$

Use of (2-19) and (2-22) with (2-18) yields the boundary condition for the $\chi_n(\vec{R},\vec{r})$

$$\chi_n(\vec{R},\vec{r}) \xrightarrow[R \to \infty]{} \psi_{B_n}(\vec{r}) e^{i\beta \vec{k}_n \cdot \vec{r}_B} \tag{2-23}$$

The exponential factor in (2-23) is usually negligible for direct processes in atom-atom and electron-atom collisions; however, in the case of rearrangement collisions, the exponential factor may be very important.

It is necessary to say something about the functions $\chi_n(\vec{R},\vec{r})$. Generally, when only direct processes are considered, the χ_n are chosen to be a complete orthonormal set; however, this set can obviously be chosen in a number of different ways. Formally, since the summation in (2-17) is over all states of the set, all basis sets should serve equally well. In practice, the summation in (2-17) is truncated so that it

includes only the "important" states in the interaction. Hence, it is necessary to choose the χ_n so that the truncated version of (2-17) adequately describes the system.

For high energy collisions, for which the two colliding atomic systems retain their distinctness over most of the trajectory, the χ_n are chosen to be just the product of the unperturbed eigenfunctions of the colliding systems (2-23).

However, for low energy collisions, for which the two systems influence one another over a large part of the trajectory, the χ_n are chosen to be a set of quasi-molecular functions. This choice of a set of molecular wave functions for low energy collisions is especially desireable, since it automatically takes into account the fact that the natural axis of quantization is along the internuclear line for slow collisions.

The equations satisfied by the channel eigenfunctions, F_n, are now determined. By taking the inner product of χ_n and the system wave equation

$$(\chi_n,(H-E)\Psi) = 0 \tag{2-24}$$

the desired equations may be found.

In order to simplify the expansion of (2-24), the Hamiltonian is decomposed as

$$H = H' - \frac{\hbar^2}{2\mu} \nabla_R^2 \tag{2-25}$$

where H' is the part of the Hamiltonian which does not contain the translational kinetic energy. That is

$$H' = -\frac{\hbar^2}{2m}\nabla_r^2 + V_{Ae} + V_{Be} + V_{AB} \tag{2-26}$$

The total energy of the system is

$$E = \frac{\hbar^2 k_n^2}{2\mu} + \varepsilon_n \tag{2-27}$$

where ε_n is the total binding energy of the system and k_n is the wave vector of the relative motion of the system in the n^{th} channel.

Use of (2-17), (2-25), (2-26), and (2-27) in (2-24) yields

$$\sum_m (\chi_n, (H - E)F_m\chi_m) = 0$$

which may be rewritten as

$$\sum_m (\chi_n, \left[\frac{\hbar^2}{2\mu}\nabla_R^2 + \frac{\hbar^2}{2\mu}k_n^2\right]F_m\chi_m) = \sum_m (\chi_n, \left[H' - E\right]\chi_m)F_m \tag{2-28}$$

The matrix elements of the interaction are defined by

$$V_{nm}(\vec{R}) = (\chi_n, \left[H' - \varepsilon_m\right]\chi_m) \tag{2-29}$$

where the integration is carried out over all electronic coordinates.

(Note that $\left(-\frac{\hbar^2}{2m}\nabla_r^2 + V_{Be} - \varepsilon_m\right)\chi_m = 0.$)

Substitution of (2-29) in (2-28) yields

$$\sum_m \left(\chi_n, \left[\frac{\hbar^2}{2\mu}\nabla_R^2 + \frac{\hbar^2}{2\mu}k_m^2\right]\chi_m F_m\right) = \sum_m V_{nm}F_m \tag{2-30}$$

The term $\nabla_R^2 F_m\chi_m$ in (2-30) may be expanded as

$$\nabla_R^2 F_m\chi_m = \chi_m\nabla_R^2 F_m + 2(\vec{\nabla}_R F_m)\cdot(\vec{\nabla}_R\chi_m) + F_m\nabla_R^2\chi_m \tag{2-31}$$

Use of (2-31) in (2-30) yields

$$\left[\frac{\hbar^2}{2\mu}\nabla_R^2 F_n + \frac{\hbar^2}{2\mu}k_n^2 - V_{nn}\right]F_n(\vec{R}) =$$

$$= \sum_{m\neq n} V_{nm}F_m - \sum_m \frac{\hbar^2}{2\mu}\left[(\chi_n, \nabla_R^2\chi_m)F_m + 2(\chi_n, \vec{\nabla}_R\chi_m)\cdot\vec{\nabla}_R F_m\right] \tag{2-32}$$

Generally, the basis functions χ_n are chosen to be slowly varying functions of $\vec{R}$, so that the terms involving $\nabla_R^2\chi_m$ may be neglected with respect to those involving $\nabla_R\chi_m$. Alternatively, the matrix element (2-29) may be redefined as

$$V_{nm}^{(new)}(\vec{R}) = V_{nm}(\vec{R}) + \frac{\hbar^2}{2\mu}(\chi_n, \nabla_R^2\chi_m)$$

Usually, the former method is chosen. Then, (2-32) is rewritten as

$$\left[\frac{\hbar^2}{2\mu}\nabla_R^2 F_n + \frac{\hbar^2}{2\mu}k_n^2 - V_{nn}\right]F_n = \sum_{m\neq n} V_{nm}F_m - \sum_m \vec{\gamma}_{nm}\cdot\vec{\nabla}_R F_m \tag{2-33}$$

where

$$\vec{\gamma}_{nm} = \frac{\hbar^2}{\mu}(\chi_n, \vec{\nabla}_R\chi_m) \tag{2-34}$$

In many cases the $\chi_n(\vec{R},\vec{r})$ are chosen to be independent of $\vec{R}$, in which case the $\vec{\nabla}_R\chi_n$ are zero and the inner product (2-34) is also zero, and (2-33) is greatly simplified.

It should be noted that (2-33) is an exact equation except for the neglect of the charge transfer channels and symmetry, and possibly the neglect of the terms in $\nabla_R^2\chi_n$.

In order to make use of the eikonal approximation in the solution of (2-33), $F_n(\vec{R})$ is broken into two parts

$$F_n(\vec{R}) = \Xi_n(\vec{R})A_n(\vec{R}) \tag{2-35}$$

where $\Xi_n(\vec{R})$ is required to satisfy the homogeneous equation

$$\left[\frac{\hbar^2}{2\mu}\nabla_R^2 + \frac{\hbar^2}{2\mu}k_n^2 - V_{nn}\right]\Xi_n(\vec{R}) = 0 \tag{2-36}$$

The homogeneous equation (2-36) has the same form as the Schrödinger

equation, where the matrix element V_{nn} plays the role of the potential. By expressing Ξ_n as

$$\Xi_n(\vec{R}) = \exp\{i\ S_n(\vec{R})\} \tag{2-37}$$

and substituting (2-37) into (2-36), results similar to (2-7) are obtained, after the neglect of terms in $\nabla_R^2 S_n$. Hence, within the context of the eikonal formulation S_n may be written as

$$S_n(\vec{\rho},Z) = k_n Z + \int_{-\infty}^{Z} \left[\sqrt{k_n^2 - \frac{2\mu}{\hbar^2} V_{nn}} - k_n\right] dZ \tag{2-38}$$

The integration in (2-38) is performed along a straight line which may be represented as

$$\vec{R} = \vec{\rho} + \vec{Z} \tag{2-39}$$

where $\vec{\rho}$ is the classical impact-parameter, perpendicular to the Z-axis.

The validity of the straight line trajectory assumption requires the kinetic energy of the system to be much greater than the energy of interaction, i.e. in the n^{th} channel, the inequality

$$\frac{\hbar^2 k_n^2}{2\mu} >> V_{nn} \tag{2-40}$$

must be satisfied. If the requirement (2-40) is not satisfied, then

the validity of the use of the eikonal assumption is in doubt. However, the fact that the eikonal treatment obviates the need for a detailed knowlege of the trajectory, $\vec{R}(t)$, makes the use of the eikonal assumption attractive even when (2-40) is not well satisfied.

For convenience the "local wave vector", $\kappa_n(\vec{R})$, is defined by

$$\kappa_n^2(\vec{R}) = k_n^2 - \frac{2\mu}{\hbar^2} V_{nn}(\vec{R}) \tag{2-41}$$

Use of (2-35), (2-37), and (2-41) yields

$$\begin{aligned} \nabla_R^2 F_n &= \nabla_R^2 \{\Xi_n(\vec{R}) A_n(\vec{R})\} \\ &\simeq \Xi_n \frac{\partial^2 A_n}{\partial Z^2} + 2i\kappa_n \Xi_n \frac{\partial A_n}{\partial Z} - \kappa_n^2 \Xi_n A_n \end{aligned} \tag{2-42}$$

where the variation of A_n in the direction perpendicular to the Z-axis has been assumed to be small which is the case if the relative motion is primarily in the direction of the Z-axis. Further, the assumption is made that

$$\frac{\partial^2 A_n}{\partial Z^2} << \kappa_n \frac{\partial A_n}{\partial Z} \tag{2-43}$$

The basis for this last assumption is that the relative motion is well described by a distorted plane wave (2-37), and hence, most of the var-

iation of $F_n(\vec{R})$ is contained in $\Xi_n(\vec{R})$.

The term $\vec{\nabla}_R F_n$ may be expanded as

$$\vec{\nabla}_R F_n(\vec{R}) = \vec{\nabla}_R \left[\Xi_n(\vec{R}) A_n(\vec{R})\right]$$

$$= A_n \vec{\nabla}_R \Xi_n + \Xi_n \vec{\nabla}_R A_n \qquad (2\text{-}44)$$

$$= i\kappa_n \Xi_n A_n \hat{Z} + \Xi_n \frac{\partial A_n}{\partial Z} \hat{Z}$$

By assuming that the second term on the right hand side is much less than the first, the derivative may be approximated by

$$\vec{\nabla}_R F_n \simeq i\kappa_n F_n \hat{Z} \qquad (2\text{-}45)$$

Now, use of (2-35), (2-37), (2-42), (2-43), and (2-45) in (2-33) yields

$$2i\left(\frac{\hbar^2}{2\mu}\right)\kappa_n \Xi_n \frac{\partial A_n}{\partial Z} = \sum_{m\neq n} V_{nm} \Xi_m A_m - \sum_m i\kappa_m \vec{\gamma}_{nm} \cdot \hat{Z}\, \Xi_m A_m \qquad (2\text{-}46)$$

By using (2-37) in (2-46), the following equations for the A_n are obtained

$$2i\left(\frac{\hbar^2}{2\mu}\right)\kappa_n \frac{\partial A_n}{\partial Z} = \left[\sum_{m\neq n} V_{nm} A_m - \sum_m i\kappa_m \vec{\gamma}_{nm} \cdot \hat{Z}\, A_m\right] e^{i(S_m - S_n)} \qquad (2\text{-}47)$$

Hence, the system wave function may be written as

$$\Psi(\vec{R},\vec{r}) = \sum_n A_n(\vec{\rho},Z)\ e^{iS_n(\vec{\rho},Z)}\chi_n(\vec{R},\vec{r}) \tag{2-48}$$

where the χ_n satisfy the asymptotic boundary conditions

$$\chi_n(\vec{R},\vec{r}) \xrightarrow[R\to\infty]{} \psi_{B_n}(\vec{r})\ e^{i\vec{k}_n\cdot\vec{r}_B}$$

Further, $S_n(\vec{\rho},Z)$ is defined by (2-38) and the $A_n(\vec{\rho},Z)$ are the solutions of (2-47).

By using (2-41), (2-38) may be more compactly written as

$$S_n(\vec{\rho},Z) = k_n Z + \int_{-\infty}^{Z} \{\kappa_n(\vec{R}) - k_n\}dZ \tag{2-49}$$

For convenience, new coefficients $B_n(\vec{\rho},Z)$ are defined by

$$B_n(\vec{\rho},Z) = A_n(\vec{\rho},Z)\ \exp i\left[\int_{-\infty}^{Z} \{\kappa_n - k_n\}\ dZ\right] \tag{2-50}$$

(Note that $|B_n| = |A_n|$.) By using (2-50), A_n may be expressed in terms of B_n as

$$A_n = B_n\ \exp -i\left[\int_{-\infty}^{Z} [\kappa_n - k_n]\ dZ\right] \tag{2-51}$$

and the derivative of A_n may then be written as

$$\frac{\partial A_n}{\partial Z} = \left[\frac{\partial B_n}{\partial Z} - i(\kappa_n - k_n)B_n\right] \exp\left[-i\int_{-\infty}^{Z} (\kappa_n - k_n)\, dZ\right] \tag{2-52}$$

Substitution of (2-51) and (2-52) into the coupled-equations (2-47) yields

$$\begin{aligned} i\hbar \frac{\partial B_f}{\partial Z} = \hbar(k_f - \kappa_f)B_f + \frac{\mu}{\hbar\kappa_f} \sum_{n\neq f} V_{fn}B_n\, e^{i(k_n - k_f)Z} \\ -i\frac{\mu}{\hbar\kappa_f} \sum_n \kappa_n \vec{\gamma}_{fn}\cdot\hat{Z}\, B_n\, e^{i(k_n - k_f)Z} \end{aligned} \tag{2-53}$$

The theory presented up to this point has been concerned with finding the system wave function $\Psi(\vec{R},\vec{r})$, which may be written as

$$\Psi(\vec{R},\vec{r}) = \sum_n B_n(\vec{\rho},Z)\, e^{ik_nZ}\, \chi_n(\vec{R},\vec{r}) \tag{2-54}$$

where the B_n satisfy the coupled-equations (2-53), subject to the initial conditions

$$B_n(\vec{\rho},-\infty) = \delta_{ni} \tag{2-55}$$

where i denotes the initial state of the system.

In order to find expressions for the differential and total cross

sections, the scattering amplitude for transition from the initial state (i) to the final state (f) is now considered. The scattering amplitude is defined by

$$f_{fi}(\theta,\phi) = -\frac{\mu}{2\pi\hbar^2}\langle\chi_f|V|\Psi\rangle \tag{2-56}$$

By using (2-54), the expression (2-56) for the scattering amplitude may be rewritten as

$$f_{fi}(\theta,\phi) = -\frac{\mu}{2\pi\hbar^2}\int d\vec{R}'\int d\vec{r}'\ \chi_f^*(\vec{R}',\vec{r}')e^{-\vec{k}_f\cdot\vec{R}'}V(\vec{R}',\vec{r}')\Psi_i(\vec{R}',\vec{r}')$$
$$\times e^{ik_nZ'}\ e^{-i\vec{k}_f\cdot\vec{R}'}\ e^{i\beta(\vec{k}_n-\vec{k}_f)\cdot\vec{r}_B'} \tag{2-57}$$

Further, since $\beta\sim10^{-3}$, the last exponential in the above expression may be approximated by unity, when only direct precesses are considered. Then by making use of (2-29), (2-57) yields

$$f_{fi}(\theta,\phi) = -\frac{\mu}{2\pi\hbar^2}\int d\vec{R}\sum_n V_{fn}(\vec{R})B_n(\vec{\rho},Z)\ e^{i(\vec{k}_i-\vec{k}_f)\cdot\vec{R}}\ e^{i(k_n-k_i)Z} \tag{2-58}$$

where the fact that $\vec{k}_i$ is parallel to the Z-axis has been used. The momentum transfer vector, $\vec{K}$, is defined by

$$\vec{K} = \vec{k}_i - \vec{k}_f \tag{2-59}$$

Substitution of (2-59) into (2-58) yields the basic equation for the scattering amplitude within the context of this treatment

$$f_{fi}(\theta,\phi) = -\frac{\mu}{2\pi\hbar^2}\int d\vec{R}\sum_n V_{fn}(\vec{R})B_n(\vec{\rho},Z)\ e^{i\vec{K}\cdot\vec{R}}\ e^{i(k_n-k_i)Z} \qquad (2\text{-}60)$$

Although the integration in (2-60) could be performed directly, an important special case reduces (2-60) to a more manageable form. This special case occures whenever the ϕ-dependence of the matrix elements (2-29) is just a complex phase; i.e.

$$V_{fn}(R,\theta,\phi) = V_{fn}(R,\theta)\ e^{i\Delta_{nf}\phi} \qquad (2\text{-}61)$$

where $\Delta_{nf} = m_n - m_f$, the difference between the magnetic quantum numbers of the states n and f. The decomposition (2-61) is very improtant, because it holds, in general, whenever the interaction potential $V(\vec{R},\vec{r})$ may be expressed as the sum of central potentials; e.g., the sum of two-body Coulomb interactions in the case of electron-atom collisions.

When the decomposition (2-61) is possible, it is convenient to define new phase-independent coefficients $C_n(\rho,Z)$ by

$$C_n(\rho,Z)\ e^{i\Delta_{in}\phi} = B_n(\vec{\rho},Z) \qquad (2\text{-}62)$$

where, obviously, $|C_n| = |B_n|$. Then, after multiplying (2-53) through

by $e^{i\Delta_{fi}\phi}$, the following equations for the C_n are obtained

$$i\hbar \frac{\partial C_f}{\partial Z} = \hbar(k_f - \kappa_f)C_f + \frac{\mu}{\hbar\kappa_f} \sum_{n\neq f} V_{fn}C_n e^{i(k_n-k_f)Z}$$

$$- \frac{i}{\hbar\kappa_f} \sum_n \kappa_n \vec{\gamma}_{fn}\cdot\hat{Z}\, C_n e^{i(k_n-k_f)Z} \tag{2-63}$$

For convenience, it is assumed in the remainder of this chapter that the basis functions, χ_n, are chosen to be independent of the relative position, $\vec{R}$. The reason this assumption is made is to simplify the remainder of the derivation; also, the basis functions actually chosen in the work discussed in the later chapters are independent of $\vec{R}$. The effect of this assumption is to reduce the inner product (2-34) to zero.

Now the summation (2-60) is considered. By using (2-62) and (2-53) the summation may be reexpressed as

$$\sum_n V_{fn}B_n e^{i(k_n-k_i)Z} = e^{i(k_f-k_i)Z} \sum_n V_{fn}B_n e^{i(k_n-k_f)Z}$$

$$= e^{i\Delta_{if}\phi}\, e^{i(k_f-k_i)Z} \sum_n V_{fn}C_n e^{i(k_n-k_f)Z}$$

$$= e^{i\Delta_{if}\phi}\, e^{i(k_f-k_i)Z}\left\{\frac{i\hbar^2\kappa_f}{\mu}\frac{\partial C_f}{\partial Z} + \left[V_{ff} - \frac{\hbar^2\kappa_f}{\mu}(k_f - \kappa_f)\right]C_f\right\}$$

Use of the above summation in (2-60) yields

$$f_{fi}(\theta,\phi) = -\frac{\mu}{2\pi\hbar^2}\int d\vec{R}\; e^{i(\vec{K}\cdot\vec{R}+\Delta_{if}\phi)}\; e^{i(k_f-k_i)Z} \times\left\{\frac{i\hbar^2\kappa_f}{\mu}\frac{\partial C_f}{\partial Z} + \left[V_{ff} - \frac{\hbar^2\kappa_f}{\mu}(k_f - \kappa_f)\right] C_f\right\} \tag{2-64}$$

The dot product $\vec{K}\cdot\vec{R}$ may be written as

$$\vec{K}\cdot\vec{R} = \vec{K}'\cdot\vec{\rho} + K_z Z = K'\rho\,\cos(\phi-\Phi) + K_z Z$$

where $\vec{K}'$ is the component of the momentum transfer perpendicular to the Z-axis.

By using the integral

$$\int_0^{2\pi} e^{i(n\Phi + z\,\cos\,\Phi)}\, d\Phi = 2\pi i^n J_n(z)$$

in (2-64), the scattering amplitude becomes

$$f_{fi}(\theta,\phi) = -\,i^{\Delta+1}\int^{\infty} J_{\Delta}(K'\rho)\left[I_1(\rho,\theta) - iI_2(\rho,\theta)\right]\rho\; d\rho \tag{2-65}$$

where J_Δ is a Bessel function of the first kind of order $\Delta \equiv \Delta_{if}$, and and the Z-integrations I_1 and I_2 are given by the expressions

$$I_1(\rho,\theta) = \int_{-\infty}^{\infty} \kappa_f(\rho,Z) \frac{\partial C_f}{\partial Z}(\rho,Z)\ e^{i\alpha Z}\ dZ \tag{2-66}$$

and

$$I_2(\rho,\theta) = \int_{-\infty}^{\infty} \left[\kappa_f(\kappa_f - k_f) + \frac{\mu}{\hbar^2} V_{ff}\right] C_f(\rho,Z)\ e^{i\alpha Z}\ dZ \tag{2-67}$$

where the θ-dependence in (2-66) and (2-67) is contained in the parameter

$$\alpha(\theta) = K_z + k_f - k_i = k_f(1 - \cos\theta) \tag{2-68}$$

which is the difference between the Z-component of the momentum transfer and the minimum value of the momentum transfer. Further, for large k_f, α becomes large when significant deviations from 0° scattering occur, causing the exponential factor $e^{i\alpha Z}$ to damp out the integrals I_1 and I_2. Thus the differential cross sections at a fixed large angle of scattering should decrease with increasing energy.

Equations (2-65) through (2-68) form the basic results of the present theory. The differential and total cross sections are subsequently obtained from the following equations

$$\frac{d\sigma}{d\Omega}(\theta,\phi) = \frac{k_f}{k_i} \left|f_{fi}(\theta,\phi)\right|^2 \tag{2-69}$$

and

$$\sigma_{fi} = \int \frac{d\sigma}{d\Omega}(\theta,\phi)\ d\Omega \tag{2-70}$$

Equations (2-65) through (2-70) form what will be called the multichannel eikonal approximation or full eikonal approximation. It should be noted that no approximations beyond those of the eikonal approximation itself have been made, but the results (2-65) through (2-68) are valid only for central potentials and basis sets, χ_n, which are independent of the relative separation $\vec{R}$; for other cases the scattering amplitude must be computed from the more general form (2-60).

CHAPTER III

APPROXIMATIONS TO THE MULTICHANNEL EIKONAL THEORY

In Chapter II the full eikonal theory has been presented. The present chapter deals with approximations, which have been presented by other investigators. The relationships between these theories and the present theory will be shown. For reference purposes, Figure 3 at the end of the chapter gives a diagramatic presentation of the relations between the different approximations presented in this chapter.

For convenience, the important equations of Chapter II are presented again. The system wave function is

$$\Psi(\vec{R},\vec{r}) = \sum_n C_n(\rho,Z)\ e^{i\Delta\Phi}\ e^{ik_n Z}\ \chi_n(\vec{r}) \tag{3-1}$$

where the coefficients C_n are the solutions of the coupled-equations

$$i\hbar \frac{\partial C_f}{\partial Z} = \hbar(k_f - \kappa_f)C_f + \frac{\mu}{\hbar\kappa_f} \sum_{n\neq f} V_{fn}C_n\ e^{i(k_n-k_f)Z} \tag{3-2}$$

solved subject to the intiial conditions

$$C_n(\rho,-\infty) = \delta_{ni}\ e^{-i\Delta\Phi}$$

and where it has again been assumed that the basis functions are independent of the relative separation $\vec{R}$. The local wave number κ_n is given by

$$\kappa_n(\vec{R}) = \left[k_n^2 - \frac{2\mu}{\hbar^2} V_{nn}(\vec{R})\right]^{1/2} \tag{3-3}$$

The scattering amplitude from the initial state i to the final state f is

$$f_{fi}(\theta,\phi) = - i^{\Delta+1} \int_0^\infty J_\Delta(K'\rho) \left[I_1(\rho,\theta) - iI_2(\rho,\theta)\right] \rho \, d\rho \tag{3-4}$$

where the integrals I_1 and I_2 are given by

$$I_1(\theta,\phi) = \int_{-\infty}^{\infty} \kappa_f(\rho,Z) \frac{\partial C_f}{\partial Z}(\rho,Z) \, e^{i\alpha Z} \, dZ \tag{3-5}$$

and

$$I_2(\rho,\theta) = \int_{-\infty}^{\infty} \left[\kappa_f(\kappa_f - k_f) + \frac{\mu}{\hbar^2} V_{ff}\right] C_f(\rho,Z) \, e^{i\alpha Z} \, \rho \, d\rho \tag{3-6}$$

Here the coefficient α is

$$\alpha(\theta) = K_z - (k_i - k_f) = k_f(1 - \cos\theta) \tag{3-7}$$

The Born Approximation

Perhaps the simplest approximation which can be made is to neglect all couplings except that which connects the initial and final states, i.e. set $C_n = \delta_{ni}$ in (3-2). Then (3-4) directly yields

$$f_{fi}(\theta,\phi) = -\frac{\mu}{2\pi\hbar^2}\int V_{fi}(\vec{R})\ \exp\ (i\vec{K}\cdot\vec{R})\ d\vec{R}$$

which is the Born-wave scattering amplitude. In fact, the Born approximation follows directly from each of the approximations A, B, and C to be discussed below, a fact that has been shown explicitly by Flannery and McCann (1973) for approximation C(0), which is a special case of approximation C.

Approximation A

The first multistate approximation to the full treatment follows from expanding the local wave vector κ_f in the integral (3-6) as

$$\kappa_f(\vec{R}) = k_f - \frac{\mu}{\hbar^2 k_f} V_{ff}(\vec{R}) \qquad (3\text{-}8)$$

The expansion (3-8) is valid in the limit of high energies, when

$$\frac{\hbar^2 k_f}{2\mu} >> V_{ff}$$

that is, when the translational energy is significantly greater than the energy of interaction.

With the aid of the expansion (3-8) it is seen that the integrand in (3-6) vanishes to order $O(V_{ff}^2/k_f^2)$, which is the order of the expansion (3-8). Thus the scattering amplitude reduces to

$$f_{fi}^A(\theta,\phi) = -\frac{\mu}{2\pi\hbar^2}\int e^{i(\vec{K}\cdot\vec{R}+\Delta\Phi)}\, d\vec{R} \sum_{n=1}^{N} C_n^A(\rho,Z)V_{fn}(R,\theta)\, e^{i(k_n-k_i)Z} \quad (3\text{-}9)$$

$$= -i^{\Delta+1}\int_0^\infty J_\Delta(K'\rho)\,\rho\, d\rho \int_{-\infty}^{\infty} \kappa_f \frac{\partial C_f^A}{\partial Z} e^{i\alpha Z}\, dZ \quad (3\text{-}10)$$

where the coefficients C_n^A satisfy

$$\frac{i\hbar^2}{\mu}\kappa_f \frac{\partial C_f^A}{\partial Z} = \sum_{n=1}^{N} C_n^A(\rho,Z)\, V_{fn}(\rho,Z)\, e^{i(k_n-k_f)Z} \quad (3\text{-}11)$$

Approximation B

A second approximation to the multistate theory is arrived at by setting the local wave numbers equal to their asymptotic values, i.e. by setting $\kappa_n = k_n$ in (3-10) and (3-11).

As previously mentioned, both approximations A and B yield the Born-wave results upon substitution of $C_n = \delta_{in}$ in (3-9). An improvment over the Born approximation for elastic scattering results by including

only the initial state coefficient in (3-11), i.e. by setting $C_n^B = C_i^B \delta_{in}$ in (3-11) with $\kappa_i = k_i$. In this case

$$C_i^B(\rho,Z) = \exp -\left[\frac{i}{\hbar v_i}\int_{-\infty}^{Z} V_{ii}(\rho,Z')\, dZ'\right]$$

The corresponding scattering amplitude is

$$f_{ii}(\theta,\phi) = -\, ik_i \int_0^\infty J_o(2k_i\rho \sin\frac{\theta}{2})\, [\exp 2i\chi(\rho) - 1]\rho\, d\rho \qquad (3\text{-}12)$$

where

$$\chi(\rho) = -\frac{1}{\hbar v_i}\int_0^\infty V_{ii}\left[(\rho^2 + Z^2)^{1/2}\right] dZ \qquad (3\text{-}13)$$

Equations (3-12) and (3-13) are just the usual eikonal approximation for elastic scattering by a fixed potential (cf. Glauber 1959, Bransden 1970).

Another form of approximation B is obtained when the system wave function (3-1) is projected onto the distorted wave

$$\chi_f(\vec{r})\, \exp\, i[\vec{k}_f\cdot\vec{R} - \frac{1}{\hbar v_f}\int_\infty^Z V_{ff}\, dZ] \qquad (3\text{-}14)$$

for the final state, rather than onto the undistorted wave $\chi_f(\vec{r})\, e^{i\vec{k}_f\cdot\vec{R}}$.

Then the resulting distorted-wave scattering amplitude is

$$f_{fi}^{DW}(\theta,\phi) = -i^{\Delta+1} \int_0^\infty J_\Delta(K'\rho)\rho \, d\rho \left[\int_{-\infty}^\infty k_f \frac{\partial C_f^B}{\partial Z} \exp i(\alpha Z + \frac{1}{\hbar v_f} \int_\infty^Z V_{ff} \, dZ') \, dZ \right]$$

where the C_f^B satisfy (3-11) with $\kappa_f = k_f$. A special case of this distorted-wave result is the two-state approximation, which includes only the initial and final states in (3-11). Then the distorted-wave scattering amplitude reduces to

$$f_{fi}^{DWB}(\theta,\phi) = -\frac{i^\Delta \mu}{\hbar^2} \int_0^\infty J_\Delta(k_f \rho \sin\theta) \, \rho \, d\rho \int_{-\infty}^\infty V_{fi}(\rho,Z) \times \exp i\{[(k_i - k_f) + \alpha]Z + \delta\Phi(Z)\} \, dZ \tag{3-15}$$

where

$$\delta\Phi(Z) = -\frac{1}{\hbar v_i} \int_{-\infty}^Z V_{ii} \, dZ - \frac{1}{\hbar v_f} \int_Z^\infty V_{ff} \, dZ \tag{3-16}$$

Equations (3-15) and (3-16) are identical to the distorted-wave Born result derived by Chen et al. (1972) from a different approach. In fact, the distorted-wave Born approach is nearly equivalent to a two-state calculation in approximation B, since the DWB method includes the matrix elements V_{ii}, V_{ff}, and V_{fi}, while the two-state method also includes the back-coupling term V_{if}.

Approximation C(α)

By using conservation of energy, the exponential factor, $k_n - k_f$, in the coupled-equations (3-11) may be written as

$$k_n - k_f = \frac{2\varepsilon_{fn}}{\hbar(v_f + v_n)} \tag{3-17}$$

where $\varepsilon_{fn} = \varepsilon_f - \varepsilon_n$. For collisions in which the energy of relative motion is much greater than the energy of excitation, the velocities will be nearly the same in all channels, i.e. $v_n = v_i$, and they will be nearly constant over the entire interaction region. Under these conditions, the following approximation may be made

$$k_n - k_f \simeq \frac{\varepsilon_{fn}}{\hbar v_i} \tag{3-18}$$

Use of (3-18) reduces the scattering amplitude of approximation B to

$$f^C_{fi}(\theta,\phi) = -\, i^{\Delta+1}\, k_i \int_0^\infty J_\Delta(K'\rho) \int_{-\infty}^{\infty} \frac{\partial C^C_f}{\partial Z}\, e^{i\alpha Z}\, dZ\, \rho\, d\rho \tag{3-19}$$

where

$$\alpha \simeq K_z - \frac{\varepsilon_{fi}}{\hbar v_i} \tag{3-20}$$

and the C_f^C satisfy the coupled-equations

$$i\hbar \frac{\partial C_f^C}{\partial Z} = \frac{1}{v_i} \sum_{n=1}^{N} C_n^C(\rho,Z) V_{fn}(\rho,Z) \exp i\frac{\epsilon_{fn} Z}{\hbar v_i} \tag{3-21}$$

Further, for high energy collisions in which most of the scattering occurs at small angles, it is seen that $\alpha \simeq 0$, since for small angles

$$K_z \simeq \frac{\epsilon_{fi}}{\hbar v_i}$$

Hence, by setting $\alpha = 0$ in (3-19), the familiar impact-parameter scattering amplitude (Flannery and McCann 1973) is recovered

$$f_{fi}^{C(0)}(\theta,\phi) = - i^{\Delta+1} k_i \int_0^\infty J_\Delta(K'\rho) [C_f^C(\rho,\infty) - \delta_{fi}]\rho \, d\rho \tag{3-22}$$

where $K'^2 \equiv K^2 - \epsilon_{fi}^2/\hbar^2 v_i^2$.

Results similar to (3-21) and (3-22) have been derived bv Byron (1970) and by Bransden and his colleagues (Bransden and Coleman 1972; Bransden, Coleman, and Sullivan 1972). Bransden et al. have also included a second order potential in their derivation of (3-21), which takes some account of the terms neglected in the truncation of the multistate expansion.

There is a definite computational advantage in the use of (3-22)

to calculate the scattering amplitude, since only the asymptotic values of the C_f are required, and these are obtained from the integration of the coupled-equations (3-21). However, the other versions of (3-22), approximations A, B, and C(α), require explicit knowlege of the C_f and their derivatives along the entire trajectory, i.e. in the more accurate versions of the theory the Z-integration must be performed directly, whereas in approximation C(0) the Z-integration is performed during the solution of the coupled equations, thus reducing the amount of computation necessary.

Further, in the limit of large impact velocities, the computation of the total cross section is also greatly simplified. From (2-69) and (2-70), it is seen that

$$\sigma_{fi} = \frac{k_f}{k_i} \int_0^{2\pi} \int_0^{\pi} |f_{fi}(\theta,\phi)|^2 \sin\theta \, d\theta \, d\phi$$

By using (3-22), the above expression may be rewritten as

$$\sigma_{fi} = 2\pi \int_0^{\pi} \{J_\Delta(K'\rho) \, J_\Delta(K'\rho') \, [C_f^C(\rho,\infty) - \delta_{fi}][C_f^C(\rho',\infty) - \delta_{fi}]^* \times \rho \, d\rho \, \rho' \, d\rho'\} \sin\theta \, d\theta \tag{3-23}$$

where $K_f = k_i$. Now

$$K' = k_f \sin\theta$$

and

$$dK' = k_f \cos\theta \, d\theta \simeq k_f \, d\theta$$

for small angle scattering. Hence, (3-23) may be rewritten as

$$\sigma_{fi} \simeq \int_0^{k_i+k_f} \int_0^{\infty} \int_0^{\infty} J_\Delta(K'\rho) \, J_\Delta(K'\rho') \, [C_f^C(\rho,\infty) - \delta_{fi}][C_f^C(\rho',\infty) - \delta_{fi}]^* \times \rho \, d\rho \, \rho' \, d\rho' \, K' \, dK'$$

However, when $k_i + k_f$ is very large, the following integral may be used

$$\int_0^{\infty} J_\Delta(K'\rho) \, J_\Delta(K'\rho') \, K' \, dK' = \frac{1}{\rho}\delta(\rho - \rho')$$

and hence, the expression for the total cross section becomes

$$\sigma_{fi} = \int_0^{\infty} |C_f^C(\rho,\infty) - \delta_{fi}|^2 \, \rho \, d\rho \qquad (3\text{-}24)$$

which is the usual impact-parameter result. It should be noted that the customary derivation of (3-24) arises from the assumption that the $|C_n|^2$ are the probabilities for transition. This assumption stems from the fact that the coupled-equations (3-21) may be derived from the time-dependent perturbation equations via the substitution $Z = v_i t$, in which

case the $|C_n|^2$ do represent the probability for transition. However, a comparison between cross sections calculated from (3-24) and from a direct integration of the differential cross sections often exhibits a large discrepancy, which is due to the incorrect assumption that the velocity is unchanging over the trajectory, and even more, to the fact that $k_i + k_f$ is not reasonably approximated by infinity.

Generally, (3-24) is valid for heavy-particle collisions for which $k_i + k_f \sim O(10^3)$; however, for electron-atom collisions $k_i + k_f$ is typically on the order of ten, and hence, the use of (3-24) is not justified.

The Glauber Approximation

An important variation of approximation C(0) is found by considering the high energy limit of (3-21). This limit is obtained when the following assumption is valid

$$\frac{\varepsilon_{fn}}{v_i} \simeq 0 \tag{3-25}$$

Then, inclusion of all states in the summation of (3-21) yields the coupled-equations

$$i\hbar \frac{\partial C_f^G}{\partial Z} = \frac{1}{v_i} \sum_n C_n^G(\rho,Z)\ V_{fn}(\rho,Z) \tag{3-26}$$

The equations (3-26) may be solved exactly, yielding

$$C_f^G(\rho,Z) = \langle \chi_f | \exp[-\frac{i}{\hbar v_i} \int_{-\infty}^{Z} V(\vec{R},\vec{r})\, dZ] | \chi_i \rangle \qquad (3\text{-}27)$$

The corresponding scattering amplitude is

$$f_{fi}^G(\theta,\phi) = -\frac{ik_i}{2\pi} \int e^{i\vec{K}\cdot\vec{\rho}}\, \chi_f^*(\vec{r})[e^{i\chi(\vec{\rho},\vec{r})} - 1]\chi_i(\vec{r})\, d\vec{r}\, d\vec{\rho} \qquad (3\text{-}28)$$

where

$$\chi(\vec{\rho},\vec{r}) = -\frac{1}{hv_i} \int_{-\infty}^{\infty} V(\vec{r},\vec{\rho},Z)\, dZ \qquad (3\text{-}29)$$

Equations (3-28) and (3-29) are identical to the expressions derived by Glauber (1970).

It is important to note that although, in principle, the Glauber approximation is a subset of approximation C(0), there is a fundamental difference, since approximation C(0) does not include couplings to all states, whereas, the Glauber approximation does. This inclusion of couplings to all channels is important, because it yields the correct long range polarization interaction, which is very important for elastic scattering and for low energy scattering in general.

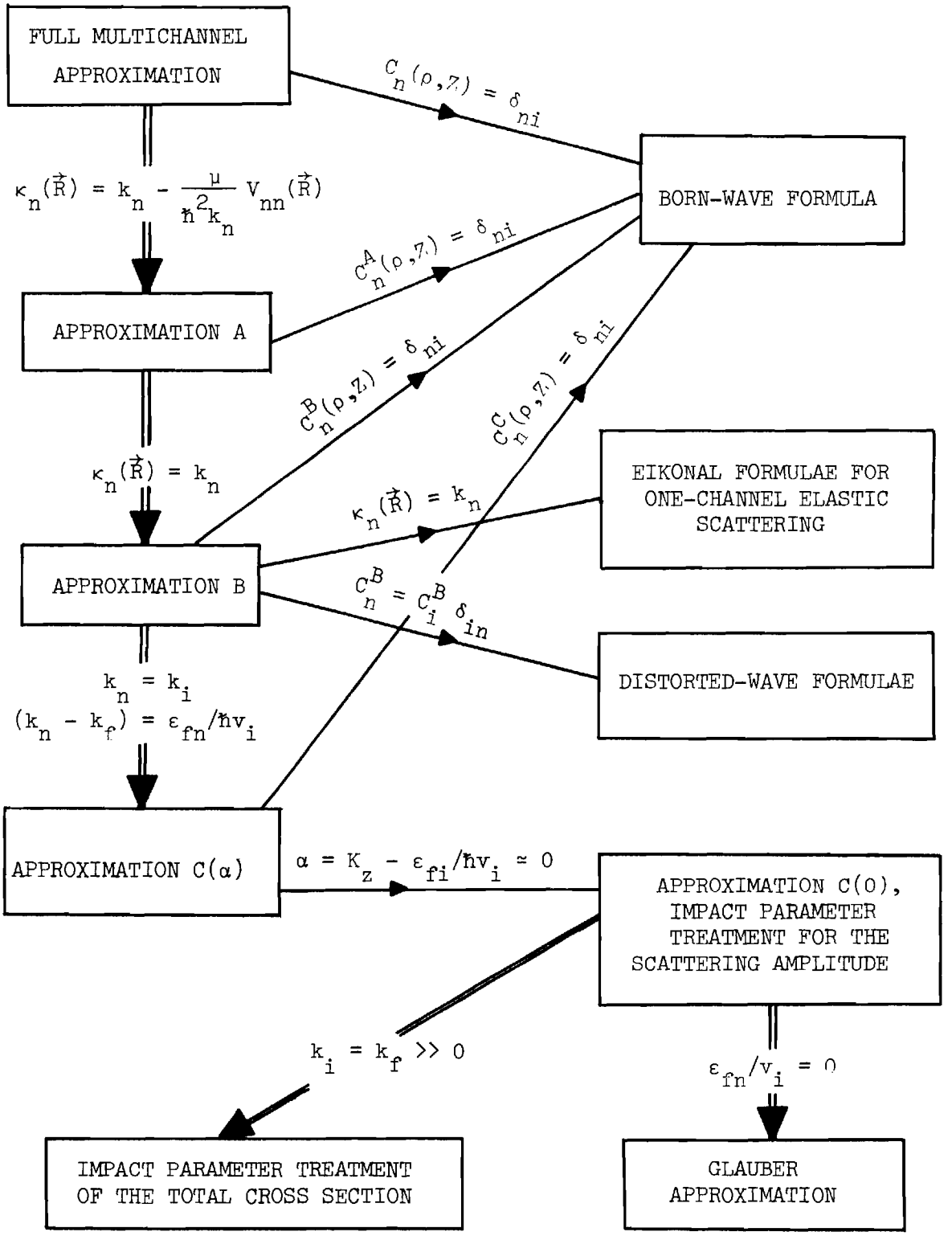

Figure 3. Schematic Diagram Illustrating Approximations To The Multichannel Eikonal Treatment.

CHAPTER IV

ELECTRON-ATOM SCATTERING

In the present chapter the full eikonal treatment of Chapter II and the subsequent approximations of Chapter III are applied to electron-atom scattering. In particular, the following reactions are considered

$$e + H(1s) \rightarrow e + H(1s, 2s, 2p_0, 2p_{\pm 1}) \tag{4-1}$$

and

$$e + He(1\ ^1S) \rightarrow e + He(1\ ^1S, 2\ ^1S, 2\ ^1P_0, 2\ ^1P_{\pm 1}) \tag{4-2}$$

In the full eikonal treatment, the lowest five states of the respective target atom have been closely coupled. Differential and total cross sections have been calculated and are displayed along with experimental data and with other theoretical calculations.

Electron-Hydrogen Scattering

Differential and total cross sections for the reaction (4-1) have been calculated for incident electron energies in the range $13.6\ \text{eV} \leq E_i \leq 200\ \text{eV}$.

Total Cross Sections

In Table 1, total cross sections obtained from the full eikonal treatment and from approximations A, B, C(α), and the impact-parameter

Table 1. Total Cross Sections (πa_o^2) at Impact Energy E_i(eV) for the Processes e + H(1s) → e + H($n\ell$), $n\ell$ = 1s,2s,$2p_0$,$2p_{\pm1}$.

E_i(eV)	$n\ell$	Full Eikonal Treatment	Approximate Eikonal Treatments A	B	C(α)	Impact-Parameter Treatment C(0)	IP
20	1s	0.841	0.923	0.703	0.651	0.714	1.056
	2s	0.145	0.174	0.131	0.070	0.122	0.147
	$2p_o$	0.398	0.524	0.319	0.347	0.373	0.447
	$2p_{\pm1}$	0.322	0.355	0.297	0.307	0.931	0.720
	2p	0.720	0.879	0.616	0.654	1.304	1.167
50	1s	0.365	0.378	0.332	0.373	0.371	0.519
	2s	0.090	0.095	0.085	0.076	0.089	0.083
	$2p_o$	0.350	0.360	0.347	0.352	0.303	0.279
	$2p_{\pm1}$	0.515	0.522	0.514	0.515	0.717	0.569
	2p	0.865	0.882	0.861	0.867	1.020	0.848
100	1s	0.224	0.229	0.202	0.202	0.213	0.271
	2s	0.052	0.053	0.050	0.049	0.053	0.054
	$2p_o$	0.190	0.192	0.191	0.196	0.176	0.173
	$2p_{\pm1}$	0.439	0.441	0.439	0.443	0.506	0.484
	2p	0.629	0.633	0.630	0.639	0.682	0.657

approximation are displayed.

The comparison between the columns C(0) and IP (impact-parameter) of Table 1 is a direct measure of the error in the calculations of the total cross section introduced by the use of (3-24) to calculate the cross section, rather than by direct integration of the differential cross section.

In general, the entries in column IP exceed those of C(0) except in the $2p_{\pm 1}$ channel. The overestimate for the $\Delta = 0$ channels and the underestimate for the $\Delta = 1$ channel is due to the integration over non-physical momentum transfers in (3-23), which is implicit in the use of (3-24).

The inclusion of the phase α by approximation $C(\alpha)$ (cf. equation (3-19)) causes a reduction in the total cross sections over those of C(0), which is expected, because the phase factor exp $i\alpha Z$ in (3-19) tends to damp out the integral. Acknowledgement of the different asymptotic speeds v_n via approximation B yields cross sections which are generally larger than those of approximation $C(\alpha)$, particularly at the lower energies, where the difference in the asymptotic speeds is more pronounced. The effect of the adoption of the local wave vector κ_n rather than its asymptotic limit k_n via approximation A is displayed in columns A and B of Table 1. The overall effect is an increase in the cross sections at all energies, such that the impact-parameter (IP) approximation appears to yield better results than the approximation merits, i.e. the effects of the successive refinements introduced in approximations C(0), $C(\alpha)$, B, and A tend to cancel one another.

Finally, the cross sections given by the full eikonal treatment

displayed in Table 1 are slightly less than those of approximation A. In conclusion, the changes introduced by the various modifications of the full eikonal treatment, displayed in Table 1, are significant at the lower energies, but become negligible at the higher energies, as expected, since all the approximations become valid at sufficiently high impact energy.

Comparison With Other Theories and Experiment

The elastic and inelastic total cross sections, obtained from the full eikonal treatment, are displayed in Table 2 for various impact energies, E_i. The present 2s and 2p excitation cross sections are compared in Figures 4a and 4b with the calculations of other investigators: the pseudo-state method of Burke and Webb (1970), the second-order potential approach of Sullivan et al. (1972), and the polarized orbital distorted-wave model of McDowell et al. (1973). The results of approximation B have also been displayed in Figures 4a and 4b along with those of the Born approximation, and of the impact-parameter treatment. The 2p experimental data of Long et al. (1968), normalized to the present value of $0.453\ \pi a_o^2$ at 200 eV (rather than to the corresponding Born result of $0.485\ \pi a_o^2$, which is 7% higher), and the values of $\sigma_{1s-2s} + 0.23\ \sigma_{1s-3p}$ measured by Kauppila et al. (1970) are also shown in Figures 4a and 4b, respectively.

The agreement between the present treatment, the pseudo-state values and experimental data is very good for the 2p excitation. The results of approximation B are indistinguishable from the full treatment for energies above 50 eV. The difference between the second-order potential method and the impact-parameter calculations is a direct measure

Table 2. Elastic and Inelastic Cross Sections (πa_o^2) From the Full Eikonal Approximation for the Processes

$e + H(1s) \rightarrow e + H(n\ell)$, $n\ell = 1s, 2s, 2p_o, 2p_{\pm 1}$.

E_i (eV) \ $n\ell$	1s	2s	$2p_o$	$2p_{\pm 1}$	2p
13.6	1.290	0.120	0.345	0.115	0.460
20.0	0.841	0.145	0.398	0.322	0.720
30.0	0.615	0.124	0.387	0.449	0.836
50.0	0.365	0.090	0.350	0.515	0.865
100.0	0.224	0.052	0.190	0.439	0.629
200.0	0.129	0.028	0.118	0.335	0.453

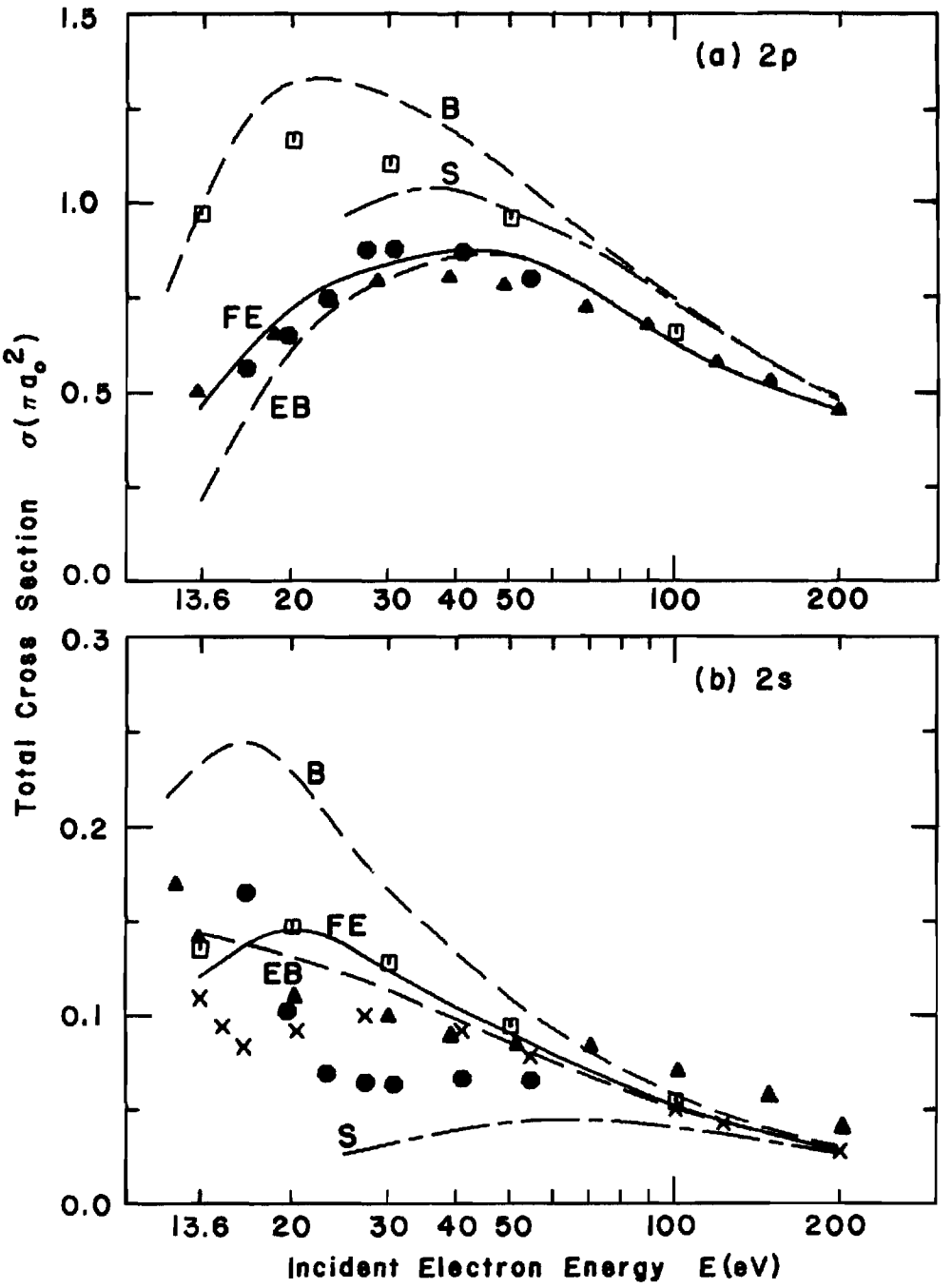

Figure 4. Total Cross Sections for the 2p and 2s Excitations of H(1s) by Electrons. (The curves shown are: FE, full eikonal treatment; EB, approximation B; ●, pseudo-state method; S, second-order potential method; ▣, impact-parameter method; B, Born approximation; ×, polarized-orbital method; ▲, experiment.)

of the effect of the second-order coupling introduced by Bransden and Coleman (1972) which takes account of the long-range polarization interaction in the incident channel. The present full eikonal treatment is a considerable improvement over both the Born and impact-parameter approximations.

In the 2s-channel there is a much wider variation in the theoretical cross sections, especially at impact energies less than 50 eV. Unfortunately, the measured values of Kauppila et al. do not resolve the matter, because these measurements include the cascade contribution, $0.23\ \sigma_{1s-3p}$, which has not been calculated. Direct comparison between the full eikonal treatment and experiment will be possible only when the n=3 channels are included in the summation (2-63). It should be noted that the inclusion of the local wave vector $\kappa_n(\vec{R})$ rather than its asymptotic value k_n (approximation B) introduces a maximum in the 2s cross section. The close agreement of the present treatment with the polarized wave model of McDowell et al. for energies greater than 40 eV is probably fortuitous, since the latter includes exchange and polarization effects. The closeness of the impact-parameter results to the present full treatment is felt to be largely due to a cancellation of errors, as previously mentioned.

Differential Cross Sections

An examination of the differential cross sections permits further insight into the validity of the various theoretical treatments. It will be seen that the differential cross section provides a more sensitive comparison between theory and experiment.

Elastic Scattering. Results of the present theory for elastic scattering at 50 eV and 100 eV are shown in Figure 5 along with the measurement of Teubner et al. (1973), the calculations of Winters et al. (1973), and the Glauber results of Franco and of Mathur (1974).

Although the experimental results are subject to a 35% error, a comparison between the full eikonal treatment and the calculations of Winters et al. clearly demonstrates the necessity of the inclusion of polarization and electron-exchange, which are important in small angle and large angle scattering, respectively, and which are included in the treatment of Winters et al. but neglected in the present treatment.

Inelastic Scattering. Figures 6a and 6b display the $2p_0$, $2p_{\pm1}$, and total 2p differential cross sections at 50 eV and 100 eV, respectively. The distorted-wave calculations of Chen et al. (1972) at 50 eV and 100 eV along with the Glauber calculations of Tai et al. (1970) at 100 eV are also shown in the figures. A comparison between the present treatment and that of Chen et al. shows the effect of the 2s-2p coupling, which has been neglected by Chen et al., is to decrease the 2p scattering at small angles.

Figures 7a and 7b display the corresponding 2s differential cross sections at 50 eV and 100 eV, respectively. Two-state calculations have also been carried out for the 2s channel and the results agree closely with the distorted-wave Born calculation of Chen et al. who found that electron-exchange, the importance of which increases with angle, is very small in the 2s channel. Figures 7a and 7b show that the more important effect arises from the coupling of the 2s channel with the 2p channel, particularly for small momentum transfers. Further, the Glauber approx-

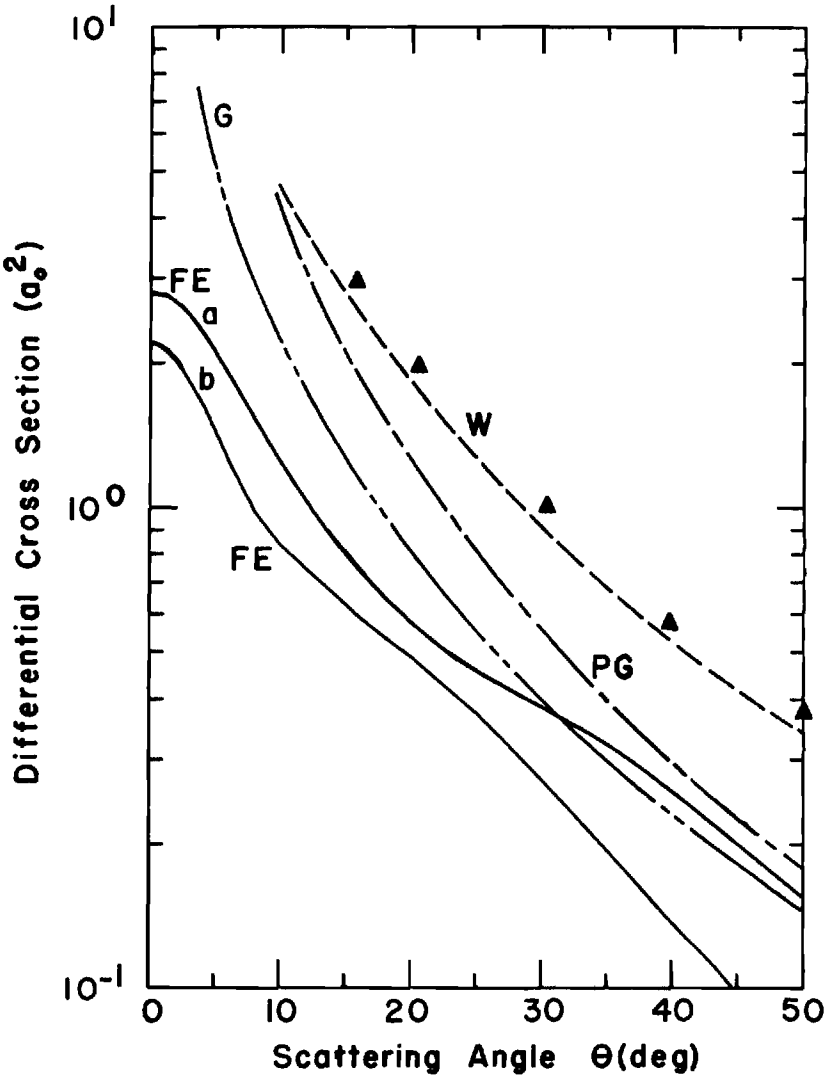

Figure 5. Differential Cross Sections for Elastic Scattering of Electrons by H(1s) at 50 eV. (——present four-state treatment at (a) 50 eV, (b) 100 eV;—-- Glauber approximation (Franco 1968);—·—·—Polarized Glauber approximation (Mathur 1974);— — — second-order potential theory with exchange (Winters et al. 1973); ▲ Experimental results of Teubner et al. (1973).)

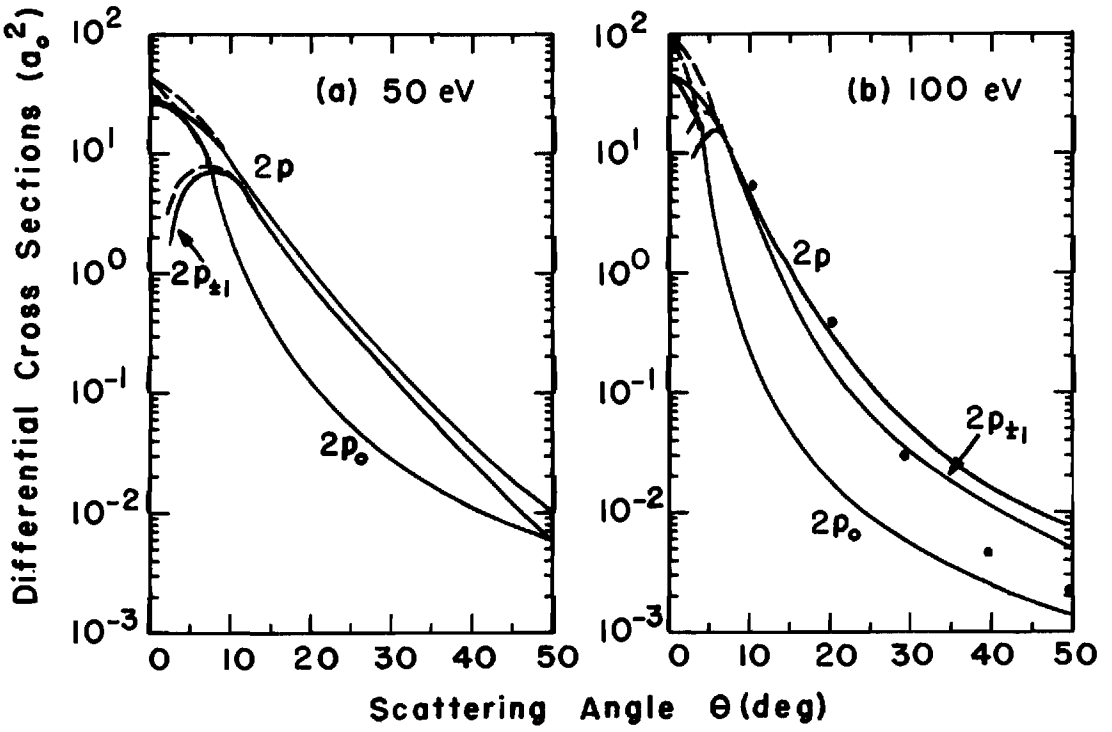

Figure 6. Differential Cross Sections for the $2p_o$, $2p_{\pm1}$, and 2p Excitations of H(1s) by Electron Impact at (a) 50 eV and (b) 100 eV. (The solid lines represent the present four-state treatment; the dashed curves represent the distorted-wave Born treatment of Chen et al. (1972); and • is the Glauber calculation of Tai et al. (1970).)

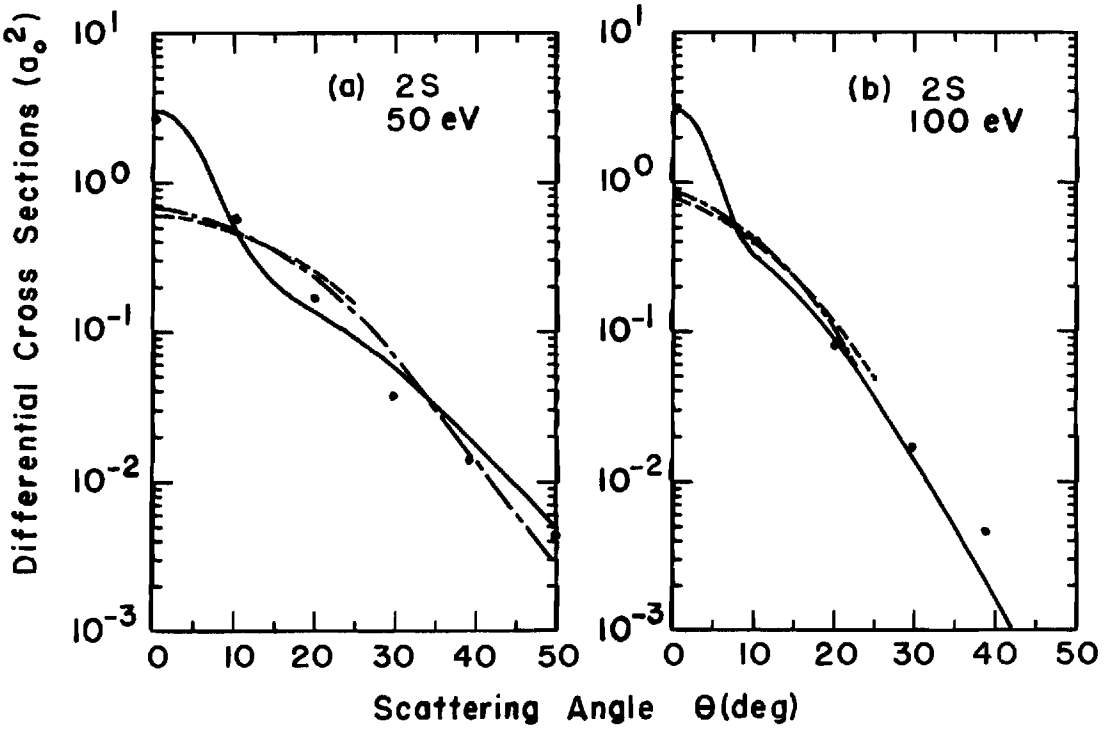

Figure 7. Differential Cross Sections for the 2s Excitation of H(1s) by Electron Impact at (a) 50 eV and (b) 100 eV. (The solid curves represent the present four-state treatment; the dashed curve is the distorted-wave Born calculation of Chen et al. (1972); the dash-dotted curve is the present two-state calculation; and • is the Glauber calculation of Tai et al. (1970).)

imation is in good agreement with the four-channel calculations except at large momentum transfers.

Electron-Helium Scattering

In an effort to further probe the reliability of the present method, the reaction (4-2) is now considered. The use of helium as a target atom, however, introduces the problem of the use of nonexact wave functions. This problem and its effect on the interaction potentials and the cross sections are subsequently discussed.

Wave Functions

In the case of electron-hydrogen collisions the exact wave functions of the target are known, and hence, the interaction potentials $V_{ij}(\vec{R})$ may be determined exactly. However, in the case of electron-helium collisions, the target atom wave functions are not exactly known. It is, therefore, of considerable interest to determine the effect of the use of different helium atom wave functions both on the resulting matrix elements and ultimately on the computed cross sections. In an effort to assess the sensitivity of the theory to the choice of helium-atom wave functions, two sets of functions have been used.

The first set is that chosen by Flannery (1970a), and subsequently used by Berrington et al. (1973) for electron-helium collisions. Following Flannery, the ground state wave function for helium is taken to be the Hartree-Fock function of Byron and Joachain (1966)

$$\Psi_{1^1S}(\vec{r}_1,\vec{r}_2) = \frac{1.6966}{\pi}\left[\exp(-1.4\ r_1) + 0.799\ \exp(-2.61\ r_2)\right] \times \left[\exp(-1.4\ r_2) + 0.799\ \exp(-2.61\ r_1)\right]$$

The function

$$\Psi_{2^1P}(\vec{r}_1,\vec{r}_2) = \frac{0.37831}{\sqrt{\pi}} \{r_1 \exp[-(0.485\ r_1 + 2r_2)]\ Y_{1m}(\hat{r}_1) + r_2 \exp[-(0.485\ r_2 + 2r_1)]\ Y_{1m}(\hat{r}_2)\}$$

of Goldberg and Clogston (1939) is taken for the 2^1P states. And for the 2^1S state the unrestricted Hartree-Fock function of Cohen and McEachran (1967) has been fit by Flannery to the simple analytical form

$$\Psi_{2^1S}(\vec{r}_1,\vec{r}_2) = \frac{N}{\pi\sqrt{1+\Delta^2}} \{\exp(-2r_1)[\exp(-\lambda r_1) - cr_1 \exp(-\mu r_1)] + \exp(-2r_1)[\exp(-\lambda r_2) - cr_2 \exp(-\mu r_2)]\}$$

with the following parameters: $\lambda = 1.1946$, $\mu = 0.4733$, $N = 0.70640$, $\Delta = 0.007322$, and $c = 0.26832$, such that the 2^1S function is orthogonal to the ground state function.

The second set of wave functions has been taken to be the analytical Hartree-Fock frozen-core wave functions of Crothers and McEachran (1970) and of McEachran and Cohen (1969). These wave functions may be expressed as

$$\Psi_{n\ell m}(\vec{r}_1,\vec{r}_2) = N_{n\ell}[\phi_o(r_1)\ \phi_{n\ell m}(\vec{r}_2) + \phi_o(r_2)\ \phi_{n\ell m}(\vec{r}_1)] \qquad (4\text{-}3)$$

where the ground-state electron is described by

$$\phi_o(r) = 2^{5/2}\, e^{-2r}\, Y_{oo}(\hat{r})$$

and the active electron has the wave function

$$\phi_{n\ell m}(\vec{r}) = \sum_{j=2\ell+1}^{J} a_j^{(n,\ell)}\, (2r)^{\ell}\, e^{-\beta r}\, L_j^{2\ell+1}(2\beta r)\, Y_{\ell m}(\hat{r})$$

where the coefficients $a_j^{(n,\ell)}$ $(2\ell+1 \leq j \leq J)$ have been given by Crothers and McEachran (1970) for the ^1S states and by McEachran and Cohen (1969) for the 2^1P state; the electron coordinate $\vec{r}$ is in atomic units; the exponential factor $\beta=2/n$; and the associated Laguerre polynomials are defined by the expression

$$L_j^{2\ell+1}(2\beta r) = \sum_{k=0}^{j-2\ell-1} \frac{(-1)^{k+1}\, (j!)^2\, (2\beta)^k}{k!\,(j-k-2\ell-1)!\,(k+2\ell+1)!}\, r^k$$

For the purposes of the calculation of the interaction potentials, it is more convenient to reexpress the $\phi_{n\ell m}(\vec{r})$ as

$$\begin{aligned} \phi_{n\ell m}(\vec{r}) &= R_{n\ell}(r)\, Y_{\ell m}(\hat{r}) \\ &= \sum_{N=\ell+1}^{J-\ell} B_N^{(n,\ell)}\, e^{-\beta r}\, r^{N-1}\, Y_{\ell m}(\hat{r}) \end{aligned} \tag{4-4}$$

where

$$B_N^{(n,\ell)} = \sum_{j=N+\ell}^{J} \frac{a_j^{(n,\ell)}\ 2^{\ell}\ (-1)^{N-\ell}\ (j!)^2\ (2\ )^{N-\ell-1}}{(N-\ell-1)!(j-N-\ell)!(N+\ell)!}$$

The coefficients $B_N^{(n,\ell)}$ and the energies of the states are given in Table 3 for the 1^1S, 2^1S, and the 2^1P states.

The normalization $N_{n\ell}$ in (4-3) is given by

$$N_{n\ell} = \{2[H(n\ell) + G^2(n\ell)]\}^{-1/2}$$

where

$$H(n\ell) = \langle \phi_{n\ell m} | \phi_{n\ell m} \rangle$$

$$= \sum_{N=\ell+1}^{J-\ell} \sum_{N'=\ell+1}^{J-\ell} B_N\ B_{N'} \int_0^{\infty} e^{-2\beta r}\ r^{N+N'}\ dr$$

$$= \sum_{N=\ell+1}^{J-\ell} \sum_{N'=\ell+1}^{J-\ell} B_N\ B_{N'} \frac{(N+N')!}{(2\beta)^{N+N'+1}}$$

and

Table 3. The Coefficients $B_N^{(n,\ell)}$, β, ε_n of Equation (4-4) for the 1s, 2s, and 2p Electrons of Helium.

$N \backslash B_N$	1s	2s	2p
1	-1.838533(0)*	-5.567741(-1)	0.000000
2	2.933174(-2)	5.273189(-1)	-1.276768(-1)
3	-1.233197(0)	-4.105320(-1)	-5.894823(-2)
4	-4.714342(-3)	3.144444(-1)	-1.516479(-2)
5	1.076863(-1)	-9.015757(-2)	-1.379295(-2)
6	-7.992620(-2)	1.726613(-2)	4.985414(-3)
7	2.039978(-2)	-1.585770(-3)	-1.207334(-3)
8	-2.624857(-3)	7.300876(-5)	1.166106(-4)
9	1.243260(-4)	-3.067930(-7)	-5.231240(-6)
β	2.0	1.0	1.0
$-\varepsilon_n$(calc)	0.87251	0.14344	0.12245
$-\varepsilon_n$(expt)	0.90357	0.14595	0.12384

*The number in parentheses indicates the power of ten by which the number is to be multiplied.

$$G(n\ell) = \langle \phi_o | \phi_{n\ell m} \rangle$$

$$= 2^{5/2}\, \delta_{\ell 0} \sum_{N=1}^{J} B_N \int_0^{\infty} e^{-(\beta+2)}\, r^{N+1}\, dr$$

$$= 2^{5/2}\, \delta_{\ell 0} \sum_{N=1}^{J} B_N \frac{(N+1)!}{(\beta+2)^{N+2}}$$

The coefficients $H(n\ell)$ and $G(n\ell)$ are presented in Table 4 along with the normalization factor $N_{n\ell}$. Another important quantity is the overlap between states with the same angular momentum quantum numbers. Table 5 presents the overlaps $\langle \Psi_{n\ell m} | \Psi_{n'\ell'm'} \rangle$ for the n + 1, 2 states.

Interaction Potentials

The matrix elements $V_{ij}(\vec{R})$ for the static interaction

$$V(\vec{R},\vec{r}_1,\vec{r}_2) = -\frac{2}{R} + \frac{1}{|\vec{R} - \vec{r}_1|} + \frac{1}{|\vec{R} - \vec{r}_1|}$$

may be determined analytically for both sets of wave functions described in the previous section.

By using the expression

$$\frac{1}{|\vec{R} + \vec{r}|} = \frac{1}{2\pi^2} \int \frac{\exp[i\vec{q}\cdot(\vec{R}+\vec{r})]}{q^2}\, d\vec{q}$$

Table 4. The Values of $H(n\ell)$, $G(n\ell)$, and the Normalization $N_{n\ell}$ of the Wave Functions $\Psi_{n\ell m}$.

n	ℓ	H(nℓ)
1	0	5.2079(-2)*
2	0	5.8774(1)
2	1	3.8117(2)
3	0	2.4459(3)
3	1	8.9201(3)
3	2	8.9954(7)
4	0	2.0856(3)
4	1	1.6150(5)
4	2	1.3401(9)

n	ℓ	G(nℓ)
1	0	-2.1112(-1)
2	0	-6.2716(-1)
3	0	1.9922(0)
4	0	1.1546(0)

n	ℓ	$N_{n\ell}$
1	0	2.2745(0)
2	0	9.1927(-2)
2	1	3.6218(-2)
3	0	1.4286(-2)
3	1	7.4869(-3)
3	2	7.4555(-5)
4	0	1.5479(-2)
4	1	1.7595(-3)
4	2	1.9316(-5)

*The number in parentheses indicates the power of ten by which the entry is to be multiplied.

Table 5. Values of the Overlaps $\langle \Psi_{n\ell m} | \Psi_{n'\ell'm'} \rangle$ for the Hartree-Fock Wave Functions.

n	ℓ	n'	ℓ'	$\langle \Psi_{n\ell m} \lvert \Psi_{n'\ell'm'} \rangle$
1	0	2	0	4.2686(-5)*
1	0	3	0	-6.5299(-6)
1	0	4	0	-8.9454(-5)
2	0	3	0	-1.8388(-3)
2	0	4	0	1.6679(-3)
3	0	4	0	4.8714(-4)
2	1	3	1	1.5357(-3)
2	1	4	1	-2.2109(-3)
3	1	4	1	1.7104(-2)
3	2	4	2	2.2958(-3)

and the integrals

$$\int r^{k+\ell} \exp(-\alpha r + i\vec{q}\cdot\vec{r})\, Y_{\ell m}(\hat{r})\, d\vec{r}$$

$$= 4\pi(2iq)^{\ell}\,(k+1)!\, Y_{\ell m}(\hat{q}) \sum_{p=1}^{p_{max}} \frac{(-1)^{p+1}\,(k+\ell+2-p)!}{(p-1)!\,(k+3-2p)!} \frac{(2\alpha)^{k+3-2p}}{(\alpha^2 + q^2)^{k+\ell+3-p}}$$

with $p_{max} = \frac{1}{2}(k+2)$ or $\frac{1}{2}(k+3)$ for k even or odd, respectively, (Flannery 1969) and

$$\int \frac{\sin(qR)}{q(\alpha^2 + q^2)^{n+1}}\, dq = \frac{\pi}{2\alpha^{2n+2}} \{1 - \frac{\exp(-\alpha R)}{2^n\, n!} F_n(\alpha R)\}$$

(Gradshteyn and Ryzhik 1965) with

$$F_n(z) = (z + 2n)F_{n-1}(z) - z \frac{dF_{n-1}(z)}{dZ}, \quad F_o(z) = 1$$

Flannery has evaluated the $V_{ij}(\vec{R})$ for the first set of wave functions.

By using the second set of wave functions (4-3) the matrix elements of the interaction may be expressed as

$$V_{n\ell m,n'\ell'm'}(\vec{R}) = -\frac{2}{R}\,\delta_{nn'}\,\delta_{\ell\ell'}\,\delta_{mm'}$$

$$+\{\langle\phi_o|\frac{1}{|\vec{R}-\vec{r}|}|\phi_o\rangle\langle n\ell m|n'\ell'm'\rangle + \langle n\ell m|\frac{1}{|\vec{R}-\vec{r}|}|n'\ell'm'\rangle \qquad (4\text{-}5)$$

$$+ \langle\phi_o|\frac{1}{|\vec{R}-\vec{r}|}|n'\ell'm'\rangle\langle n\ell m|\phi_o\rangle + \langle n\ell m|\frac{1}{|\vec{R}-\vec{r}|}|\phi_o\rangle\langle\phi_o|n'\ell'm'\rangle\}$$

where

$$\langle \phi_o | \frac{1}{|\vec{R}-\vec{r}|} | \phi_o \rangle = \frac{1}{R} - e^{-4R}\left(\frac{1}{R} + 2\right) \tag{4-6}$$

And the other integrals may be evaluated analytically by using the expression

$$\frac{1}{|\vec{R} - \vec{r}|} = \sum_{L=0}^{\infty} \sum_{M=-L}^{L} \frac{4\pi}{2L+1} \frac{r_<^L}{r_>^{L+1}} Y_{LM}(\hat{R}) Y_{LM}^*(\hat{r})$$

where $r_<$ and $r_>$ are the lesser and greater, respectively, of R and r; and the integrals

$$\int_0^R r^n e^{-\alpha r} dr = \frac{n!}{\alpha^{n+1}} - e^{-\alpha R} \sum_{k=0}^{n} \frac{n!}{k!} \frac{R^k}{\alpha^{n-k+1}} \tag{4-7}$$

$$\int_R^{\infty} r^n e^{-\alpha r} dr = e^{-\alpha R} \sum_{k=0}^{n} \frac{n!}{k!} \frac{R^k}{\alpha^{n-k+1}} \tag{4-8}$$

and

$$D(\ell\ell'L;mm'M) = \int Y_{\ell m}(\hat{r})\ Y_{\ell' m'}(\hat{r})\ Y_{LM}^*(\hat{r})\ d\hat{r}$$

$$= \left[\frac{(2\ell+1)(2\ell'+1)}{4\pi(2L+1)}\right]^{1/2} C(\ell\ell'L,000)\ C(\ell\ell'L,mm'M)$$

where the C's are Clebsch-Gordan coefficients.

Each integral in the expansion of (4-5) of the matrix element will have a form similar to (4-6), i.e. designating $\langle n\ell m|\,|\vec{R} - \vec{r}|^{-1}|n'\ell'm'\rangle$ by $I(n\ell m,n'\ell'm')$, the form of the integrals will be

$$I(n\ell m,n'\ell'm') = -\frac{a}{R^M} + e^{-\alpha R}\left(\frac{a}{R^M} + \frac{b}{R^{M-1}} + \cdots + cR^N\right) \qquad (4\text{-}9)$$

times an appropriate angular factor. The exponent M in the outside factor is dependent on ℓ and ℓ'; namely, $\ell = \ell' = 0$, $M = -1$ (this term, however, always cancels either with the nuclear term in (4-5) or with other outside factors); $\ell = 0$, $\ell' = 1$, $M = -2$; $\ell = \ell' = 1$, $M = -1, -3$ (where the two terms come from the angular momentum expansion of $|\vec{R}-\vec{r}|^{-1}$, and again the R^{-1} term is cancelled out). The exponential factor β is given by $\beta = 2/n + 2/n'$. The exponent of the largest power in (4-9) is determined by the number of terms in the expansion (4-4) of the wave functions . The coefficients in (4-10) are presented in Appendix 1 for the matrix elements involving the n = 1 and 2 states of helium.

A brief comparison of the matrix elements computed from the two sets of wave functions is presented in Tables 6 and 7 for the diagonal and non-diagonal matrix elements, respectively. In general, the agreement is within a few percent. However, the worst agreement is seen to be between elements involving the 2^1S state, and as will be shown the cross sections computed from these sets of wave functions shows little change for the 2^1P states, but do show significant change for the 2^1S state.

Table 6. A Comparison of the Diagonal Matrix Elements Calculated from the First V(1) and Second V(2) Set of Wave Functions for Selected Values of R.

R(au)	$V_{1^1S}(1)$	$V_{1^1S}(2)$	$V_{2^1S}(1)$	$V_{2^1S}(2)$	$V_{2^1P}(1)$	$V_{2^1P}(2)$
0.01	-1.966(2)*	-1.967(2)	-1.977(2)	-1.977(2)	-1.978(2)	-1.978(2)
0.02	-9.663(1)	-9.668(1)	-9.776(1)	-9.773(1)	-9.777(1)	-9.776(1)
0.04	-4.664(1)	-4.668(1)	-4.777(1)	-4.773(1)	-4.777(1)	-4.777(1)
0.06	-2.999(1)	-3.003(1)	-3.111(1)	-3.108(1)	-3.111(1)	-3.111(1)
0.08	-2.167(1)	-2.171(1)	-2.279(1)	-2.276(1)	-2.279(1)	-2.279(1)
0.10	-1.669(1)	-1.673(1)	-1.780(1)	-1.777(1)	-1.780(1)	-1.780(1)
0.20	-6.836(0)	-6.874(0)	-7.903(0)	-7.876(0)	-7.903(0)	-7.904(0)
0.40	-2.212(0)	-2.244(0)	-3.166(0)	-3.149(0)	-3.167(0)	-3.168(0)
0.60	-9.286(-1)	-9.518(-1)	-1.756(0)	-1.750(0)	-1.760(0)	-1.761(0)
0.80	-4.319(-1)	-4.477(-1)	-1.138(0)	-1.141(0)	-1.145(0)	-1.146(0)
1.00	-2.123(-1)	-2.226(-1)	-8.103(-1)	-8.203(-1)	-8.195(-1)	-8.204(-1)
2.00	-8.765(-3)	-9.667(-3)	-2.587(-1)	-2.824(-1)	-2.826(-1)	-2.830(-1)
3.00	-4.560(-4)	-5.295(-4)	-1.042(-1)	-1.242(-1)	-1.364(-1)	-1.364(-1)
4.00	-2.552(-5)	-3.170(-5)	-4.114(-2)	-5.557(-2)	-7.426(-2)	-7.411(-2)
5.00	-1.469(-6)	-1.985(-6)	-1.404(-2)	-2.442(-2)	-4.365(-2)	-4.347(-2)
6.00	-8.564(-8)	-1.225(-7)	-2.749(-3)	-1.048(-2)	-2.722(-2)	-2.706(-2)
7.00	-5.026(-9)	-6.734(-9)	1.526(-3)	-4.398(-3)	-1.783(-2)	-1.770(-2)
8.00	-2.961(-10)	-2.873(-10)	2.793(-3)	-1.813(-3)	-1.220(-2)	-1.210(-2)
9.00	-1.749(-11)	-7.538(-12)	2.866(-3)	-7.333(-4)	-8.659(-3)	-8.581(-3)
10.00	-1.035(-12)	-1.198(-13)	2.531(-3)	-2.904(-4)	-6.346(-3)	-6.286(-3)
20.00	-5.664(-25)	-3.137(-24)	3.984(-4)	-4.180(-9)	-7.971(-4)	-7.890(-4)
30.00	-3.170(-37)	-1.851(-38)	1.181(-4)	-2.806(-15)	-2.362(-4)	-2.338(-4)
40.00	0.000	0.000	4.982(-5)	-3.461(-22)	-9.964(-5)	-9.862(-5)
50.00	0.000	0.000	2.551(-5)	-1.628(-29)	-5.102(-5)	-5.050(-5)

*The number in the parentheses indicates the power of ten by which the entry is to be multiplied.

Figure 7. A Comparison of the Non-diagonal Matrix Elements Calculated From the First V(1) and Second V(2) Set of Wave Functions for Selected Values of R.

	$1\,^1S - 2\,^1S$		$1\,^1S - 2\,^1P$		$2\,^1S - 2\,^1P$	
R(au)	V(1)	V(2)	V(1)	V(2)	V(1)	V(2)
0.01	2.747(-1)*	2.530(-1)	1.493(-3)	-1.362(-3)	-3.995(-4)	1.208(-4)
0.02	2.745(-1)	2.571(-1)	2.876(-3)	-2.722(-3)	-3.511(-4)	2.418(-4)
0.04	2.737(-1)	2.584(-1)	5.721(-3)	-5.435(-3)	-5.002(-4)	4.854(-4)
0.06	2.723(-1)	2.578(-1)	8.552(-3)	-8.131(-3)	-7.498(-4)	7.323(-4)
0.08	2.705(-1)	2.565(-1)	1.136(-2)	-1.080(-2)	-1.004(-3)	9.840(-4)
0.10	2.683(-1)	2.546(-1)	1.414(-2)	-1.344(-2)	-1.269(-3)	1.242(-3)
0.20	2.528(-1)	2.405(-1)	2.733(-2)	-2.601(-2)	-2.701(-3)	2.654(-3)
0.40	2.101(-1)	2.019(-1)	4.906(-2)	-4.685(-2)	-6.405(-3)	6.312(-3)
0.60	1.658(-1)	1.620(-1)	6.390(-2)	-6.137(-2)	-1.136(-2)	1.118(-2)
0.80	1.269(-1)	1.265(-1)	7.259(-2)	-7.021(-2)	-1.739(-2)	1.708(-2)
1.00	9.520(-2)	9.703(-2)	7.643(-2)	-7.451(-2)	-2.414(-2)	2.372(-2)
2.00	1.970(-2)	2.193(-2)	6.186(-2)	-6.248(-2)	-5.757(-2)	5.768(-2)
3.00	3.697(-3)	4.305(-3)	3.940(-2)	-4.055(-2)	-7.602(-2)	7.757(-2)
4.00	6.645(-4)	7.917(-4)	2.482(-2)	-2.577(-2)	-7.869(-2)	8.072(-2)
5.00	1.164(-4)	1.389(-4)	1.642(-2)	-1.711(-2)	-7.226(-2)	7.384(-2)
6.00	2.003(-5)	2.285(-5)	1.151(-2)	-1.200(-2)	-6.235(-2)	6.319(-2)
7.00	3.400(-6)	3.368(-6)	8.472(-3)	-8.840(-3)	-5.218(-2)	5.238(-2)
8.00	5.711(-7)	4.068(-7)	6.490(-3)	-6.772(-3)	-4.315(-2)	4.293(-2)
9.00	9.509(-8)	2.966(-8)	5.128(-3)	-5.351(-3)	-3.565(-2)	3.521(-2)
10.00	1.572(-8)	-2.614(-9)	4.154(-3)	-4.334(-3)	-2.961(-2)	2.910(-2)
20.00	1.880(-16)	-9.450(-17)	1.039(-3)	-1.084(-3)	-7.623(-3)	7.424(-3)
30.00	1.804(-24)	-6.117(-27)	4.616(-4)	-4.816(-4)	-3.388(-3)	3.300(-3)
40.00	1.565(-32)	-5.304(-38)	2.596(-4)	-2.709(-4)	-1.906(-3)	1.856(-3)
50.00	0.000	0.000	1.662(-4)	-1.734(-4)	-1.220(-3)	1.188(-3)

*The number in parentheses indicates the power of ten by which the entry is to be multiplied.

Results and Discussion

Figures 8a and 8b display the differential cross sections for the 2^1P channel at 50 eV and 100 eV, respectively. The present results show little variation with the change of wave functions. The differential cross sections are also compared with the recent results of the second-order potential theory (Berrington et al. 1973), in which the first set of wave functions were employed. Even though the long-range polarization is expected to be most effective for small angle scattering, the resulting increase in the cross sections of Berrington et al. is relatively small at small angles and vanishes with increasing angle and energy. Figures 8a and 8b also show that the present treatment causes a further reduction in the cross section at large angles.

The differential cross sections for the 2^1S channel are displayed in Figures 9a and 9b for 50 eV and 100 eV, respectively. The use of different wave functions causes a more significant change in the 2^1S channel, and, in fact, there is a difference of about 30% at intermediate angles for 50 eV incident energy. This difference decreases with increasing energy. The fact that the change in wave functions causes such a large change in the 2^1S channel and a relatively small change in the 2^1P channel seems to result from two causes. First, the 2^1S cross sections are, in general, more sensitive to any change in the calculation. Second, the major disagreement between the matrix elements for the two sets of wave functions occurs between the elements involving the 2^1S state. The second-order potential calculations of Berrington et al. are also shown in the figures. In the 2^1S channel there is general agreement between the present treatment and that of Berrington et al. at

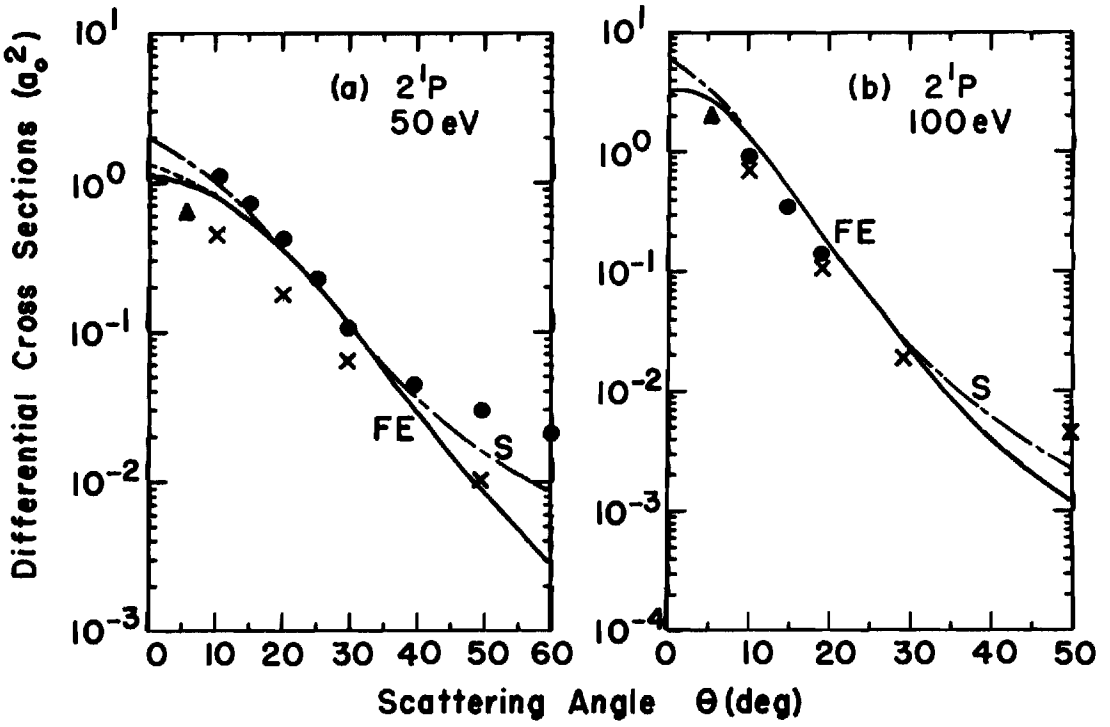

Figure 8. Differential Cross Sections for the $2\ ^1P$ Excitation of Helium at (a) 50 eV and (b) 100 eV. (The solid line FE is the present four-state calculation with the first set of wave functions; the dashed curve is the present treatment with the second set of wave functions; the dash-dotted curve is the second-order potential method; × is the experiment of Crooks and Rudd; ▲ is the experiment of Chamberlain; ● is the experiment of Truhlar et al. at 55.5 eV and of Vriens et al. at 100 eV.)

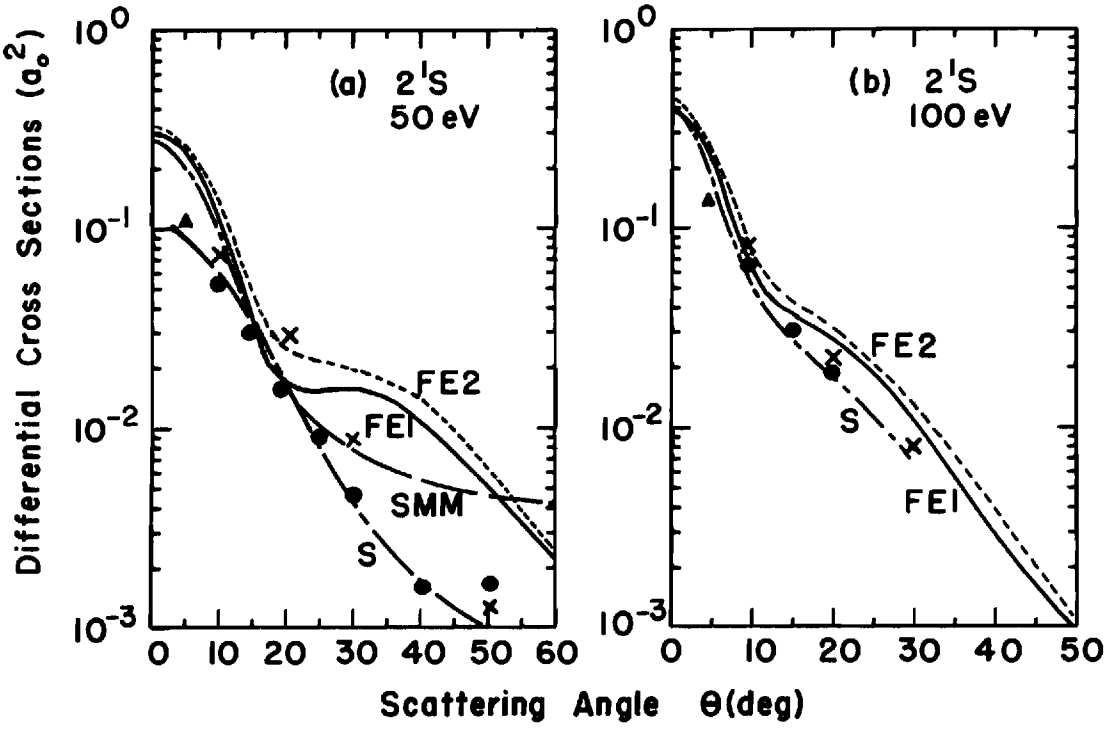

Figure 9. Differential Cross Sections for the $2\ ^1S$ Excitation of Helium by Electron Impact at (a) 50 eV and (b) 100 eV. (FE1 and FE2 are the present treatment with the first and second wave function sets, respectively; the dash-dotted curve is the second-order potential method; × is the experiment of Crooks and Rudd; the long dashed curve is the experiment of Simpson et al.; ▲ is the experiment of Chamberlain et al.; and ● is the experiment of Rice et al. at 55.5 eV, and of Vriens et al. at 100 eV.)

small angles; however, the intermediate angles show considerable disagreement.

The 2^1S and 2^1P experimental data of various groups has also been shown in the figures for comparison. The general agreement with theory is satisfactory only for small and intermediate angle scattering, although there is significant discrepancy between the experimental observations themselves, especially in the 2^1S channel.

The percentage polarization P of the radiation emitted from the 2^1P level is obtained from

$$P = \frac{100(\sigma_o - \sigma_1)}{\sigma_o + \sigma_1}$$

where σ_m is the cross section for the excitation of the m^{th} substate of the 2^1P level (Percival and Seaton 1958), and is given in Table 8 along with the 2^1P cross sections. It should be noted that experimental measurement of the polarization fraction is very difficult.

The 2^1P and 2^1S total cross sections are given in Tables 8 and 9, and are displayed in Figures 10a and 10b, respectively. The figures also present the theoretical calculations of Berrington et al. (1973), and the Born approximation; and the experimental results of Donaldson et al. (1972), Jobe and St. John (1967), Moustafa Moussa et al. (1969), and of van Eck and de Jongh (1970) for the 2^1P excitation; and the data of Rice et al. (1972), Lassetre et al. (1970), Miller et al. (1968), Vriens et al. (1968), and of Simpson et al. (1966) for the 2^1S excitation.

Table 8. Inelastic Cross Sections (πa_o^2) for the Process

$e + He(1\ ^1S) \quad e + He(2\ ^1P)$

	FE[a]				2 ^1P		
E_i(eV)	2 ^1P_o	2 $^1P_{\pm1}$	2 ^1P	P[b]	S[c]	IP[d]	Born[e]
50	0.0732	0.0600	0.1332	41.9	0.215	0.232	0.1694
80	0.0637	0.0750	0.1387	25.9	--	--	0.1596
100	0.0547	0.0759	0.1306	18.1	0.155	0.161	0.1485
200	0.0347	0.0671	0.1018	1.7	0.105	0.107	0.1069
300	0.0237	0.0577	0.0814	-9.8	0.0822	0.083	0.0841
400	0.0173	0.0500	0.0673	-18.2	0.0681	0.069	0.0700
500	0.0120	0.0466	0.0586	-32.0	0.0581	0.058	0.0602

a: Present four-channel treatment (second set of wave functions)
b: Percentage polarization of emitted radiation
c: Second-order potential method (Berrington et al. 1973)
d: Impact-parameter approximation (Berrington et al. 1973)
e: Born approximation (Bell et al. 1969)

Table 9. Inelastic Cross Sections (πa_o^2) for the Process

$$e + He(1\ ^1S) \rightarrow e + He(2\ ^1S)$$

E_i (eV)	FE[a]	S[b]	IP[c]	Born[d]
50	0.0215	0.0225	0.031	0.0390
80	0.0175	--	--	0.0270
100	0.0153	0.0154	0.0182	0.0222
200	0.0096	0.0093	0.0102	0.0118
300	0.0070	0.0066	0.0071	0.0080
400	0.0054	0.0052	0.0054	0.0060
500	0.0045	0.0042	0.0044	0.0048

a: Present four-channel treatment (second set of wave functions)
b: Second-order potential method (Berrington et al. 1973)
c: Impact-parameter method (Berrington et al. 1973)
d: Born approximation (Bell et al. 1969)

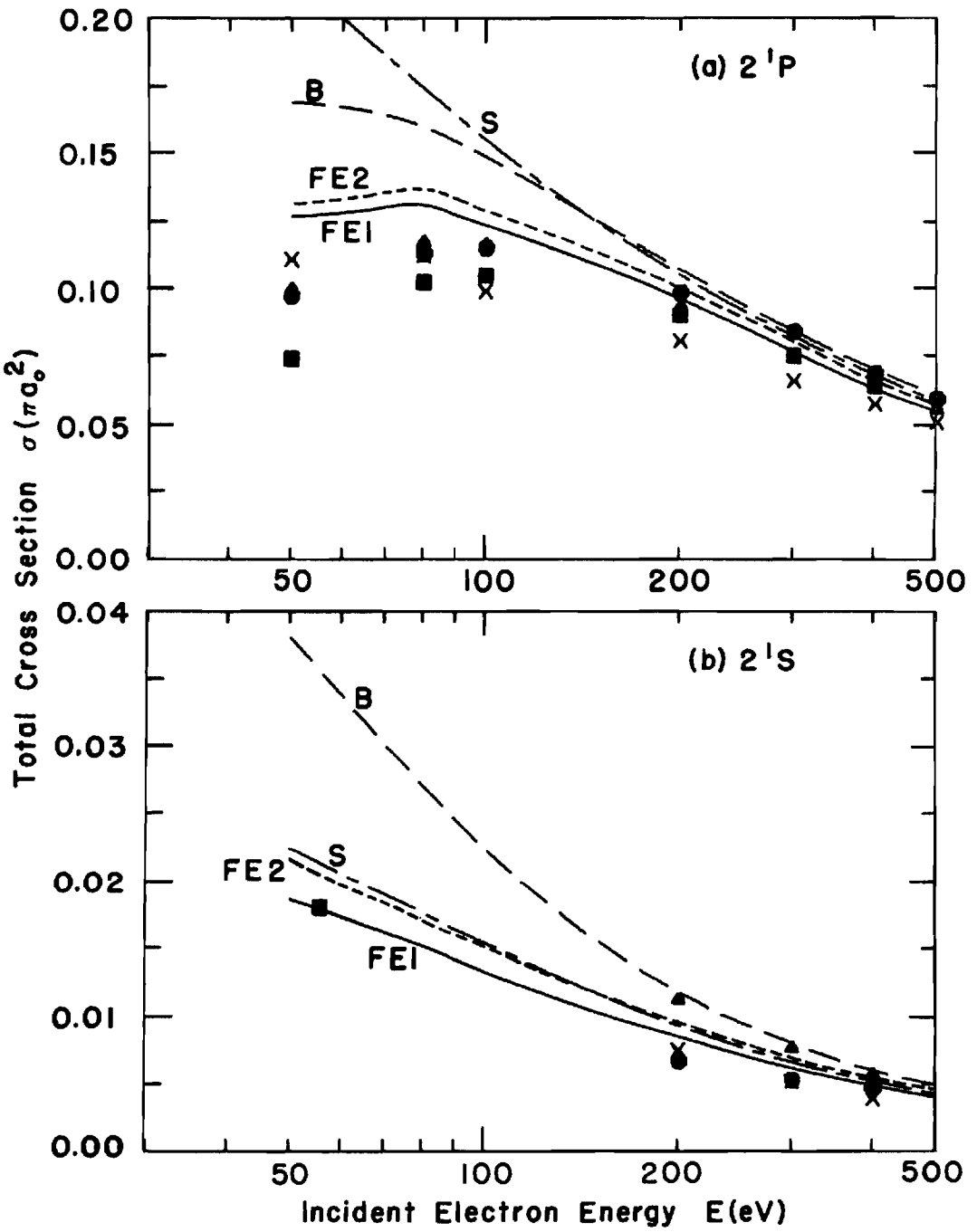

Figure 10. Total Cross Sections for the 2 ^{1}P and 2 ^{1}S Excitation of Helium by Electron Impact. (FE1 and FE2 are the present theory for the first and second set of wave functions; B is the Born approximation; S is the second-order potential method. Experiment (2 ^{1}P): ▲ Donaldson; ✕ Moustafa-Moussa; ● van Eck; ■ Jobe. Experiment (2 ^{1}S): ▲ Lassettre; ✕ Miller; ● Vriens.)

As exhibited in the figures, the present theory represents a considerable improvement over the Born and second-order potential approximations for the total cross sections. Further, the present treatment has a peak in the 2^1P cross section at about 80 eV, which is consistent with the experimental data. The total cross sections are seen to be not overly sensitive to the change in wave functions, with the 2^1S channel showing the greatest difference.

CHAPTER V

ATOM-ATOM SCATTERING

The present theory has been applied to both hydrogen-hydrogen collisions for excitation of the target atom to the 1s, 2s, and 2p states, and to hydrogen-helium collisions for the excitation of the target hydrogen atom to the 1s, 2s, and 2p states. The atom-atom calculations have all been done in the context of the approximation C(0) of Chapter III, although selected calculations have been carried out in the full treatment. The full treatment shows no differecne from the C(0) treatment for the reactions and energies considered.

The results for hydrogen-hydrogen collisions have recently been published in the Physical Review A, Volume 9, pages 1947 to 1953, May 1974. This article appears in Appendix III of this dissertation. The theory used for heavy-particle collisions has also been published in the Physical Review A, Volume 8, pages 2915 to 2921, December 1973; and, for completeness, it has been included in Appendix II of this dissertation.

The results for hydrogen-helium collisions have recently been published in the Journal of Physics B: Atom. Molec. Phys., Volume 7, pages 840 to 849, and a copy of this article appears in Appendix IV.

CHAPTER VI

ION-ATOM SCATTERING

The present theory, within the context of approximation C(0), has been applied to both helium-ion hydrogen scattering and to proton-helium scattering. The results for helium-ion excitation of hydrogen to the 1s, 2s, and 2p states have been accepted for publication by the Journal of Physics B: Atom. Molec. Phys., and the proofs appear in Appendix V. The results for the excitation of helium to the 2^1S and 2^1P states by protons have been accepted for publication in the Journal of Physics B: Atom. Molec. Phys., and the proofs appear in Appendix VI.

APPENDIX I

MATRIX ELEMENTS FOR e-He COLLISIONS

This appendix presents FORTRAN functions for the matrix elements used in the electron-helium scattering calculations. These matrix elements are based on the Hartree-Fock frozen-core wave functions of Crothers and McEachran (1970) and of McEachran and Cohen (1969).

```
      FUNCTION V1S(ZR,ZFI)
      DOUBLE PRECISION R,A,B
      R=ZR
      A=
     &+((  -.53884272 4E+00)*R**( -1)+(  -.1077685 5E+01)*R**(  0))
     &  *DEXP(-R*(    .40000000 E+01))
     &+((  -.53884272 4E+00)*R**( -1)+(  -.1450729 1E+01)*R**(  0)
     &+(  -.14921774 3E+01)*R**(  1)+(  -.1237271 3E+01)*R**(  2)
     &+(  -.46699724 0E+00)*R**(  3)+(  -.2109222 1E+00)*R**(  4)
     &+(  -.28497198 6E-01)*R**(  5)+(  -.5766102 9E-02)*R**(  6)
     &+(  -.87612083 3E-02)*R**(  7)+(   .3084636 0E-02)*R**(  8)
     &+(  -.57393368 4E-03)*R**(  9)+(  -.1647132 3E-03)*R**( 10)
     &+(   .12529055 6E-03)*R**( 11)+(  -.4061864 5E-04)*R**( 12)
     &+(   .78548185 0E-05)*R**( 13)+(  -.9411566 6E-06)*R**( 14)
     &+(   .65161843 3E-07)*R**( 15)+(  -.1932129 1E-08)*R**( 16))
     &  *DEXP(-R*(    .40000000 E+01))
      B=
     &+2.*((  -.46115727 6E+00)*R**( -1)+(  -.1072344 0E+01)*R**(  0)
     &+(  -.60012058 7E+00)*R**(  1)+(  -.4054381 1E+00)*R**(  2)
     &+(   .25636329 3E-02)*R**(  3)+(  -.6527038 3E-02)*R**(  4)
     &+(  -.10923710 4E-01)*R**(  5)+(   .3931482 7E-02)*R**(  6)
     &+(  -.70129044 7E-03)*R**(  7)+(   .4221410 7E-04)*R**(  8))
     &  *DEXP(-R*(    .40000000 E+01))
      V1S=A+B
      RETURN
      END
```

```
      FUNCTION V2S(ZR,ZFI)
      DOUBLE PRECISION R,A
      R=ZR
      A=
     $+((  -.993352138E+00)*R**( -1)+(  -.198670428E+01)*R**(  0)
     $  *DEXP(-R*(   .400000000E+01))
     $+((  -.993352138E+00)*R**( -1)+(  -.174110746E+01)*R**(  0)
     $+(  -.149551064E+01)*R**(  1)+(  -.936608681E+00)*R**(  2)
     $+(  -.340239008E+00)*R**(  3)+(  -.158390965E+00)*R**(  4)
     $+(  -.802107832E-02)*R**(  5)+(  -.180966856E-01)*R**(  6)
     $+(   .482785422E-02)*R**(  7)+(  -.220661065E-02)*R**(  8)
     $+(   .516779447E-03)*R**(  9)+(  -.102136287E-03)*R**( 10)
     $+(   .134900269E-04)*R**( 11)+(  -.131015904E-05)*R**( 12)
     $+(   .777336359E-07)*R**( 13)+(  -.280288363E-08)*R**( 14)
     $+(   .215986469E-10)*R**( 15)+(  -.470611135E-13)*R**( 16))
     $  *DEXP(-R*(   .200000000E+01))
     $+(.*((  -.664786185E-02)*R**( -1)+(   .117940502E-02)*R**(  0)
     $+(   .334535934E-01)*R**(  1)+(   .460964263E-02)*R**(  2)
     $+(   .104874021E-01)*R**(  3)+(  -.287848325E-02)*R**(  4)
     $+(   .812141344E-03)*R**(  5)+(  -.872421250E-04)*R**(  6)
     $+(   .515792156E-05)*R**(  7)+(  -.222348686E-07)*R**(  8))
     $  *DEXP(-R*(   .300000000E+01))
      V2S=V
      RETURN
      END
```

```
      FUNCTION V2PO(ZR,ZFI)
      DOUBLE PRECISION R,A,B,C
      PI=4.*ATAN(1.0)
      R=ZR
      FI=ZFI+PI/2.
      A=
     $+((  -.100000000E+01)*R**( -1)+(  -.200000000E+01)*R**(  0))
     $  *DEXP(-R*(    .400000000E+01))
      B=
     $+((  -.100000000E+01)*R**( -1)+(  -.175872453E+01)*R**(  0)
     $+(  -.151744907E+01)*R**(  1)+(  -.850782399E+00)*R**(  2)
     $+(  -.344966044E+00)*R**(  3)+(  -.107446494E+00)*R**(  4)
     $+(  -.266390375E-01)*R**(  5)+(  -.533917948E-02)*R**(  6)
     $+(  -.956443013E-03)*R**(  7)+(  -.144661132E-03)*R**(  8)
     $+(  -.184418117E-04)*R**(  9)+(  -.420213955E-05)*R**( 10)
     $+(   .875122376E-06)*R**( 11)+(  -.331187094E-06)*R**( 12)
     $+(   .520348288E-07)*R**( 13)+(  -.614589923E-08)*R**( 14)
     $+(   .377407662E-09)*R**( 15)+(  -.136829542E-10)*R**( 16))
     $  *DEXP(-R*(    .200000000E+01))
      C=
     $      .315594714E+02*R**( -3)
     $+((  -.315594714E+02)*R**( -3)+(  -.631189428E+02)*R**( -2)
     $+(  -.631189428E+02)*R**( -1)+(  -.420792952E+02)*R**(  0)
     $+(  -.210396476E+02)*R**(  1)+(  -.837978745E+01)*R**(  2)
     $+(  -.273314316E+01)*R**(  3)+(  -.741011048E+00)*R**(  4)
     $+(  -.164257308E+00)*R**(  5)+(  -.315778965E-01)*R**(  6)
     $+(  -.545303074E-02)*R**(  7)+(  -.800244132E-03)*R**(  8)
     $+(  -.996254475E-04)*R**(  9)+(  -.221930617E-04)*R**( 10)
     $+(   .441267548E-05)*R**( 11)+(  -.167871863E-05)*R**( 12)
     $+(   .261465369E-06)*R**( 13)+(  -.308321183E-07)*R**( 14)
     $+(   .184703831E-08)*R**( 15)+(  -.684147708E-10)*R**( 16))
     $  *DEXP(-R*(    .200000000E+01))
      C=C   +    .564132367E+00*SQRT(5./(16.*PI))*(3.*COS(FI)*COS(FI)-1.)
      V2PO=A+B+C
      RETURN
      END
```

```
 FUNCTION V2P1(ZR,ZFI)
 DOUBLE PRECISION R,A,B,C
 PI=4.*ATAN(1.0)
 R=ZR
 FI=ZFI+PI/2.
 A=
$+((  -.100000000E+01)*R**( -1)+(  -.200000000E+01)*R**(  0))
$  *DEXP(-R*(    .400000000E+01))
 B=
$+((  -.100000000E+01)*R**( -1)+(  -.175872453E+01)*R**(  0)
$+(  -.151744907E+01)*R**(  1)+(  -.850782399E+00)*R**(  2)
$+(  -.344966044E+00)*R**(  3)+(  -.107446494E+00)*R**(  4)
$+(  -.266390375E-01)*R**(  5)+(  -.533917948E-02)*R**(  6)
$+(  -.956443013E-03)*R**(  7)+(  -.144661132E-03)*R**(  8)
$+(  -.184418117E-04)*R**(  9)+(  -.420213955E-05)*R**( 10)
$+(   .875122376E-06)*R**( 11)+(  -.331187094E-06)*R**( 12)
$+(   .520348288E-07)*R**( 13)+(  -.614589923E-08)*R**( 14)
$+(   .377407662E-09)*R**( 15)+(  -.136829542E-10)*R**( 16))
$  *DEXP(-R*(    .200000000E+01))
 C=
$      .315594714E+02*R**( -3)
$+((  -.315594714E+02)*R**( -3)+(  -.631189428E+02)*R**( -2)
$+(  -.631189428E+02)*R**( -1)+(  -.420792952E+02)*R**(  0)
$+(  -.210396476E+02)*R**(  1)+(  -.837978745E+01)*R**(  2)
$+(  -.273314316E+01)*R**(  3)+(  -.741011048E+00)*R**(  4)
$+(  -.168257308E+00)*R**(  5)+(  -.318778965E-01)*R**(  6)
$+(  -.545303074E-02)*R**(  7)+(  -.800244132E-03)*R**(  8)
$+(  -.998254475E-04)*R**(  9)+(  -.221930617E-04)*R**( 10)
$+(   .441287548E-05)*R**( 11)+(  -.167871883E-05)*R**( 12)
$+(   .261465369E-06)*R**( 13)+(  -.308321183E-07)*R**( 14)
$+(   .183703831E-08)*R**( 15)+(  -.684147708E-10)*R**( 16))
$  *DEXP(-R*(    .200000000E+01))
 C=C  *  -.317066184E+00*SQRT(5./(16.*PI))*(3.*COS(FI)*COS(FI)-1
 V2P1=A+B+C
 RETURN
 END
```

```
      FUNCTION V152S(ZR,ZFI)
      DOUBLE PRECISION R,A,B,C,D
      PI=4.*ATAN(1.0)
      R=ZR
      FI=ZFI+PI/2.
      A=
     $+((   .553261672E-01)*R**( -1)+(   .110652334E+00)*R**(  0))
     $  *DEXP(-R*(   .400000000E+01))
      B=
     $+((   .553261672E-01)*R**( -1)+(   .269611734E+00)*R**(  0)
     $+(   .559867450E+00)*R**(  1)+(   .374099380E+00)*R**(  2)
     $+(   .305553490E+00)*R**(  3)+(   .526330682E-01)*R**(  4)
     $+(   .434889758E-01)*R**(  5)+(  -.346929136E-02)*R**(  6)
     $+(   .179952251E-02)*R**(  7)+(   .120533762E-02)*R**(  8)
     $+(  -.742180521E-03)*R**(  9)+(   .274602447E-03)*R**( 10)
     $+(  -.627096136E-04)*R**( 11)+(   .991169655E-05)*R**( 12)
     $+(  -.103110750E-05)*R**( 13)+(   .651329579E-07)*R**( 14)
     $+(  -.209998905E-08)*R**( 15)+(   .847611148E-11)*R**( 16))
     $  *DEXP(-R*(   .300000000E+01))
      C=
     $+((  -.553688528E-01)*R**( -1)+(   .982305359E-02)*R**(  0)
     $+(   .278628998E+00)*R**(  1)+(   .383928893E-01)*R**(  2)
     $+(   .873476967E-01)*R**(  3)+(  -.239743723E-01)*R**(  4)
     $+(   .676418005E-02)*R**(  5)+(  -.726624061E-03)*R**(  6)
     $+(   .429594065E-04)*R**(  7)+(  -.185190245E-06)*R**(  8))
     $  *DEXP(-R*(   .300000000E+01))
      D=
     $+((  -.553688528E-01)*R**( -1)+(  -.128751077E+00)*R**(  0)
     $+(  -.720534841E-01)*R**(  1)+(  -.486789391E-01)*R**(  2)
     $+(   .307802612E-03)*R**(  3)+(  -.783668980E-03)*R**(  4)
     $+(  -.131155540E-02)*R**(  5)+(   .472033517E-03)*R**(  6)
     $+(  -.842014443E-04)*R**(  7)+(   .506843725E-05)*R**(  8))
     $  *DEXP(-R*(   .400000000E+01))
      V152S=A+B+C+D
      RETURN
      END
```

```
      FUNCTION V1S2P0(ZR,ZFI)
      DOUBLE PRECISION R,A,B
      PI=4.*ATAN(1.D)
      R=ZR
      FI=ZFI+PI/2.
      A=
     $     .570838900E+00*R**( -2)
     $+(  -.570838900E+00)*R**( -2)+(  -.171251670E+01)*R**( -1)
     $+(  -.256877505E+01)*R**(  0)+(  -.244446521E+01)*R**(  1)
     $+(  -.155365178E+01)*R**(  2)+(  -.737398054E+00)*R**(  3)
     $+(  -.241249554E+00)*R**(  4)+(  -.608044135E-01)*R**(  5)
     $+(  -.151745062E-01)*R**(  6)+(  -.118605547E-02)*R**(  7)
     $+(  -.859748933E-03)*R**(  8)+(  -.680157219E-05)*R**(  9)
     $+(   .491021839E-04)*R**( 10)+(  -.360087885E-04)*R**( 11)
     $+(   .103526059E-04)*R**( 12)+(  -.188345558E-05)*R**( 13)
     $+(   .213939336E-06)*R**( 14)+(  -.139053815E-07)*R**( 15)
     $+(   .435587498E-09)*R**( 16))
     $  *DEXP(-R*(    .300000000E+01))
      A=A  *    .118163590E+01*SQRT(3./(4.*PI))*COS(FI)
      B=
     $     .179891010E+00*R**( -2)
     $+(  -.179891010E+00)*R**( -2)+(  -.539673030E+00)*R**( -1)
     $+(  -.809509544E+00)*R**(  0)+(  -.697941596E+00)*R**(  1)
     $+(  -.272428313E+00)*R**(  2)+(  -.703120483E-01)*R**(  3)
     $+(  -.109099451E-01)*R**(  4)+(   .204404314E-02)*R**(  5)
     $+(  -.128958160E-02)*R**(  6)+(   .154329962E-03)*R**(  7)
     $+(  -.947323255E-05)*R**(  8))
     $  *DEXP(-R*(    .300000000E+01))
      B=B  *    .118163590E+01*SQRT(3./(4.*PI))*COS(FI)
      V1S2P0=A+B
      RETURN
      END
```

```
      FUNCTION V1S2P1(ZR,ZFI)
      DOUBLE PRECISION R,A,B
      PI=4.*ATAN(1.0)
      R=ZR
      FI=ZFI+PI/2.
      A=
     $      .570838900E+00*R**( -2)
     $+(  -.570838900E+00)*R**( -2)+(  -.171251670E+01)*R**( -1)
     $+(  -.256877505E+01)*R**(  0)+(  -.244446521E+01)*R**(  1)
     $+(  -.155365178E+01)*R**(  2)+(  -.737398054E+00)*R**(  3)
     $+(  -.241249554E+00)*R**(  4)+(  -.608044135E-01)*R**(  5)
     $+(  -.151745062E-01)*R**(  6)+(  -.118605547E-02)*R**(  7)
     $+(  -.859748933E-03)*R**(  8)+(  -.680157219E-05)*R**(  9)
     $+(   .491021839E-04)*R**( 10)+(  -.360087885E-04)*R**( 11)
     $+(   .103526050E-04)*R**( 12)+(  -.188345558E-05)*R**( 13)
     $+(   .213939336E-06)*R**( 14)+(  -.139053815E-07)*R**( 15)
     $+(   .433587498E-09)*R**( 16))
     $  *DEXP(-R*(   .300000000E+01))
      A=A  *   .118163590E+01*(-SQRT(3./(4.*PI)))*SIN(FI)
      B=
     $      .179891010E+00*R**( -2)
     $+(  -.179891010E+00)*R**( -2)+(  -.539673030E+00)*R**( -1)
     $+(  -.809509544E+00)*R**(  0)+(  -.697941596E+00)*R**(  1)
     $+(  -.272428313E+00)*R**(  2)+(  -.703120483E-01)*R**(  3)
     $+(  -.109099451E-01)*R**(  4)+(   .208404314E-02)*R**(  5)
     $+(  -.128958160E-02)*R**(  6)+(   .154329062E-03)*R**(  7)
     $+(  -.947323255E-05)*R**(  8))
     $  *DEXP(-R*(   .300000000E+01))
      B=B  *   .118163590E+01*(-SQRT(3./(4.*PI)))*SIN(FI)
      V1S2P1=A+B
      RETURN
      END
```

```
      FUNCTION V2S2P0(ZR,ZFI)
      DOUBLE PRECISION R,A,B
      PI=4.*ATAN(1.0)
      R=ZR
      FI=ZFI+PI/2.
      A=
     $     -.516502072E+01*R**( -2)
     $+(    .516502072E+01)*R**( -2)+(    .103300414E+02)*R**( -1)
     $+(    .103300414E+02)*R**(  0)+(    .685238258E+01)*R**(  1)
     $+(    .337472372E+01)*R**(  2)+(    .126606305E+01)*R**(  3)
     $+(    .386952613E+00)*R**(  4)+(    .891483666E-01)*R**(  5)
     $+(    .172334105E-01)*R**(  6)+(    .353764250E-02)*R**(  7)
     $+(    .627874159E-05)*R**(  8)+(    .287233710E-03)*R**(  9)
     $+(   -.712696082E-04)*R**( 10)+(    .177221961E-04)*R**( 11)
     $+(   -.254171909E-05)*R**( 12)+(    .268978408E-06)*R**( 13)
     $+(   -.162367991E-07)*R**( 14)+(    .585629603E-09)*R**( 15)
     $+(   -.240736693E-11)*R**( 16))
     $  *DEXP(-R*(    .200000000E+01))
      A=A   *    .118163590E+01*SQRT(3./(4.*PI))*COS(FI)
      B=
     $      .215986158E-01*R**( -2)
     $+(   -.215986158E-01)*R**( -2)+(   -.647958475E-01)*R**( -1)
     $+(   -.971937713E-01)*R**(  0)+(   -.837983645E-01)*R**(  1)
     $+(   -.327091081E-01)*R**(  2)+(   -.844201676E-02)*R**(  3)
     $+(   -.130990267E-02)*R**(  4)+(    .250220660E-03)*R**(  5)
     $+(   -.154833628E-03)*R**(  6)+(    .185296284E-04)*R**(  7)
     $+(   -.113740376E-05)*R**(  8))
     $  *DEXP(-R*(    .300000000E+01))
      B=B   *    .118163590E+01*SQRT(3./(4.*PI))*COS(FI)
      V2S2P0=A+B
      RETURN
      END
```

```
      FUNCTION V2S2P1(ZR,ZFI)
      DOUBLE PRECISION R,A,B
      PI=4.*ATAN(1.0)
      R=ZR
      FI=ZFI+PI/2.
      A=
     &     -.516502072E+01*R**( -2)
     &+((   .516502072E+01)*R**( -2)+(   .103300414E+02)*R**( -1)
     &+(   .103300414E+02)*R**(  0)+(   .685238258E+01)*R**(  1)
     &+(   .337472372E+01)*R**(  2)+(   .126606305E+01)*R**(  3)
     &+(   .386952613E+00)*R**(  4)+(   .891483666E-01)*R**(  5)
     &+(   .172334165E-01)*R**(  6)+(   .353764250E-02)*R**(  7)
     &+(   .627874159E-03)*R**(  8)+(   .287233710E-03)*R**(  9)
     &+(  -.712696082E-04)*R**( 10)+(   .177221961E-04)*R**( 11)
     &+(  -.251171909E-05)*R**( 12)+(   .268978408E-06)*R**( 13)
     &+(  -.162367991E-07)*R**( 14)+(   .585629603E-09)*R**( 15)
     &+(  -.240736693E-11)*R**( 16))
     &  *DEXP(-R*(   .200000000E+01))
      A=A   *    .118163590E+01*(-SQRT(3./(4.*PI)))*SIN(FI)
      B=
     &     .215986158E-01*R**( -2)
     &+((  -.215986158E-01)*R**( -2)+(  -.647958475E-01)*R**( -1)
     &+(  -.971937713E-01)*R**(  0)+(  -.837983645E-01)*R**(  1)
     &+(  -.327091081E-01)*R**(  2)+(  -.844201676E-02)*R**(  3)
     &+(  -.130990267E-02)*R**(  4)+(   .250220660E-03)*R**(  5)
     &+(  -.154833628E-03)*R**(  6)+(   .185296284E-04)*R**(  7)
     &+(  -.113740376E-05)*R**(  8))
     &  *DEXP(-R*(   .300000000E+01))
      B=B   *    .118163590E+01*(-SQRT(3./(4.*PI)))*SIN(FI)
      V2S2P1=A+B
      RETURN
      END
```

```
      FUNCTION V2P0P1(ZR,ZFI)
      DOUBLE PRECISION R,A
      PI=4.*ATAN(1.0)
      R=ZR
      FI=ZFI+PI/2.
      A=
     $      .315594714E+02*R**( -3)
     $+(   -.315594714E+02)*R**( -3)+(   -.631189428E+02)*R**( -2)
     $+(   -.631189428E+02)*R**( -1)+(   -.420792952E+02)*R**(  0)
     $+(   -.210396476E+02)*R**(  1)+(   -.837978745E+01)*R**(  2)
     $+(   -.273314316E+01)*R**(  3)+(   -.741011048E+00)*R**(  4)
     $+(   -.168257308E+00)*R**(  5)+(   -.318778965E-01)*R**(  6)
     $+(   -.545303074E-02)*R**(  7)+(   -.800244132E-03)*R**(  8)
     $+(   -.998254475E-04)*R**(  9)+(   -.221930617E-04)*R**( 10)
     $+(    .441287548E-05)*R**( 11)+(   -.167871883E-05)*R**( 12)
     $+(    .261465369E-06)*R**( 13)+(   -.308321183E-07)*R**( 14)
     $+(    .188703831E-08)*R**( 15)+(   -.684147708E-10)*R**( 16))
     $  *DEXP(-R*(    .20000000E+01))
      A=A   *    .549174740E+00*(-SQRT(5./(12.*PI)))*3.*SIN(FI)*COS(FI)
      V2P0P1=A
      RETURN
      END
```

```
      FUNCTION V2PP1(ZR,ZFI)
      DOUBLE PRECISION R,A
      PI=4.*ATAN(1.0)
      R=ZR
      FI=ZFI+PI/2.
      A=
     &      .31559471 4E+02*R**( -3)
     &+(   -.31559471 4E+02)*R**( -3)+(   -.63118942 8E+02)*R**( -2)
     &+(   -.63118942 8E+02)*R**( -1)+(   -.42279295 2E+02)*R**(  0)
     &+(   -.21039647 6E+02)*R**(  1)+(   -.83797874 5E+01)*R**(  2)
     &+(   -.27331431 6E+01)*R**(  3)+(   -.74101104 8E+00)*R**(  4)
     &+(   -.16825730 8E+00)*R**(  5)+(   -.31877896 5E-01)*R**(  6)
     &+(   -.54530307 4E-02)*R**(  7)+(   -.80024413 2E-03)*R**(  8)
     &+(   -.99825447 5E-04)*R**(  9)+(   -.22193061 7E-04)*R**( 10)
     &+(    .44128754 8E-05)*R**( 11)+(   -.16787188 3E-05)*R**( 12)
     &+(    .26146536 9E-06)*R**( 13)+(   -.30832118 3E-07)*R**( 14)
     &+(    .18870383 1E-08)*R**( 15)+(   -.68414770 8E-10)*R**( 16))
     $  *DEXP(-R*(    .20000000 0E+01))
      A=A   *   -.77065036 5E+00*SQRT(5./(48.*PI))*3.*SIN(FI)*SIN(FI)
      V2PP1=A
      RETURN
      END
```

APPENDIX II

DIFFERENTIAL CROSS SECTIONS IN THE MULTISTATE IMPACT-PARAMETER DESCRIPTION OF HEAVY-PARTICLE COLLISIONS

This appendix is a reprint of the article which appeared in Physical Review, Volume 8, pages 2915 to 2921, December 1973.

PHYSICAL REVIEW A VOLUME 8, NUMBER 6 DECEMBER 1973

Differential Cross Sections in the Multistate Impact-Parameter Description of Heavy-Particle Collisions

M. R. Flannery and K. J. McCann
School of Physics, Georgia Institute of Technology, Atlanta, Georgia 30332
(Received 11 June 1973)

Differential cross sections are derived from a multistate impact-parameter treatment of heavy-particle collisions. Various approximations are suggested and their relationship with previous expressions are discussed. The equivalence between the differential cross sections in the impact-parameter and wave versions of the Born approximation is established for elastic and inelastic scattering and is illustrated explicitly for the 1s, 2s, $2p_0$, and $2p_{\pm1}$ excitations of atomic hydrogen by proton and hydrogen-atom impact.

I. INTRODUCTION

Application of the multistate impact-parameter description of heavy-particle collisions has been limited mainly to the evaluation of total inelastic-scattering cross sections. Attention has only recently been focused on the corresponding theoretical differential cross sections. Wilets and Wallace[1] expressed the scattering amplitude $f(\theta)$ as a Fraunhofer integral of the asymptotic transition amplitudes over the impact parameter. Byron[2] and Brandsden and Coleman[3] independently derived identical formulas for $f(\theta)$ which differ somewhat from the result of Wilets and Wallace. The relationship between the two formulas is not obvious.

Moreover, a conceptual difficulty arises in that the exact quantum-mechanical expression for $f(\theta)$ involves the electrostatic interaction between the colliding systems averaged over the exact stationary-state wave function satisfying the correct asymptotic boundary condition and the final stationary-state wave function for the isolated atoms. The impact-parameter approach, however, is normally derived from the Dirac method of variation of constants,[4] which is a time-dependent formulation.

In this paper, we will attempt to resolve this conflict and use the multistate description to present yet another expression for $f(\theta)$, which, upon successive approximation, reduces to the results cited above.

Also, the equivalence relationship between the impact-parameter and wave versions of Born's approximation for the *total* cross section has already been established by Crothers and Holt[5] and by McCarroll and Salin.[6] The relationship between the corresponding differential cross sections has been clarified by Byron.[3] An important consequence of the present theory is that both versions of Born's approximation for both elastic and inelastic collisions do yield identical expressions for the differential cross section. This point will be illustrated by the consideration of specific transitions in H^+-H(1s) and H(1s)-H(1s) collisions.

II. THEORY

A. Scattering Amplitude and Impact-Parameter Method for Stationary States

In the center-of-mass reference frame, the scattering amplitude for a transition between an initial state i and a final state f of the collision system is

$$f_{if}(\theta,\varphi) = -\frac{1}{4\pi}\frac{2M_{AB}}{\hbar^2}\langle \Psi_f(\vec{k}_f;\vec{r},\vec{R})\,|\,V(\vec{r},\vec{R}) \times |\Psi_i^+(\vec{k}_i;\vec{r},\vec{R})\rangle_{\vec{r},\vec{R}}\,, \tag{1}$$

in which $V(\vec{r},\vec{R})$ is the instantaneous electrostatic interaction between the two structured collision partners A and B of the system with reduced mass M_{AB}. The composite internal electronic coordinates are denoted by $\vec{r}$ taken relative to the center of mass O of the nuclei with relative separation $\vec{R}$. The angles θ and φ are the spherical angles of the A-B final relative momentum vector $\vec{k}_f$ with polar axis directed along the incident relative momentum $\vec{k}_i$. Equation (1) can be derived either from a time-dependent or a stationary-state treatment of the collision process,[7] but in either description Ψ_f represents the final *stationary* state of the isolated atoms and Ψ_i^+ is the appropriate solution of the time-independent Schrödinger equation

$$\left(-\frac{\hbar^2}{2M_{AB}}\nabla_R^2 + H_e(\vec{r}) + V(\vec{r},\vec{R})\right)\Psi_n^+(\vec{r},\vec{R}) = E_n\Psi_n^+(\vec{r},\vec{R}) \tag{2}$$

subject to the asymptotic boundary condition

$$\Psi_i^+(\vec{r},\vec{R}) \underset{\text{large } R}{\sim} \sum_n \left[e^{i\vec{k}_n\cdot\vec{R}_B}\delta_{ni} + f_{in}(\theta,\varphi)\frac{e^{ik_nR_B}}{R_B}\right] \times \varphi_n(\vec{r}_{aj},\vec{r}_{bj})\,. \tag{3}$$

The purely electronic functions φ_n form a complete set of normalized eigenfunctions of the Hamiltonian H_e describing the electronic motion of the isolated atoms with internal energy $\mathcal{E}_n$ and satisfy

$$H_e(\vec{r}_{aj}, \vec{r}_{bj})\varphi_n(\vec{r}_{aj}, \vec{r}_{bj}) = \mathcal{E}_n\varphi_n(\vec{r}_{aj}, \vec{r}_{bj}), \tag{4}$$

where $\vec{r}_{aj}$ and $\vec{r}_{bj}$ denote the composite electronic coordinates relative to each respective parent nucleus. The total constant energy E_+ in (2) is the sum of the kinetic energy of relative motion $\hbar^2k_n^2/2M_{AB}$ and the energy E_n^e of the electrons relative to O, the center of mass of the nuclei, i.e., $E_n^e = \mathcal{E}_n +$ (the translational kinetic energy of the electrons relative to O). The vector $\vec{R}_B$ specifies the center of mass of the M-electron atom B of mass M_B relative to the center of mass of the N-electron atom A of mass M_A and is given by

$$\vec{R}_B = \vec{R} - \frac{m}{M_A}\sum_{i=1}^{N}\vec{r}_{ai} + \frac{m}{M_B}\sum_{j=1}^{M}\vec{r}_{bj}, \tag{5}$$

where m is the electronic mass. The plane wave $e^{i\vec{k}_n\cdot\vec{R}_B}$ in the boundary condition (3) therefore contains $e^{i\vec{k}_n\cdot\vec{R}}$ together with phase factors that account for the translational motions of the electrons relative to O. As an aid to further clarity, assume that the collision system contains only one electron. The generalization of the subsequent formulas for excitation of many-electron systems is trivial. Let

$$\Psi_i(\vec{r}, \vec{R}) = e^{i\vec{k}_i\cdot\vec{R}}\chi_i(\vec{r}, \vec{R}) \tag{6}$$

such that (2) is rewritten as

$$[H_e(\vec{r}) + V]\Psi_i - \frac{\hbar^2}{2M_{AB}}\{e^{i\vec{k}_i\cdot\vec{R}}\nabla_R^2\chi + 2[\vec{\nabla}_R e^{i\vec{k}_i\cdot\vec{R}}]\cdot\vec{\nabla}_R\chi\} = E_i^e\Psi_i(\vec{r}, \vec{R}). \tag{7}$$

For heavy-particle collisions, assume (a) that the chief dependence of Ψ_i on $\vec{R}$ is contained in $e^{i\vec{k}_i\cdot\vec{R}}$ such that $\nabla_R^2\chi$ can be neglected, (b) that the relative motion is directed mainly along $\hat{n}$, a unit vector along the Z axis, such that

$$\vec{\nabla}_R e^{i\vec{k}_i\cdot\vec{R}} = k_i\hat{n}e^{i\vec{k}_i\cdot\vec{R}},$$

and (c) that

$$\nabla_r^2 = \nabla_{r_a}^2 + (m/M_A)\vec{\nabla}_R\cdot\vec{\nabla}_{r_a} = \nabla_{r_a}^2, \tag{8}$$

such that $H_e(\vec{r}) = H_e(\vec{r}_a)$. With these approximations, (7) becomes

$$[H_e(\vec{r}_A) + V(\vec{r}_a, \vec{R}) - E_i^e]\chi_i(\vec{r}_a, \vec{R}) = i\hbar v_i\left(\frac{\partial\chi_i}{\partial Z}\right)_{\vec{r}\ \text{fixed}} = i\hbar v_i\left[\left(\frac{\partial\chi_i}{\partial Z}\right)_{\vec{r}_a\ \text{fixed}} + \frac{M_{AB}}{M_A}\left(\frac{\partial\chi_i}{\partial z_a}\right)\right], \tag{9}$$

where v_i is the incident speed and where[6] the presence of $z_a = \vec{r}_a\cdot\hat{n}$ in (9) results in correct acknowledgment of the electron's translational motion. Further reduction is obtained by the substitution

$$\chi_i(\vec{r}_a, \vec{R}) = \psi_i(\vec{r}_a, \vec{R})e^{i\mathcal{E}_i Z/\hbar v_i}\exp[im(M_{AB}/M_A)v_i z_a/\hbar] \tag{10}$$

and, since

$$E_i^e = \mathcal{E}_i + \tfrac{1}{2}m(M_{AB}/M_A)v_i^2,$$

ψ_i therefore satisfies

$$[H_e(\vec{r}_a) + V(\vec{r}_a, \vec{R})]\psi_i(\vec{r}_a, \vec{R}) = i\hbar v_i\frac{\partial\psi_i}{\partial Z}. \tag{11}$$

We note, on writing $Z = v_i t$, that Eq. (11), which has been derived from a *stationary-state description* of the scattering, is formally identical to the time-dependent Schrödinger equation obtained by considering the motion of the electrons above in a "time-dependent" potential field $V(\vec{r}_a, \vec{R}(t))$ generated by the motion of the nuclei. This procedure would be analogous to the Born-Oppenheimer approximation for the separation of electronic and nuclear motions. For direct excitation, the stationary-state function $\psi_i(\vec{r}_a, \vec{R})$ can be expanded in terms of the isolated atomic functions φ_n in (4) as

$$\psi_i(\vec{r}_a, \vec{R}) = \sum_n a_n(\vec{R})\varphi_n(\vec{r}_a)e^{-i\mathcal{E}_n z/\hbar v_i} \tag{12}$$

which, on insertion into (11) and with the aid of (4), followed by projection on direct-excitation channel m, yields the following coupled differential equations:

$$\frac{\partial a_m(\vec{R})}{\partial Z} = -\frac{i}{\hbar v_i}\sum_n a_n(\vec{R})\langle\varphi_m|V|\varphi_n\rangle_{\vec{r}_a}e^{i\mathcal{E}_{mn}z/\hbar v_i}, \tag{13}$$

which when solved subject to the asymptotic condition $a_n(\rho, Z\to-\infty) = \delta_{in}$ provides Ψ_i^+ as a function of $\vec{r}_a$ and $\vec{R}$. Thus, the initial wave function Ψ_i^+ develops in $\vec{R}$ as

$$\Psi_i^+(\vec{r}, \vec{R}) = e^{i\vec{k}_i\cdot\vec{R}}\exp\left[im\left(\frac{M_{AB}}{M_A}\right)\frac{v_i z_a}{\hbar}\right] \times e^{i\mathcal{E}_i Z/\hbar v_i}\psi_i(\vec{r}_a, \vec{R}) \tag{14}$$

and, as $Z\to-\infty$, reduces to the correct stationary-state incident wave $e^{i\vec{k}_i\cdot\vec{R}_B}\varphi_i(\vec{r}_a)$. The final-state wave function Ψ_f in (1) is the solution of (2) with $V = 0$, and is therefore

$$\Psi_f(\vec{r}, \vec{R}) = e^{i\vec{k}_f\cdot\vec{R}}\exp\left[im\left(\frac{M_{AB}}{M_A}\right)\frac{v_f z_a}{\hbar}\right]\varphi_f(\vec{r}_a). \tag{15}$$

Hence, with the assumption that the relative speed in the above phase factors is unaffected, i.e.,

$v_i = v_f$, the substitution of (14) and (15) in (1) yields

$$f_{if}(\theta,\varphi) = -\frac{1}{4\pi}\frac{2M_{AB}}{\hbar^2}\int e^{i\vec{K}\cdot\vec{R}} \times\left(\sum_n a_n(\vec{R})\langle\varphi_f(\vec{r}_a)|\,V(\vec{r}_a,\vec{R})\,|\varphi_n(\vec{r}_a)\rangle \times e^{i\delta_{in}Z/\hbar v_i}\right)d\vec{R}, \tag{16}$$

where $\delta_{in} = \delta_i - \delta_n$ and $\vec{K}$ is the momentum change $\vec{k}_i - \vec{k}_f$. The electrostatic interactions averaged over the electronic motions can be written as[9]

$$\langle\varphi_f|\,V|\varphi_n\rangle = V_{fn}(R,\Theta)e^{i(m_n - m_f)\Phi}, \tag{17}$$

where m_f is the magnetic quantum number of electronic state f and $\vec{R} \equiv (R,\Theta,\Phi)$. Thus, (13) is

$$\frac{\partial a_n(\vec{R})}{\partial Z} = -\frac{i}{\hbar v_i}\sum_n a_n(Z,\rho,\Phi)V_{mn}(R,\Theta) \times e^{im_{nf}\Phi}e^{i\delta_{mn}Z/\hbar v_i}, \tag{18}$$

with $m_{nf} = m_n - m_f$, $\vec{R} = (Z,\rho,\Phi)$ in a cylindrical coordinate frame, and with $a_n(-\infty,\rho,\Phi) = \delta_{in}$ as the boundary condition. Introduction of the phase-independent amplitudes $C_n (\equiv a_n e^{im_n\Phi})$ produces

$$\frac{\partial C_m(\rho,Z)}{\partial Z} = -\frac{i}{\hbar v}\sum_n C_n(\rho,Z)V_{mn}(\rho,Z)e^{i\delta_{mn}Z/\hbar v_i}, \tag{19}$$

a set of phase-independent equations capable of numerical solution as functions of ρ and Z. Hence, with the aid of (19) and (16),

$$f_{if}(\theta,\varphi) = -\frac{ik_f}{2\pi}\int e^{i(\vec{K}\cdot\vec{\rho}+m_{if}\Phi)}e^{i\delta_{if}Z/\hbar v_i}\frac{\partial C_f(\rho,Z)}{\partial Z}d\vec{R}, \tag{20}$$

which is the basic formula for the scattering amplitude as determined from the present approach. This formula is essentially identical with that derived by Byron[2] [see Eq. (17b) of his paper]. The generalization of the above equation to excitation in many-electron atomic systems is simple when exchange and transfer of electrons between the two nuclei is neglected.

We note that the above formula is also reproduced when we arbitrarily insert the following fully *time-dependent* initial and final wave functions:

$$\Psi_i^+(\vec{k}_i;\vec{r},\vec{R}(t),t) = \left(\sum_n a_n(t)\varphi_n(\vec{r}_a)e^{-iE_n t/\hbar}\right) \times e^{i\vec{k}_i\cdot\vec{R} - i\hbar k_i^2 t/2M_{AB}} \tag{21}$$

and

$$\Psi_f(\vec{k}_i;\vec{r},\vec{R}(t),t) = [\varphi_f(\vec{r}_c)e^{-iE_f t/\hbar}] \times e^{i\vec{k}_f\cdot\vec{R} - i\hbar k_f^2 t/2M_{AB}} \tag{22}$$

into the scattering amplitude (1) and use the conservation of energy together with the substitution $Z = v_i t$.

B. Approximations to Scattering Amplitude

Approximation 1. The first approximation is based on the fact that for heavy-particle collisions, the Z component of the momentum change can be expanded as

$$K_Z = \vec{K}\cdot\hat{n} = k_i - k_f + 2k_f\sin^2\tfrac{1}{2}\theta = k_i - k_f = \frac{\delta_{fi}}{\hbar v_i}\left(1 + \frac{\delta_{fi}}{2M_{AB}v_i^2} + \cdots\right). \tag{23}$$

Hence, the scattering amplitude (20) becomes

$$f_{if}(\theta,\varphi) = -\frac{ik_i}{2\pi}\int e^{i(\vec{K}'\cdot\vec{\rho}}[e^{im_{if}\Phi}C_f(\rho,\infty) - \delta_{if}]d\vec{\rho}, \tag{24}$$

where

$$K'^2 = K^2 - K_Z^2 = K^2 - \delta_{fi}^2/\hbar^2 v_i^2$$

approximates the square of the momentum change perpendicular to the incident direction, such that $\vec{K}'\cdot\vec{\rho} = K'\rho\cos(\varphi - \Phi)$. Therefore both the Φ and the Z integrations can be performed analytically to yield

$$f_{if}(\theta,\varphi) = -ik_i i^{\Delta}e^{i\Delta\varphi}\int_0^\infty J_\Delta(K'\rho) \times[C_f(\rho,\infty) - \delta_{if}]\rho\,d\rho, \tag{25}$$

where J_Δ are Bessel functions of integral order $\Delta = m_{if}$, the change in magnetic quantum number. The total cross section σ_{if} follows directly from (24) when we write

$$K^2 = k_i^2 + k_f^2 - 2k_i k_f\cos\theta = K'^2 + K_Z^2 \tag{26}$$

to yield

$$\sigma_{if}(k_i) = (k_f/k_i)\int|f_{if}(\theta,\varphi)|^2\,d(\cos\theta)\,d\varphi = \frac{1}{4\pi^2}\int_{K'=0}^{[(k_i+k_f)^2 - K_Z^2]^{1/2}}\int_{\varphi=0}^{2\pi}e^{i(\vec{\rho}-\vec{\rho}')\cdot\vec{K}'}d\vec{K}'\int[e^{i\Delta\Phi}C_f(\rho,\infty) - \delta_{if}]\,d\vec{\rho} \times\int[e^{-i\Delta\Phi'}C_f^*(\rho',\infty) - \delta_{if}]\,d\vec{\rho}', \tag{27}$$

in which $d\vec{K}' = K'\,dK'\,d\Phi'$ is an element lying entirely in the XY plane. The upper limit to K' in (29) is effectively infinite for heavy particles and hence

$$\sigma_{if}(k_i) = 2\pi \int_{\rho=0}^{\infty} |C_f(\rho,\infty) - \delta_{if}|^2 \rho\, d\rho \tag{28}$$

in harmony with the prediction from (10) and (12) that $|C_f(\rho,\infty)|^2$ is the probability for excitation at impact parameter ρ, and with Byron.[2] The corresponding probability for elastic collisions is, however, $|C_i|^2 + (1 - 2\,\mathrm{Re}C_i)$ and is not $|C_i|^2$, except of course when $\mathrm{Re}C_i = \frac{1}{2}$, for all ρ, which is an impossibility.

Equation (24) above may be compared to that obtained by Byron[2] [see his Eq. (19)] who used the actual momentum change $k_f \sin\theta$ perpendicular to the incident direction, rather than the XY-component K' used here. For heavy-particle collisions, there is, however, little difference.

Approximation II. This approximation follows from the neglect of δ_{if} in (20) to give

$$f_{if}(\theta,\varphi) = -\frac{ik_i}{2\pi} \int e^{i(\vec{K}\cdot\vec{R} + m_{if}\Phi)} \frac{\partial C_i(\rho,Z)}{\partial Z}\, d\vec{R}\,. \tag{29}$$

For heavy-particle impacts at high energy, $\vec{K}$ is almost perpendicular to $\vec{n}$ such that

$$\vec{K}\cdot\vec{R} = \vec{K}\cdot\vec{\rho} = K\rho\cos(\theta - \varphi), \tag{30}$$

where K above is taken as the *total* momentum change. Substitution of (30) in (29) yields the expression

$$f_{if}(\theta,\varphi) = -\frac{ik_i}{2\pi} i^{\Delta} e^{i\Delta\varphi} \times \int_0^{\infty} J_{\Delta}(K\rho)\,[C_f(\rho,\infty) - \delta_{if}]\rho\, d\rho\,, \tag{31}$$

which is similar to (25) but with K replacing K'. We note that approximations I and II are identical *only* for elastic collisions. The differences between them will be fully explored for specific inelastic transitions in Sec. II C when we examine the Born wave approximation.

The approximation II, Eq. (31) has also been derived by Bransden and Coleman.[3] However, it is worth pointing out that $f(\theta)$ given by Bransden *et al.*[10] for the excitation of state n by electron impact is valid only then for transitions involving no change in magnetic quantum number (although, for hydrogenic states, $\sum_{l,m}|\Psi_{nlm}|^2$ is, to be sure, spherically symmetric).

Approximation III. On recognizing that $\vec{K}$ is not quite perpendicular to $\vec{k}_i$, we insert the scalar product

$$\vec{K}\cdot\vec{R} = K\rho\cos\tfrac{1}{2}\theta\cos(\varphi - \Phi) + KZ\sin\tfrac{1}{2}\theta \approx K\rho\cos\tfrac{1}{2}\theta\cos(\varphi - \Phi) \tag{32}$$

into (29) and (31) is reproduced except that the argument of the Bessel functions is $K\rho\cos\frac{1}{2}\theta$ instead of $K\rho$ as in approximation II. With $K \approx 2k_i \times \sin\frac{1}{2}\theta$ since $k_i \approx k_f$, then the argument is $k_i\rho\sin\theta$.

Approximation IV. That the Z and Φ integrations in (9) can be achieved in the last two approximations is a direct consequence of the neglect in (32) of $\sin\frac{1}{2}\theta$. A more natural approach, however, is to rotate our initial coordinate frame by $\frac{1}{2}\theta$ about the X axis such that the new Z' axis directed along the vector

$$\hat{n}' = (\vec{k}_i + \vec{k}_f)/|\vec{k}_i + \vec{k}_f|\,, \tag{33}$$

which bisects the initial and final directions and which always ensures that $\vec{K}\cdot\hat{n} = 0$ for a given scattering angle θ. Thus, the components of $\vec{R}$ are, in the new (primed) system, given as

$$\begin{bmatrix} \rho'\cos\Phi' \\ \rho\sin\Phi' \\ Z' \end{bmatrix} = \begin{bmatrix} 1 & 0 & 0 \\ 0 & \cos\frac{1}{2}\theta & \sin\frac{1}{2}\theta \\ 0 & -\sin\frac{1}{2}\theta & \cos\frac{1}{2}\theta \end{bmatrix} \begin{bmatrix} \rho\cos\Phi \\ \rho\sin\Phi \\ Z \end{bmatrix} \tag{34}$$

such that (29) reduces exactly,

$$f(\theta,\varphi) = -\frac{ik}{2\pi} \int e^{i\vec{K}\cdot\vec{\rho}'} \frac{\partial a_{if}(Z,\rho,\Phi)}{\partial Z} \times \rho'\,d\rho'\,dZ'\,d\Phi'\,, \tag{35}$$

with a_{if} maintained as functions in the old (unprimed) coordinate system.

To first order, (34) becomes

$$Z' = Z\cos\tfrac{1}{2}\theta, \quad \rho' = \rho\cos\tfrac{1}{2}\theta, \quad \cos\varphi' = \cos\varphi/\cos\tfrac{1}{2}\theta\,, \tag{36}$$

and, by substituting $dZ' = dZ\cos\frac{1}{2}\theta$ in (35), and by proceeding as above, we find

$$f_{if}(\theta,\varphi) = -ik_i\cos^{3}\tfrac{1}{2}\theta(i\cos\tfrac{1}{2}\theta\, e^{i\varphi})^{\Delta} \times \int_0^{\infty} J_{\Delta}(K\rho\cos\tfrac{1}{2}\theta)[C_{if}(\rho,\infty) - \delta_{if}]\rho\, d\rho\,. \tag{37}$$

If, instead of (36), $Z' = Z$, then a factor $\cos\frac{1}{2}\theta$ disappears from (37). If, in addition, $\phi' \approx \phi$, the $(i\cos\frac{1}{2}\theta\, e^{i\varphi})^{\Delta}$ factor also disappears and the final result is then identical to that of Wilets and Wallace[1] (when $K \approx 2k_i\sin\frac{1}{2}\theta$).

C. Born Version of Scattering Amplitude

By setting $C_n = \delta_{in}$ in the right-hand side of (19), the impact-parameter version of Born's approximation is obtained from (20) to yield

$$f_{if}^{B}(\theta,\varphi) = -\frac{1}{4\pi}\frac{2M_{AB}}{\hbar^2}\int e^{i\vec{K}\cdot\vec{R}}V_{fi}(\vec{R})\,d\vec{R}, \qquad (38)$$

the Fourier transform of the coupling interaction, a result identical with the wave version of Born's approximation.

The main advantage of (20) is, of course, its use in a multistate-state treatment, in which the set of coupled differential equations is solved numerically for $C_n(\rho, Z)$. Thus approximation I, Eq. (24), is essential as a first step and involves only the replacement of K_z by $\mathcal{E}_{fi}/\hbar v_i$, which is almost exact for heavy-particle collisions. The Born version of (24), approximation I, is

$$f_{if}^{B}(\theta,\varphi) = -\frac{1}{4\pi}\frac{2M_{AB}}{\hbar^2}\int e^{i(\vec{K}'\cdot\vec{\rho}+m_{if}\Phi)}d\vec{\rho} \times \int V_{fi}(\rho,Z)e^{i\mathcal{E}_{fi}Z/\hbar v_i}\,dZ, \qquad (39)$$

which when expressed in spherical-polar instead of cylindrical coordinates is equivalent to (38) with $K^2 = K'^2 + \mathcal{E}_{fi}^2/\hbar^2 v_i^2$.

As confirmation of this equivalence in approximation I, consider the following collision processes:

$$H^+ + H(1s) \rightarrow H^+ + H(1s, 2s, 2p_{0,\pm1}). \qquad (40)$$

The appropriate interaction potentials are[11] (in a.u.),

$$V_{1s\,1s}(R) = (1+1/R)e^{-2R}, \quad R^2 = \rho^2 + Z^2 \qquad (41a)$$

$$V_{2s\,1s}(\vec{R}) = -\frac{2}{27}\sqrt{2}(2+3R)e^{-3R/2} \qquad (41b)$$

and

$$V_{2p_{0},1s}(\vec{R}) = (Z/R)V_{2p1s}(R), \quad V_{2p_{\pm1},1s}(\vec{R}) = (\rho/\sqrt{2}R)V_{2p\,1s}(R), \qquad (41c)$$

with

$$V_{2p\,1s}(R) = 4\sqrt{2}\left(\frac{2}{3}\right)^5\left[\frac{1}{R^2} - \left(\frac{1}{R^2}+\frac{3}{2R}+\frac{9}{8}+\frac{27}{64}R\right)e^{-3R/2}\right]. \qquad (41d)$$

The inner integral of (39) for these transitions can be expressed in terms of integral Bessel functions K_n of the third kind,[11,12] as

$$\int_{-\infty}^{\infty} V_{1s\,1s}(R)\,dZ = 2[K_0(\gamma\rho) + \rho K_1(\gamma\rho)], \quad \gamma = 2 \qquad (42a)$$

$$\int_{-\infty}^{\infty} V_{2s\,1s}(R)\cos\beta Z\,dZ = -\frac{8}{27}\sqrt{2}(\alpha^3/A^3)\rho^2 K_2(A\rho), \quad \alpha = \tfrac{3}{2}, \quad A^2 = \alpha^2+\beta^2 \qquad (42b)$$

$$\int_{-\infty}^{\infty} V_{2p\,1s}(R)(Z/R)\sin\beta Z\,dZ = \tfrac{128}{243}\sqrt{2}\beta\{2K_0(\beta\rho) - [2K_0(A\rho) + \tfrac{9}{4}(\rho/A)K_1(A\rho) + \tfrac{27}{32}(\alpha\rho^2/A^2)K_2(A\rho)]\}, \qquad (42c)$$

$$\int_{-\infty}^{\infty} V_{2p\,1s}(R)(\rho/R)\cos\beta Z\,dZ = \tfrac{256}{243}\{\beta K_1(\beta\rho) - [AK_1(A\rho) + \tfrac{9}{8}\rho K_0(A\rho) + \tfrac{27}{64}\beta(\rho^2/A)K_1(A\rho)]\}, \qquad (42d)$$

with $\beta = 3/8v_i$ a.u.

The Φ integration in (39) is performed to give

$$f_{if}(\theta,\varphi) = -\frac{2M_{AB}e^2}{\hbar^2}i^{\Delta}e^{i\Delta\varphi}\int_0^{\infty} J_{\Delta}(K'\rho)\rho\,d\rho\int_{-\infty}^{\infty} V_{fi}(\vec{R})e^{i\mathcal{E}_{fi}Z}\,dZ, \qquad (43)$$

while the ρ integration in the above can be acheived by using the integral formula[12]

$$\int_0^{\infty}\rho^{n+m}K_n(A\rho)J_m(K'\rho)\rho\,d\rho = \frac{2^{n+m}K'^m A^n(n+m)!}{(K'^2+A^2)^{n+m+1}}. \qquad (44)$$

After some algebraic simplification, the following results for the scattering amplitudes are obtained:

$$f_{1s\,1s}^{B}(\theta,\varphi) = -\frac{2M_{AB}e^2}{\hbar^2}\frac{K^2+8}{(K^2+4)^2}, \qquad (45a)$$

$$f_{1s\,2s}^{B}(\theta,\varphi) = -\frac{2M_{AB}e^2}{\hbar^2}\frac{4\sqrt{2}}{(K^2+\alpha^2)^3}, \quad \alpha = \tfrac{3}{2} \qquad (45b)$$

$$f_{1s\,2p_0}^{B}(\theta,\varphi) = f_{1s\,2p}^{B}(\theta,\varphi)\cos\delta, \quad f_{1s\,2p_{\pm1}}^{B}(\theta,\varphi) = f_{1s\,2p}^{B}(\theta,\varphi)\sin\delta, \qquad (45c)$$

where

$$f_{1s\,2p}^{B}(\theta,\varphi) = -\frac{2M_{AB}e^2}{\hbar^2}\frac{6\sqrt{2}}{K(K^2+\alpha^2)^3}, \qquad (45d)$$

with $K^2 = K'^2 + \mathcal{E}_{fi}^2/v_i^2$ and $\cos\delta = \hat{K}\hat{n} = K_z/K = \mathcal{E}_{fi}/v_i$. All of these results agree exactly with those obtained from the Born wave formula (38) which can either be evaluated directly using (41) expressed in spherical polar coordinates or alternatively from

$$f_{if}^{BW}(\theta,\varphi) = -\frac{2M_{AB}c^2}{\hbar^2}\frac{\delta_{if}-F_{if}(\vec{K})}{K^2}, \tag{46}$$

where $F_{if}(\vec{K})$ is the form factor

$$\langle\varphi_i(\vec{r}_a)|e^{i\vec{K}\cdot\vec{r}_a}|\varphi_f(\vec{r}_a)\rangle$$

for atomic hydrogen, determined with the atomic axis of quantization taken along $\hat{n}$, the direction of incidence. The equivalence between the two versions of Born's approximation is achieved for approximation I via the fact that $K'^2+A^2 = K'^2+K_z^2+\alpha^2 = K^2+\alpha^2$ in the denominator of (44).

The difference between approximations I and II arises essentially from the neglect of δ_{if}/v_i in (20) with the result that K' in (39) is replaced by K. Thus, approximation II yields the Born-wave results only for elastic scattering when $K=K'$, and increases K' in (45b) and (45d) by δ_{fi}^2/v_i^2. In the limit of high-impact velocities, approximations I and II should therefore agree for inelastic collisions.

Approximations III and IV also neglect δ_{if}/v_i in (20) and attempt thereafter to take fuller account of the direction of $\vec{K}$ (rather than assuming as in approximation II that $\vec{K}$ lies entirely in the XY plane). This procedure leads to K_z in (45a)–(45d) being replaced by $K\cos\frac{1}{2}\theta$ for both cases and, for IV in addition, to the appearance of an extra multiplicative factor $\cos^{\frac{1}{2}}\theta$ for (45a) and (45b) and $\cos^{\frac{1}{2}}\theta$ for (45a). Approximations III and IV therefore result in an incorrect angular dependence, becoming worse for the larger scattering angles. Moreover, the resulting errors would be strongly amplified for the case of electron impact.

The basic reason why approximations III and IV are not as good as approximations I and II arises from the fact that, while approximation II essentially neglects K_z and is thereafter consistent with this neglect, approximations III and IV neglect K_z initially in (20) and then seek to account for K_z later by assuming that $\vec{K}$ indeed possesses a Z component.

The following neutral-neutral processes,

$$H(1s)+H(1s) \rightarrow H(1s)+H(1s,2s,2p_0,2p_{\pm1}), \tag{47}$$

have also been explored in both Born versions. The appropriate interaction potentials have already been given.[9,12] For the elastic case,

$$\int_{-\infty}^{\infty} V_{1s,1s}(\vec{R})\,dZ = 2[K_0(2\rho)+\rho K_1(2\rho)-\tfrac{1}{2}\rho^2K_2(2\rho) -\tfrac{1}{8}\rho^3K_3(2\rho)], \tag{48}$$

and the integrals for the inelastic case are also known.[12] The subsequent ρ integrations can also be performed analytically, and approximation I then yielded precisely the Born-wave values deduced from the customary formula,

$$f_{if}^{BW}(\theta,\varphi) = \frac{2M_{AB}c^2}{\hbar^2}\frac{[1-F_{1s,1s}(K)][\delta_{if}-F_{if}(\vec{K})]}{K^2}, \tag{49}$$

for H–H impacts.

Finally, as another example, assume that some reaction is assumed to proceed (with unit probability) only for collisions with impact parameter $\rho \le R_0$, a reaction radius. Then the resulting integrations in (25) can be performed analytically in terms of Bessel and Lommel functions. For the case with $\Delta=0$, the scattering amplitude is simply (with $a_i=0$, $a_f=1$ for $\rho\le R_0$, and $a_i=1$, $a_{if}=0$ otherwise)

$$f_{if}(\theta,\varphi) = -ik_iR_0J_1(KR_0)/K = -f_{ii}(\theta,\varphi) \rightarrow -\tfrac{1}{2}k_iR_0^2 \tag{50}$$

for small $K\approx 2k_i\sin\frac{1}{2}\theta$. Both the elastic and inelastic differential cross sections are therefore peaked at small scattering angles θ, with magnitude $\frac{1}{4}k_i^2R_0^4$, and have angular spread $(k_iR_0)^{-1}$. Hence, little error is introduced by setting

$$\sigma_{if} = 2\pi\int_0^{\pi}|f_{if}|^2\,d(\cos\theta) = 2\pi R_0^2\int_0^{\infty}[J_1(k_iR_0\theta)]^2\frac{d\theta}{\theta} = \pi R_0^2 = \sigma_{ii} \tag{51}$$

as predicted elsewhere[13] for collisions with a total absorbing sphere in the limit of large incident momentum k_i. The total cross section for both elastic and inelastic scattering is therefore

$$\sigma = \sigma_{ii}+\sigma_{if} = 2\pi R_0^2 = (4\pi/k_i)\,\mathrm{Im}f_{ii}(\theta=0) \tag{52}$$

in harmony with the optical theorem.

In conclusion, a basic expression (20) for the scattering amplitude $f(\theta)$ has been simply derived. The Born version of (20) is identical to the Born-wave result of $f^{BW}(\theta)$. When a multistate description is used, several approximations are explored and are presented in decreasing order of effectiveness [as determined by the comparison of the corresponding Born versions with $f^{BW}(\theta)$]. The Born version of the "best" approximation I agrees with $f^{BW}(\theta)$ in the heavy-particle limit, i.e., when $K_z=\delta_{fi}/v_i$. The possible elaboration of this approximation to electron-atom collisions is of interest. The relationship of these approximations with those previously derived[1-3] is probed.

[1]L. Wilets and S. J. Wallace, Phys. Rev. 169, 84 (1968).
[2]F. W. Byron, Phys. Rev. A 4, 1907 (1971).
[3]B. H. Bransden and J. P. Coleman, J. Phys. B 5, 537 (1972).
[4]D. R. Bates, *Quantum Theory* (Academic, New York, 1961), Vol. 1, pp. 251–97.
[5]D. S. Crothers and A. R. Holt, Proc. Phys. Soc. Lond. 88, 75 (1966).
[6]R. McCarroll and A. Salin, C. R. Acad. Scl. (Paris) 263, 329 (1966).
[7]L. S. Rodberg and R. M. Thaler, *Introduction to the Quantum Theory of Scattering* (Academic, New York, 1967), p. 225.
[8]M. R. C. McDowell and J. P. Coleman, *Introduction to the Theory of Ion Atom Collisions* (North-Holland, New York, 1970), pp. 156, 317.
[9]M. R. Flannery, Phys. Rev. 183, 231 (1969).
[10]B. H. Bransden, J. P. Coleman, and J. Sullivan, J. Phys. B 5, 546 (1972).
[11]D. R. Bates, Proc. Roy. Soc. Lond. A 245, 299 (1958).
[12]I. S. Gradshteyn and I. M. Ryzhik, *Tables of Integrals, Series and Products* (Academic, New York, 1965).
[13]N. F. Mott and H. S. W. Massey, *Theory of Atomic Collisions* (Clarendon, Oxford, England, 1965), p. 191.

APPENDIX III

DIFFERENTIAL CROSS SECTIONS FOR ELASTIC SCATTERING AND FOR THE 2s AND 2p EXCITATIONS OF H(1s) BY HYDROGEN-ATOM IMPACT

This appendix is a reprint of an article which appears in Physical Review A, Volume 9, pages 1947 to 1953, May 1974.

PHYSICAL REVIEW A VOLUME 9, NUMBER 5 MAY 1974

Differential cross sections for elastic scattering and for the 2s and 2p excitations of H(1s) by hydrogen-atom impact

M. R. Flannery and K. J. McCann
School of Physics, Georgia Institute of Technology, Atlanta, Georgia 30332
(Received 16 July 1973)

Differential cross sections are calculated using the two-state and four-state impact-parameter treatments for H(1s)-H(1s) elastic and inelastic collisions in the keV-energy region. The cross sections, computed as a function of scattering angle, are compared with those evaluated from the Born-wave and unitarized-Born approximations. Interesting differences are observed.

I. INTRODUCTION

The multistate impact-parameter description of neutral-neutral collisions in the keV energy range has been used mainly to evaluate total excitation cross sections.[1] The influence of various interaction couplings on the collisional cross section can therefore be systematically examined by including additional unperturbed eigenfunctions in the total wave function describing the collision system. An examination of the corresponding differential cross sections $\sigma(\theta)$ as a function of the scattering angle θ is, however, feasible[2,3-5] and very desirable since (a) it would provide further theoretical insight into the basic model as extra couplings are introduced, and (b) $\sigma(\theta)$ can now be measured directly for neutral-neutral collisions. The resulting comparison with theoretical predictions would provide a more sensitive test of the theoretical model.

In this paper, this multistate impact-parameter treatment is applied to the examination of the collisional processes

$$\mathrm{H}(1s) + \mathrm{H}(1s) \rightarrow \mathrm{H}(1s) + \mathrm{H}(1s, 2s, 2p_0 \text{ or } 2p_{\pm 1}) \quad (1)$$

in which the incident hydrogen atom remains in the ground state. Differential cross sections as a function of θ are calculated at several impact energies using various approximations.

The effects of nuclear symmetry, electron exchange between the nuclei, and simultaneous transitions occuring in both target and projectile atoms are explicitly neglected.

II. MULTISTATE THEORY

The basic formula for the amplitude for the scattering of two heavy particles of reduced mass M_{AB} and initial relative momentum $\vec{k}_i$ into the direction (θ, φ) about the z direction of incidence is given, in the center-of-mass reference frame, by[2]

$$f_{if}(\theta, \varphi) = -\frac{ik_i}{2\pi} \int e^{i(\vec{K}\cdot\vec{R} + m_{if}\Phi)} e^{i\mathcal{E}_{if} Z/\hbar v_i} \frac{\partial C_f}{\partial Z}\, d\vec{R}, \quad (2)$$

where the incident velocity $\vec{v}_i = \hbar\vec{k}_i/M_{AB}$. The momentum change $\vec{K}$ caused by the collision is $\vec{k}_i - \vec{k}_f$, where the final relative momentum $\vec{k}_f$ is directed along (θ, φ). The difference $\mathcal{E}_{if}$ in the electronic energies between the initial (i) and final (f) states of both atoms is $\mathcal{E}_i - \mathcal{E}_f$, and $m_{if} = m_i - m_f$ is the change in the total azimuthal quantum numbers, with the atomic axis of quantization along the incident direction. The nuclear-separation vector $\vec{R}$ has components (R, Θ, Φ) in a spherical polar frame, and (ρ, Φ, Z) in a cylindrical frame where ρ is the impact-parameter which lies perpendicular to the incident direction. A rectilinear trajectory for the relative motion is assumed, such that the transition amplitude C_m satisfies the following set of (phase Φ-independent) first-order, coupled differential equations:

$$\frac{\partial C_m(\rho, Z)}{\partial Z} = -\frac{i}{\hbar v_i} \sum_n C_n(\rho, Z) V_{mn}(\rho, Z) e^{i\mathcal{E}_{mn} Z/\hbar v_i}, \quad (3)$$

solved subject to the boundary condition $C_n(\rho, -\infty) = \delta_{ni}$, where i denotes the initial state of the collision system. The interaction matrix elements coupling the states j and k of the atoms are

$$V_{jk}(\vec{R}) = \langle \Psi_j(\vec{r}_1, \vec{r}_2) | V(\vec{r}, \vec{R}) | \Psi_k(\vec{r}_1, \vec{r}_2) \rangle, \quad (4)$$

where $V(\vec{r}, \vec{R})$ is the instantaneous electrostatic interaction between the two neutral atoms at internuclear distance $\vec{R}$, and the composite electronic coordinates are represented by $\vec{r}$. The wave functions Ψ_j are eigenfunctions of the isolated atoms with eigenenergies $\mathcal{E}_j$ and (by neglecting exchange effects and double transitions) are therefore given, for processes (1), by

$$\Psi_f(\vec{r}_1,\vec{r}_2)=\varphi_{nlm}(\vec{r}_1)\varphi_{1s}(\vec{r}_2), \tag{5}$$

where φ_{nlm} denote a set of eigenfunctions for the hydrogen atom in quantum state (nlm) and where $\vec{r}_1$ and $\vec{r}_2$ are the position vectors of each electron relative to its parent nucleus. The subsequent integrations over $\vec{r}_1$ and $\vec{r}_2$ in (4) can be performed analytically. The diagonal and off-diagonal matrix elements appropriate for a full four-state treatment have already been expressed[1,2] as functions of $\vec{R}$. With this information, the set of equations (3) can now be solved numerically.

In order to use the computed multistate transition amplitudes C_{fi}, further simplification to (2) is required. This can be achieved by noting that, for heavy-particle collisions, the z-component K_z of the momentum change $\vec{K}$ can be expanded according to

$$K_z=k_i-k_f\cos\theta\approx k_i-k_f$$
$$=(\mathcal{E}_{fi}/\hbar v_i)(1+\mathcal{E}_{fi}/2M_{AB}v_i^2+\cdots). \tag{6}$$

Hence, in the heavy-particle limit, second- and higher-order terms in the above expansion can be neglected such that (2) reduces to

$$f_{if}(\theta,\varphi)=-\frac{ik_i}{2\pi}\int\exp(i\vec{K}'\cdot\vec{\rho})$$
$$\times[e^{i\eta_{if}}C_f(\rho,\infty)-\delta_{if}]d\vec{\rho}, \tag{7}$$

where $K'^2=K^2-K_z^2=K^2-\mathcal{E}_{fi}^2/\hbar^2v_i^2$ is the square of the momentum change perpendicular to the direction of incidence along $\vec{k}_i$, and hence, $\vec{K}'\cdot\vec{\rho}=K'\rho\cos(\varphi-\Phi)$. Thus, the Φ integration in (7) is performed to give

$$f_{if}(\theta,\varphi)=-ik_i i^{\Delta}e^{i\Delta\varphi}\int_0^{\infty}J_{\Delta}(K'\rho)$$
$$\times[C_f(\rho,\infty)-\delta_{if}]\rho\,d\rho, \tag{8}$$

where J_Δ are Bessel functions of integral order $\Delta=m_{if}$.

The required differential cross section is therefore

$$\sigma_{if}(\theta)=2\pi(k_f/k_i)|f_{if}(\theta,\varphi)|^2. \tag{9}$$

III. BORN, UNITARIZED BORN, AND GLAUBER APPROXIMATIONS

The impact-parameter version of Born's approximation for elastic and inelastic scattering readily follows by inserting $C_n(\rho,Z)=\delta_{ni}$ into the right-hand side of (2) with the result that

$$\frac{\partial C_f(\rho,Z)}{\partial Z}=-\frac{i}{\hbar v_i}V_{fi}(\rho,Z)e^{i\mathcal{E}_{fi}Z/\hbar v_i} \tag{10}$$

which is in a form suitable for use in (2) directly. Hence, on transforming from the cylindrical frame (ρ,Φ,Z) to the spherical-polar coordinate frame (R,Θ,Φ), (2) yields

$$f_{if}^{B}(\theta,\varphi)=-\frac{1}{4\pi}\frac{2M_{AB}}{\hbar^2}\int V_{fi}(\vec{R})e^{i\vec{K}\cdot\vec{R}}\,d\vec{R}, \tag{11}$$

the Fourier transform of the interaction coupling the initial and final channels, a result identical with that obtained directly from the wave version of Born's approximation. The Born approximation is valid only in the limit of high impact-energy and weak interaction when the departure from probability conservation is small.

For the special case of elastic scattering, a "unitarized" Born approximation can be obtained by simply neglecting all inelastic channels with the result that [with $C_n=0$, $n\neq i$ in (3)]

$$C_i(\rho,Z)=\exp\left(-\frac{i}{\hbar v_i}\int_{-\infty}^{Z}V_{ii}(\rho,Z)\,dZ\right), \tag{12}$$

which always conserves probability, and which can also be used directly in (2). By taking the first two terms of the expansion of the exponential in (12), the usual Born expression (11) for elastic scattering is recovered.

The Born approximation for inelastic scattering ignores couplings between states other than the initial and final states, and essentially arises from a two-state treatment in which the diagonal interactions (distortion terms) and back coupling are ignored. It takes account, however, of the energy difference $\mathcal{E}_{fi}$.

An approximation which ignores the excitation differences $\mathcal{E}_{mn}$ in (3), but takes full account of all the couplings, can readily be derived. The phase-dependent set of equations, similar to (3), can then be solved exactly, to give

$$C_f(\vec{\rho},Z)=\langle\Psi_f(\vec{r}_1\vec{r}_2)|\exp\left(-\frac{i}{\hbar v_i}\int_{-\infty}^{Z}V(\vec{R},\vec{r})\,dZ\right)$$
$$\times|\Psi_i(\vec{r}_1,\vec{r}_2)\rangle. \tag{13}$$

The first two terms in the expansion of the exponential yields the Born-wave result for elastic scattering. Inserting the full expression (13) into (8) yields a result identical with the Glauber approximation.[7] However, (13) involves the calculation of various powers of the electrostatic interaction averaged over the electronic motion, and so will be not applied here.

Some of the more general features displayed by the more elaborate calculations can be readily deduced from the simple Born result (11), which for this case can be rewritten as

$$f_{if}^{B}(\theta,\varphi)=(2M_{AB}e^2/\hbar^2K^2)[\mathrm{I}-F_{is\,1s}(K)]$$
$$\times[\delta_{if}-F_{fi}(\vec{K})] \tag{14}$$

TABLE I. Various properties of the Born-wave cross sections $\sigma(\theta)/a_0^2$ [a] for H(1s) + H(1s) → H(1s) + H(nl). $\sigma_{2s}(0) = (2^8/3^8)M_{AB}^2/v^4$; $\sigma_{2p}(0) = (2^{10}/3^8)M_{AB}/v^2$; $E = \frac{1}{2}M_{AB}v^2$.

Final states	σ(small θ)	$\sigma_{max}(\theta_0)$	θ_0	σ(large θ)
1s	$32M_{AB}{}^4E^2\sin^4\frac{1}{2}\theta$	1.62×10^5	$0.093/v$	$1/(8E^2\sin^4\frac{1}{2}\theta)$ [b]
2s	$\sigma_{2s}(0) + (2^{24}/3^{12})M_{AB}{}^4E^2\sin^4\frac{1}{2}\theta$	2.50×10^4	$0.055/v$	$1/(2^{10}M_{AB}{}^4E^6\sin^{12}\frac{1}{2}\theta)$
2p	$\sigma_{2p}(0) + (2^{18}/3^{10})M_{AB}{}^3E\sin^2\frac{1}{2}\theta$	1.07×10^5	$0.036/v$	$9/(2^{15}M_{AB}{}^6E^7\sin^{14}\frac{1}{2}\theta)$

[a] Entries to be multiplied by (final speed/incident speed) ratio.
[b] Rutherford cross section.

where $F_{fi}(K) = \langle\varphi_f(\vec{r})|e^{i\vec{K}\cdot\vec{r}}|\varphi_i(\vec{r})\rangle$ is the elastic ($i=f$) or inelastic ($i\neq f$) form factor which is known explicitly for hydrogen. With this knowledge, the differential cross section $\sigma_f^B(\theta)$ can be written down, and the maximum value σ_{max} and its location at θ_0 determined. Table I summarizes the various properties and any departures from them will be fully examined in the following section when more refined descriptions are used.

IV. RESULTS AND DISCUSSION

The two-state and four-state descriptions of the scattering processes

$$H(1s)+H(1s)\rightarrow H(1s)+H(1s, 2s, 2p_0, 2p_{\pm1}) \qquad (15)$$

involved solving the full set of either two- or four-coupled equations (3) numerically for the (complex) transition amplitude $C_n(\rho,\infty)$, which were then inserted for numerical integration of (8), to yield from (9) the two-state and four-state cross sections $\sigma^T(\theta)$ and $\sigma^F(\theta)$, respectively, as a function of scattering angle θ. Calculations were performed for incident speeds $v_i = 0.5$, 1, 2, and 3 atomic units (corresponding to incident kinetic energies $25v_i^2$ keV). Illustrative results are presented only for the $v_i = 1$, 2 cases, the remainder being available upon request.

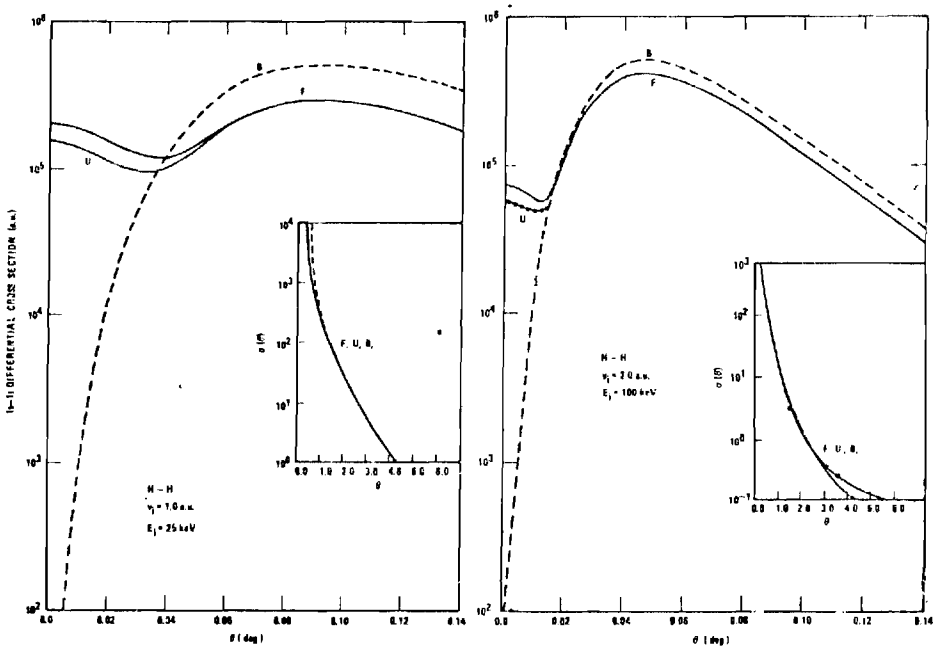

FIG. 1. 1s-1s differential cross sections. F—four-state approximation; U—unitarized-Born approximation; B—Born approximation (Born wave and impact-parameter Born).

In addition,[9] for comparison purposes, elastic and inelastic Born-wave cross sections σ^B for (15) were obtained from (14), and also the unitarized-Born elastic cross sections σ^U were calculated from (8) and (12).

A. Elastic scattering

In Figs. 1(a) and 1(b) are displayed the computed differential cross sections $\sigma(\theta)$ for elastic scattering as a function of θ at two impact energies E. The insets in each figure demonstrate the behavior of $\sigma(\theta)$ at the larger scattering angles. The four-state and unitarized Born cross sections, σ^F and σ^U respectively, are finite for scattering in the forward direction $\theta=0$, where the Born-wave cross section σ^B is zero. The minima and maxima in all the graphs are associated with the behavior of J_Λ in (8).

For large θ, σ^B exhibits an exact Rutherford dependence $\sim E^{-2}\csc^4\frac{1}{2}\theta$, a dependence that is followed in general by both σ^F and σ^U.

Finally, the closeness between σ^F and σ^U throughout the whole angular and impact-energy range is a direct manifestation that the excited 2s and 2p states cause little influence in the elastic-scattering cross sections as expected. The situation, however, for inelastic collisions is different.

B. Inelastic scattering

The four-state, two-state, and Born-wave cross sections σ^F, σ^T, and σ^B respectively, are displayed in Figs. 2(a) and 2(b) for the 2s excitation of hydrogen. The cross sections are finite at $\theta=0$, with $\sigma^B(0)>\sigma^F(0)>\sigma^T(0)$ for the slower collisions. As E increases, $\sigma^B(0)$ decreases much more rapidly than σ^F and σ^T with the result that $\sigma^B(0)\ll\sigma^T(0)\leq\sigma^F(0)$ eventually. From the analytical expression for σ^B, it can be readily deduced, with all quantities in atomic units, that $\sigma^B(0)=(2^6/3^8)M^2_{\Lambda B}\pi a_0^3/v_i^4$ for $v_i\gg 1$. In general, there is remarkable agreement of the maxima and location of the maxima at θ_0 given by the three approximations.

The main difference between σ^B and σ^F is demonstrated for the larger scattering angles when σ^B falls off very fast $[\sim E^{-1}\csc^2\frac{1}{2}\theta]^6$ in contrast to the much slower fall off for σ^F. However, this difference does not affect the total cross section appreciably. For the higher E, the scattering becomes more concentrated in the forward direction

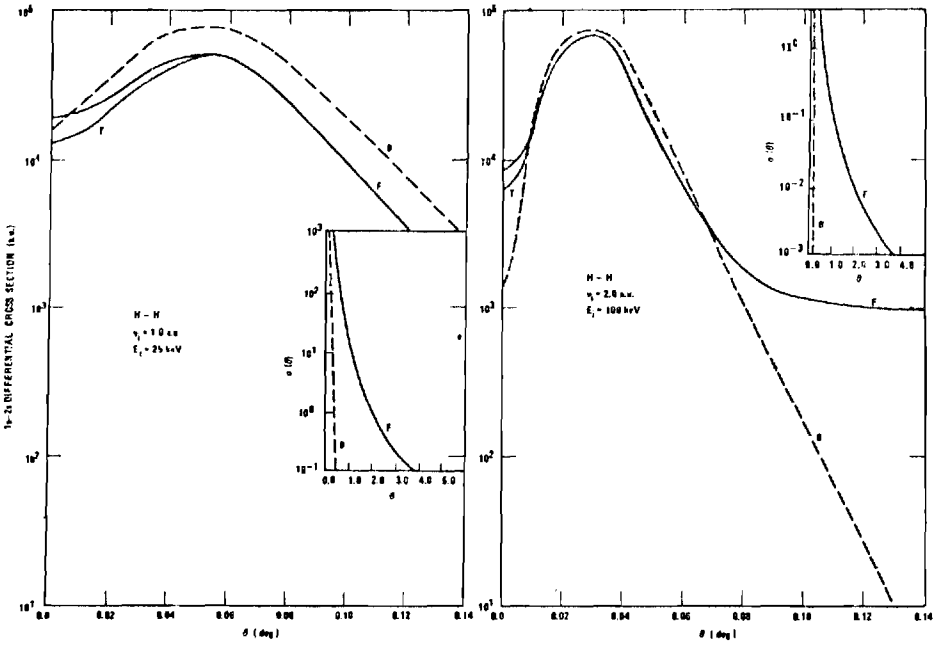

FIG. 2. 1s-2s differential cross sections. F—four-state approximation; T—two-state approximation: B—Born approximation (Born wave and impact-parameter Born).

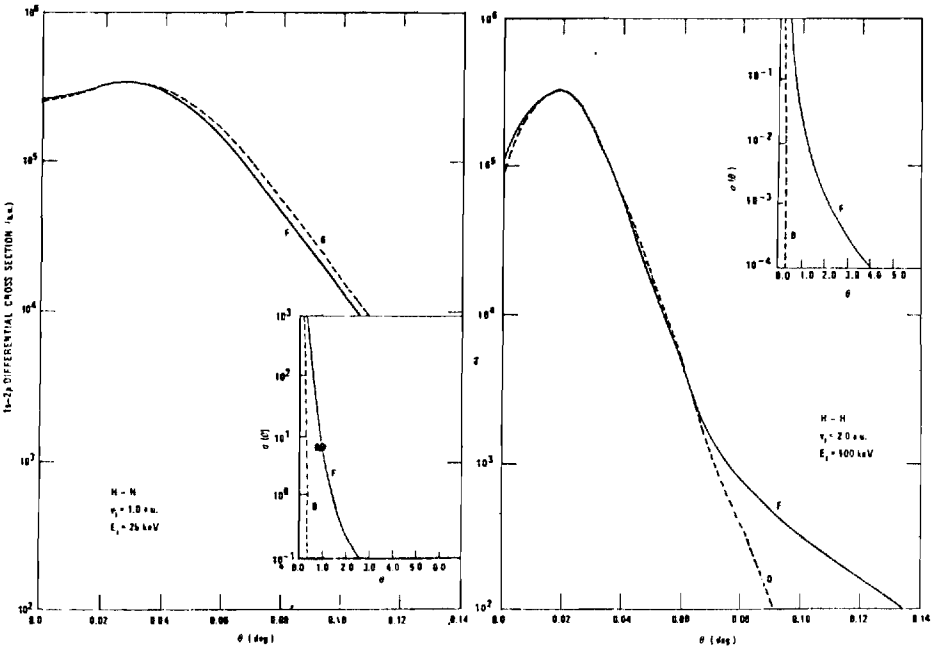

FIG. 3. $1s$-$2p$ differential cross sections. F—four-state approximation; B—Born approximation (Born wave and impact-parameter Born).

for both approximations, as expected.

In Figs. 3(a) and 3(b) are displayed the four-state and Born-wave cross sections for the $1s$-$2p$ transition. The cross sections given by the two-state approximation agreed to within 1% with σ^F. As in the previous case, the cross sections are finite for scattering in the forward direction and $\sigma^B(0) > \sigma^F(0)$ at lower energies while $\sigma^F(0) > \sigma^B(0) = (2^{10}/3^8)/(A f_{AB}^2 a_0^2/\iota_i^2)$ at higher energies.

There is excellent over-all agreement except at small and large scattering angles where σ^F decreases much more slowly than $\sigma^B \sim (E^{-1}\csc^2\frac{1}{2}\theta)^2$.

Examination of the $1s$-$2p_0$ and $1s$-$2p_{\pm 1}$ cross sections provides more detailed insight into $2p$ excitations. Accordingly, in Figs. 4(a) and 4(b) are shown the "substate" cross sections σ_{2p_0} and $\sigma_{2p_{\pm 1}}$ in both approximations. For scattering in the forward direction $\sigma^F_{2p_0}$ alone is finite, while the zero value given by $\sigma_{2p_{\pm 1}}$ results from $J_1(0) = 0$. The finite value $\sigma^F_{2p_0}(0)$ decreases with increase in E and closely follows $\sigma^B(0)$, in contrast to the $2s$ case.

TABLE II. The $(0$-$\theta_{max})$ angular-integrated cross sections σa_0^2 and the impact-parameter intergrated cross sections $\sigma' a_0^2$.

v	θ_{max}	σ_{1s}	σ'_{1s}	σ_{2s}	σ'_{2s}	σ_{2p}	σ'_{2p}
0.5	0.5	1.58^{0a}	3.24^{0}	1.44^{-1}	2.32^{-1}	3.73^{-1}	4.38^{-1}
	3.0	3.20^{0}		2.31^{-1}		4.21^{-1}	
1.0	0.1	6.89^{-1}	1.67^{0}	4.59^{-2}	8.71^{-2}	1.89^{-1}	2.16^{-1}
	3.0	1.64^{0}		8.70^{-2}		2.17^{-1}	
2.0	0.1	3.87^{-1}	6.13^{-1}	1.95^{-2}	2.26^{-2}	5.63^{-1}	5.66^{-2}
	3.0	6.09^{-1}		2.25^{-2}		5.64^{-1}	
3.0	0.1	2.39^{-1}	3.00^{-1}	9.45^{-3}	1.01^{-2}	2.48^{-2}	2.50^{-2}
	3.0	2.97^{-1}		9.87^{-3}		2.49^{-2}	

[a] Superscript indicates the power of ten by which the result is to be multiplied.

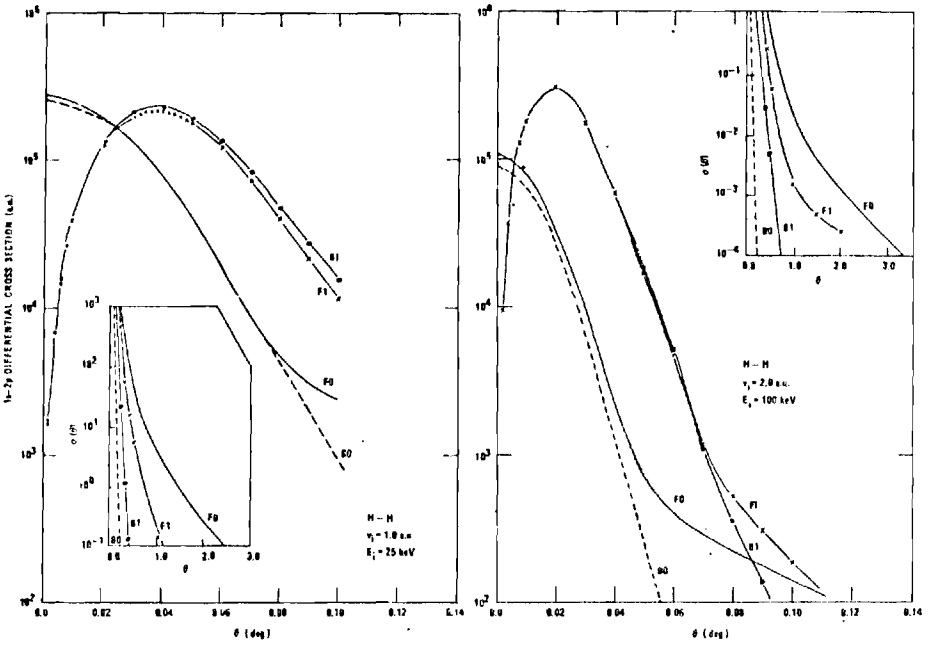

FIG. 4. $1s$-$2p_0$ and $1s$-$2p_{\pm1}$ differential cross sections. F0--four-state ($1s$-$2p_0$) approximation; F1—four-state ($1s-2p_{\pm1} = 1s-2p_{+1} + 1s-2p_{-1}$) approximation; B0—Born ($1s-2p_0$) approximation; B1—Born ($1s-2p_{\pm1}$) approximation.

With increase in E, $\sigma_{2p_{\pm1}}$ increases relative to σ_{2p_0} until it becomes the main contributor to σ_{2p}. In general, the Born results exhibit the main features of the cross sections, except, of course, at the larger scattering angles.

C. Total elastic and excitation cross sections

Finally, we have performed calculations for the total cross sections by using

$$\sigma_f(v_i) = \int_{\theta=0}^{\theta_{\max}} \sigma_{if}(\theta)\, d(\cos\theta) \tag{16}$$

and also by using

$$\sigma_f'(v_i) = 2\pi \int_0^{\infty} |C_f(\rho,\infty) - \delta_{if}|^2 \rho\, d\rho\,. \tag{17}$$

The results are given in Table II. The closeness between the cross sections calculated from the two different formulas (16) and (17) is a measure of the accuracy of the overall calculations. In general, the agreement is very good, although for the higher impact energies E and larger angles $\theta \approx 3°$, the accurate determination of $\sigma_{if}(\theta)$ is prevented by the rapid oscillation in the Bessel functions. Thus, in the table, $\theta_{\max}$ was taken to be 3°. Also, Table II demonstrates that as E increases, the scattering becomes much more concentrated in the forward direction. For example, the relative contributions arising from elastic scattering into the 0–0.1° angular range are 41%, 63%, and 99% for incident speed $v_i = 1$, 2, and 3, respectively. For $2s$ inelastic scattering, corresponding percentages are 53%, 86%, and 94%, and are 87%, 99%, and 99%, respectively, for $2p$ excitation.

[1]M. R. Flannery, Phys. Rev. 183, 231 (1969); Phys. Rev. 183, 241 (1969); J. Phys. B 2, 913 (1969).
[2]M. R. Flannery and K. J. McCann, Phys. Rev. A 8, 2915 (1973).
[3]F. W. Byron, In *Sixth International Conference of the Physics of Electronic and Atomic Collisions* (MIT, Cambridge, Mass., 1969), p. 644.
[4]F. W. Byron, R. V. Krotkov, and J. A. Medeiros, Phys. Rev. Lett. 24, 83 (1970).
[5]F. W. Byron, Phys. Rev. A 4, 1907 (1971).
[6]M. R. Flannery and H. Levy II, J. Phys. B 2, 314 (1969).
[7]R. J. Glauber, *Lectures in Theoretical Physics* (Interscience, New York, 1958), Vol. 1, p. 373.

APPENDIX IV

DIFFERENTIAL CROSS SECTIONS FOR ELASTIC AND INELASTIC HYDROGEN-HELIUM COLLISIONS

This appendix is a reprint on an article which appears in the Journal of Physics B: Atom. Molec. Phys., Volume 7, pages 840 to 849, 1974.

J. Phys. B: Atom. Molec. Phys., Vol. 7, No. 7, 1974. Printed in Great Britain.

Differential cross sections for elastic and inelastic hydrogen–helium collisions

M R Flannery and K J McCann
School of Physics, Georgia Institute of Technology, Atlanta, Georgia 30332

Received 12 October 1973

Abstract. The elastic and the 2s and 2p inelastic scattering of ground-state hydrogen atoms by helium is examined in the Born, unitarized-Born and multistate impact-parameter formulation of heavy-particle collisions, with incident energies E in the range $0.25 \leq E \leq 225$ keV. The failure of Born's approximation to provide an adequate description of both small angle elastic and inelastic scattering and large-angle inelastic scattering is graphically displayed.

1. Introduction

Although considerable interest has recently been focused on the determination of the total cross section Q for neutral neutral (H H and H He) excitation collisions as a function of impact-energy E (Flannery 1969a, b, c, Levy 1969a, b, Bell *et al* 1973), relatively little is known about the corresponding differential cross section $\sigma(\theta)$ versus scattering angle θ.

The main theoretical description for Q at intermediate E is the multistate impact-parameter treatment (MIPT) in which the influence of the various interactions, coupling the excitation channels, can be systematically examined. For excitation to a final state f, $\sigma(\theta)$ involves both the magnitude and the relative phase of the asymptotic transition amplitude a_f, and hence its examination would therefore provide a more sensitive probe into the various approximate schemes adopted than that provided by Q, which depends only on $|a_f|^2$. Also, recent advances in experimental techniques have permitted the measurement of $\sigma(\theta)$ and comparison with theory would perhaps yield further insight into the basic theoretical model.

In this paper, a theory in which the internal electronic motions of the colliding atomic systems are described by the MIPT, while the relative atom-atom motion is treated by the Eikonal approximation, is applied to the examination of the differential cross section for the processes,

$$\mathrm{H}(1s) + \mathrm{He}(1s^2) \rightarrow \mathrm{H}(1s, 2s, 2p_{0,\pm 1}) + \mathrm{He}(1s^2) \tag{1}$$

as a function of θ for various impact energies E. Such an approach has been followed by Bransden *et al* (1972) and by Sullivan *et al* (1972) for scattering of charged structureless particles (e and H^+) for target H(1s), and also by Berrington *et al* (1973) and by Begum *et al* (1973) for scattering of e and H^+ by $He(1s^2)$. Neutral-neutral collisions display, however, interesting differences.

2. Multistate theory

The basic formula for the amplitude of the scattering of two heavy particles of reduced mass M_{AB} and initial relative momentum k_i into the direction (θ, ϕ) about the Z-direction of incidence is given (Flannery and McCann 1973), in the centre-of-mass reference frame, by

$$f_{if}(\theta, \phi) = -\frac{ik_i}{2\pi}\int \exp i(\boldsymbol{K}\cdot\boldsymbol{R} + m_{if}\Phi)\exp(i\epsilon_{if}Z/\hbar v_i)\frac{\partial C_{if}}{\partial Z}\mathrm{d}\boldsymbol{R} \tag{2}$$

where the incident velocity $v_i = \hbar k_i/M_{AB}$. The momentum change $\boldsymbol{K}$ caused by the collision is $\boldsymbol{k}_i - \boldsymbol{k}_f$ and the final relative momentum k_f is directed along (θ, ϕ). The difference ϵ_{if} in the electronic energies between the initial (i) and final (f) states of both atoms is $\epsilon_i - \epsilon_f$, and $m_{if} = m_i - m_f$ is the change in the total azimuthal quantum numbers, with atomic axis of quantization along the incident direction. The nuclear-separation vector $\boldsymbol{R}$ has components (R, Θ, Φ) in a spherical polar frame, and (ρ, Φ, Z) in a cylindrical frame where ρ is the impact-parameter which lies perpendicular to the incident direction. The transition amplitude C_m satisfies the following set of (phase Φ-independent) first-order, coupled differential equations

$$\frac{\partial C_m(\rho, Z)}{\partial Z} = -\frac{i}{\hbar v_i}\sum_n C_n(\rho, Z)V'_{mn}(\rho, Z)\exp(i\epsilon_{mn}Z/\hbar v_i) \tag{3}$$

solved subject to the boundary condition $C_n(\rho, -\infty) = \delta_{ni}$, where i denotes the initial state of the collision system. The interaction matrix elements coupling the states i and k of the atoms are

$$V_{jk}(R) = \langle\Psi'_j(r)|V(r, R)|\Psi'_k(r)\rangle \tag{4}$$

where $V(r, R)$ is the instantaneous electrostatic interaction between the two neutral atoms at internuclear distance R, and where Ψ'_j are eigenfunctions for the isolated atoms with eigenenergies ϵ_j and composite electronic coordinates denoted by r.

When the Hartree–Fock potential of Strand and Bonham (1964) for $He(1s^2)$ is adopted, Flannery (1969) has shown that the interaction matrix elements $V_{jk}(R)$ can be determined as analytic functions of R. This potential for He is sufficiently accurate, since there is no observable difference in the calculated total cross sections when the potential is computed from very accurate form factors (cf Levy 1969). With this information, the set of coupled equations (3) can now be solved by customary numerical procedures.

In order to use the computed multistate transition amplitudes C_m, further simplification to (2) is required. This can be achieved by noting that, for heavy-particle collisions, the Z-component K_Z of the momentum change $\boldsymbol{K}$ can be expanded according to,

$$K_z = k_i - k_f\cos\theta \approx k_i - k_f = \frac{\epsilon_{fi}}{\hbar v_i}\left[1 + \frac{\epsilon_{fi}}{2M_{AB}v_i^2} + \ldots\right]. \tag{5}$$

Hence, in the heavy-particle limit, (2) reduces to

$$f_{if}(\theta, \phi) = \frac{ik_i}{2\pi}\int \exp(i\boldsymbol{K}'\cdot\boldsymbol{\rho})[\exp(im_{if}\Phi)C_{if}(\rho, \infty) - \delta_{if}]\,\mathrm{d}\boldsymbol{\rho} \tag{6}$$

where $K'^2 = K^2 - K_Z^2 = K^2 - \epsilon_{fi}^2/\hbar^2 v_i^2$ is the square of the momentum-change perpendicular to the direction of incidence along $\boldsymbol{k}_i$, and hence $\boldsymbol{K}'\cdot\boldsymbol{\rho} = K'\rho\cos(\phi - \Phi)$.

It is worth noting that K' appears in (6), in contrast to the total K as used by Bransden *et al* (1972) and by Berrington *et al* (1973). The Φ-integration in (6) can now be performed to give

$$f_{if}(\theta, \phi) = -ik_i i^{\Delta} e^{i\Delta\phi} \int_0^{\infty} J_{\Delta}(K'\rho)[C_f(\rho, \infty) - \delta_{if}]\rho \, d\rho \tag{7}$$

where J_{Δ} are Bessel functions of integral order $\Delta = m_{if}$.

The required differential and total cross sections are therefore,

$$\sigma_{if}(\theta) = 2\pi \frac{k_f}{k_i} |f_{if}(\theta, \phi)|^2. \tag{8a}$$

and

$$Q(r_i) = 2\pi \int_0^{\pi} |C_f(\rho, \infty) - \delta_{if}|^2 \rho \, d\rho = 2\pi \int_0^{\pi} \sigma_{if} \, d(\cos\theta) \tag{8b}$$

respectively.

A two-state treatment includes in (3) only the initial and final atomic states of the isolated atoms. In the four-state treatment other intermediate states are included eg for (1), the 1s, 2s, $2p_0$, $2p_{\pm 1}$ states are chosen such that the effect of the 2p–2s coupling on, say, the cross section for the 1s–2s transition can be assessed. Inclusion of coupling to higher hydrogenic states can be implicitly acknowledged by the use of 3s and 3p pseudo-states (Burke and Webb 1970), thus necessitating a seven-state calculation. We content ourselves at present to only a four-state calculation, since the addition of the extra pseudo-channels causes changes in the total cross section only at low incident speeds (cf Bell *et al* 1973), as expected.

2.1. Born, and unitarized Born approximations

The impact-parameter version of Born's approximation for elastic and inelastic scattering readily follows by inserting $C_n(\rho, Z) = \delta_{ni}$ into the right hand side of (3) with the usual result that

$$\frac{\partial C_f(\rho, Z)}{\partial Z} = -\frac{i}{\hbar v_i} V_{fi}(\rho, Z) \exp(i\epsilon_{fi} Z/\hbar v_i) \tag{9}$$

which is in a form suitable for use in (2) directly, without the need for approximation (5). Hence, on transforming from the cylindrical frame (ρ, Φ, Z) to the spherical-polar coordinate frame (R, Θ, Φ), (2) yields

$$f_{if}^{B}(\theta, \phi) = -\frac{1}{4\pi} \frac{2M_{AB}}{\hbar^2} \int V_{fi}(\boldsymbol{R}) \exp(i\boldsymbol{K}' \cdot \boldsymbol{R}) \, d\boldsymbol{R} \tag{10}$$

the Fourier transform of the interaction coupling the initial and final channels, a result identical with that obtained directly from the wave version of Born's approximation. The Born-approximation is valid only in the limit of high impact-energy and weak-interaction when the departure from probability-conservation is small.

For the special case of elastic scattering, a 'unitarized' Born approximation can be obtained by simply neglecting all inelastic channels with the result that (with $C_n = 0$,

$n \neq i$, in (3)),

$$C_i(\rho, Z) = \exp\left(-\frac{i}{\hbar v_i}\int_{-\infty}^{Z} V_{ii}(\rho, Z)\,dZ\right) \tag{11}$$

which always conserves probability and which also can be used directly in (2). By taking the first two terms of the expansion of the exponential in (11), the usual Born expression (10) for elastic scattering is then recovered from (7).

3. Results and discussion

By application of the preceding theory, differential cross sections have been calculated for the following processes.

$$H(1s) + He(1s^2) \rightarrow H(1s, 2s, \text{or } 2p_{0,\pm 1}) + He(1s^2) \tag{12}$$

as a function of scattering angle θ at various impact energies E.

3.1 Elastic scattering

In figures 1(*a*–*d*) are displayed the computed cross sections σ^B, σ^U and σ^F as given by the Born, unitarized-Born, and four-state approximations, respectively, for the elastic process in (12). Several distinctions emerge:

(a) For elastic scattering in the forward direction $\theta = 0$, σ^B vanishes in contrast to the finite values (which decrease with energy-increase) given by both σ^U and σ^F. This zero arises from the fact that the form factor $F_{ij}^H(K)$ for hydrogen in the customary expression obtained from (10),

$$f_{ij}(\theta, \phi) = -\frac{2M_{AH}e^2}{\hbar^2 K^2}[2 - F_{11}^{He}(K)][\delta_{ij} - F_{ij}^H(K)] \tag{13}$$

for the Born-scattering amplitude, tends to zero as $K \rightarrow 0$, while the corresponding elastic form factor F_{11}^{He} for helium $\sim 2 + K^2$. Thus the static H–He interaction $V_{ii}(R)$ vanishes when integrated over all R, a remarkable result in direct contrast with both ion-neutral elastic collisions and with neutral-neutral inelastic collisions for which $\sigma^B(0) > 0$. It is noted that equation (13) only follows from (10) when electron-exchange effects are explicitly neglected.

(b) That both σ^U and σ^F are close throughout the entire energy and angular ranges is a manifestation that the diagonal interaction V_{ii} is dominant and that the influence of the $n = 2$ channel, is comparatively weak for elastic collisions.

(c) As θ increases, σ^U (and therefore σ^F) initially decreases to a minimum at θ_0, rises to a maximum at θ_1, and ultimately approaches the Rutherford cross section, decreasing as $(2E\sin^2\frac{1}{2}\theta)^{-2} \sim (E\theta^2)^{-2}$ for large θ and E. The initial decrease is attributed to the fact that the Bessel function $J_0(K'\rho = 2k_i \sin\frac{1}{2}\theta)$ in (7) controls the behaviour of f_{ii} at small θ (since the transition amplitudes $C_f(\rho, \infty)$ vary only slowly for the distant encounters which are responsible). The function $J_0(x)$ decreases from unity with gradient $(-J_1)$ to zero at $x \approx 2{\cdot}4$ and reaches a minimum at $x \approx 4$, a behaviour which is reflected in the minimum and the maximum respectively, of σ^U and σ^F. Subsequent oscillations occurring in J_0 at the larger scattering angles are suppressed by the much more rapid variation in the transition amplitude C_f for the closer encounters that are involved at larger angles.

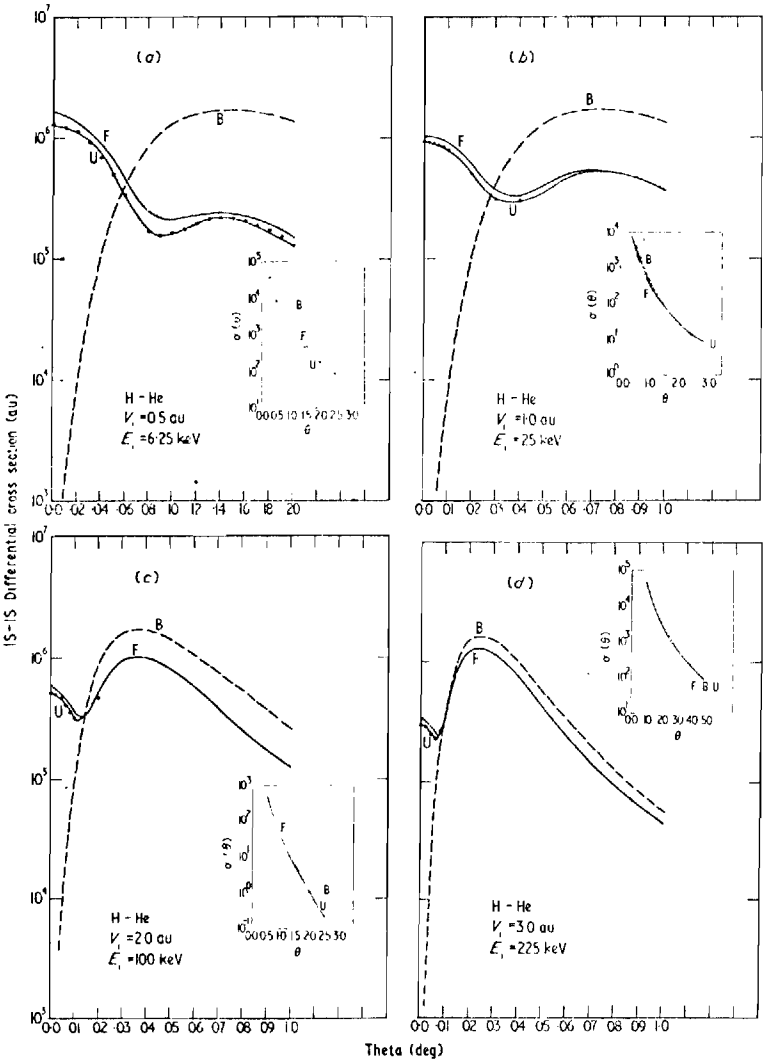

Figure 1. Differential cross sections for the elastic scattering of H(1s) by He($1s^2$) at (*a*) 6·25 keV (*b*) 25 keV (*c*) 100 keV and (*d*) 225 keV incident energy E_i. B: Born approximation. U: unitarized-Born approximation. F: four-state approximation.

(d) As E increases, both θ_0 and θ_1 shift toward the forward direction and σ^B tends to σ^U and σ^I throughout *most* of the angular range, *except* in the forward direction. This incorrect behaviour of $\sigma^B(\theta)$, for θ small, does not vanish at high impact energies, even though the interaction V_{ij} at the distant encounters involved is weak. This inherent defect of Born's approximation is attributable to the lack of conservation of probability and to the violation of the optical theorem (since f^B is always real). The resulting error however is minimized (but is never removed) for high E, since it is confined only to an ever decreasing angular region. The contribution arising from this region to the *total* cross section becomes, of course, relatively minute.

In conclusion, the Born approximation underestimates the scattering at small θ, and overestimates the scattering at larger θ. The overestimate vanishes for higher impact energies while the underestimate, although minute, remains.

3.2. *Inelastic scattering*

In figures 2(*a–d*) are displayed differential cross sections for the 1s–2s collisional excitation in H by He. Both σ^B and σ^I yield non-zero values at $\theta = 0$, and as E increases, the initially higher $\sigma^B(0)$ diminishes much faster than $\sigma^I(0)$ until it lies well below $\sigma^I(0)$.

In the intermediate angular region, the significant difference between σ^I and σ^B becomes reduced at high E. However, σ^I exhibits a much slower fall-off than $\sigma^B \sim (E\theta^2)^{-6}$, for large θ. This behaviour is expected and arises from the fact that the multistate treatment provides a more detailed description of the distortion interaction at the close encounters which are responsible for the large angles of scattering.

In summary, the Born description fails at both small and large scattering angles, although at high impact energies, σ^B and σ^I tend to agree in the intermediate angular region. The region which provides the dominant contribution to the total cross section.

The corresponding cross sections for the 1s–2p transition are shown in figures 3 (*a–d*). Here $\sigma^B(0)$ and $\sigma^I(0)$ are again non-zero, but lie much closer than that observed for the 1s–2s excitation. The coupling interaction V_{1s2p} has longer-range than V_{1s2s} and is, for the distant encounters responsible for the forward scattering, therefore less influenced by the distortion which is important only for the closer impacts and which is included in the multistate treatment. At large scattering angles, σ^I falls off, as expected, more slowly than $\sigma^B \sim (E\theta^2)^{-7}$, but faster than σ^I for the 1s–2s transition.

Finally, the cross sections for excitation of the substates $2p_0$ and $2p_{\pm 1}$ are shown together in figures 4 (*a–d*). The $2p_0$ cross sections are non-zero at $\theta = 0$ where $\sigma_{2p\pm 1}$ vanish. There is overall agreement with Born's approximation except, of course, at the larger scattering angles where $\sigma^F_{2p_0} > \sigma^F_{2p_{\pm 1}} > \sigma^B_{2p_{\pm 1}} > \sigma^B_{2p_0}$, which are all several orders of magnitude less than the cross-section maxima. For low E and small θ, the main contribution to the 2p cross section arises from $2p_0$ excitation, a contribution which rapidly diminishes as E is increased until the $2p_{\pm 1}$ excitation dominates the cross section at the largest E.

Two-state calculations have also been performed and the computed cross sections σ^T are indistinguishable from the four-state cross sections except for the forbidden 1s–2s transition for which $\sigma^T(\theta)$ lies somewhat below $\sigma^I(\theta)$, as expected, but only in a small angular region $0 < \theta < \theta_1$. The angle θ_1 becomes very small with increasing impact energy.

In conclusion, the Born-approximation fails to describe scattering in the forward direction for all collisions between neutrals. In addition, for inelastic collisions, it also fails to provide an adequate description of large-angle scattering.

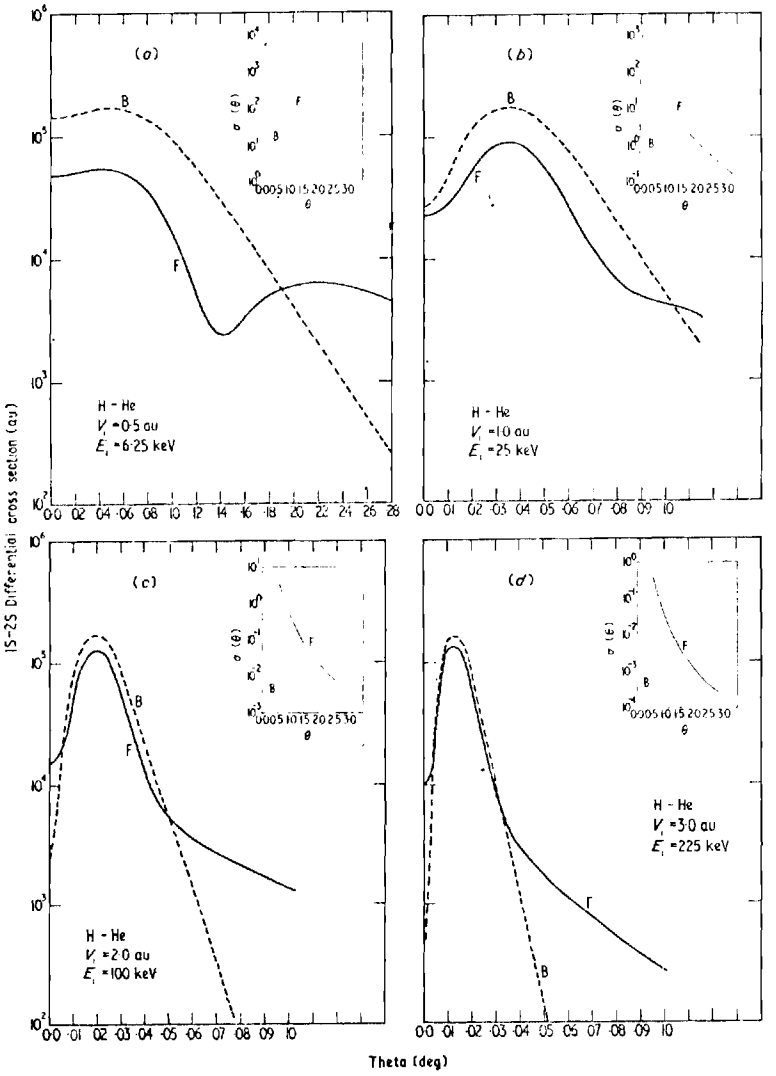

Figure 2. Differential cross sections for the 2s-excitation of atomic hydrogen by He($1s^2$) at (*a*) 6·25 keV (*b*) 25 keV (*c*) 100 keV and (*d*) 225 keV incident energy E_i. B: Born approximation. F: four-state approximation.

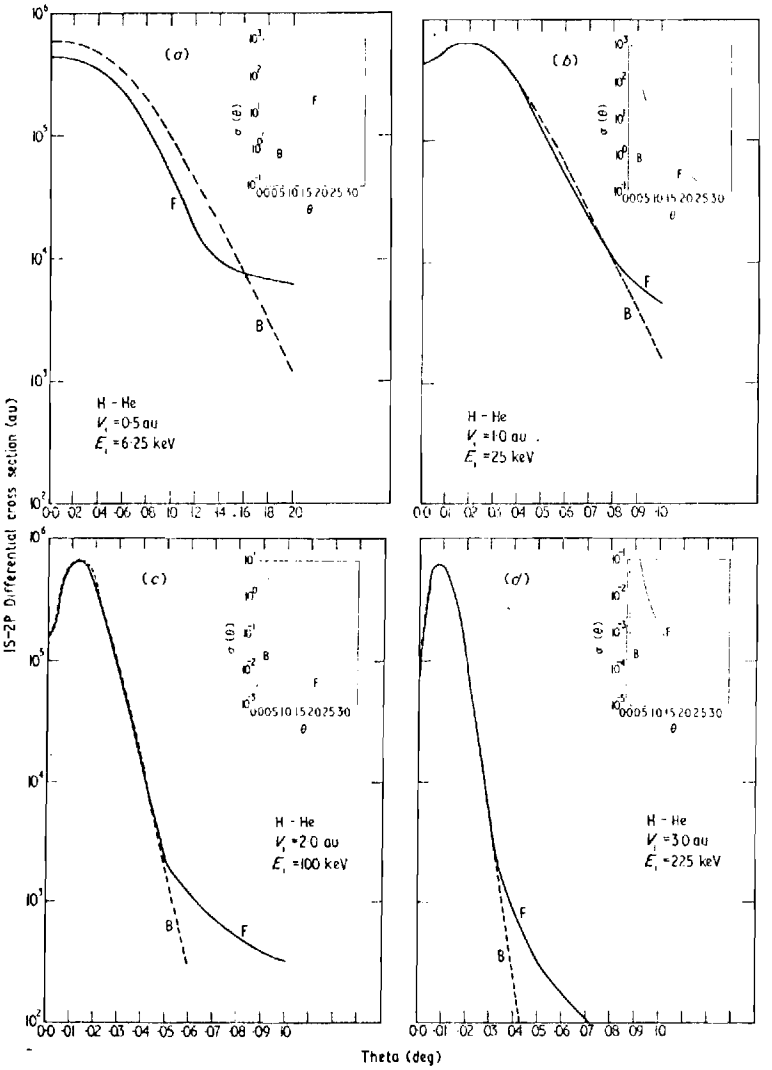

Figure 3. Differential cross sections for the 2p-excitation of atomic hydrogen by He($1s^2$) at (*a*) 6·25 keV (*b*) 25 keV (*c*) 100 keV and (*d*) 225 keV incident energy E_i. B: Born approximation. F: four-state approximation.

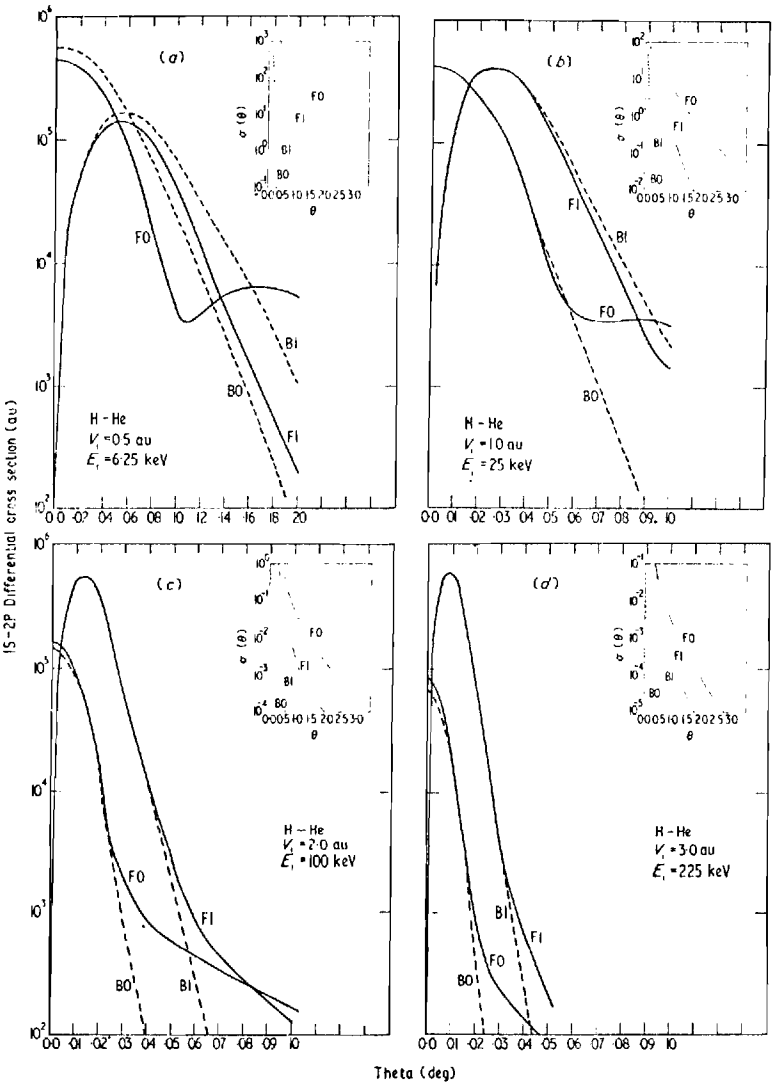

Figure 4. Differential cross sections for the $2p_0$ and $2p_{\pm 1}$ excitations of atomic hydrogen by He($1s^2$) at (*a*) 6·25 keV (*b*) 25 keV (*c*) 100 keV and (*d*) 225 keV incident energy E_i.
B0 and B1 : Born approximations for $2p_0$ and $2p_{\pm 1}$ excitations respectively.
F0 and F1 : four-state approximations for $2p_0$ and $2p_{\pm 1}$ excitations respectively.

References

Begum S, Bransden B H and Coleman J P 1973 *J. Phys.* B: *Atom. molec. Phys* **6** 837–40
Bell, K L, Kingston A E and McIlveen W A 1973 *J. Phys.* B. *Atom. molec. Phys* **6** 1246–54
Berrington K A, Bransden B H and Coleman J P 1973 *J. Phys.* B: *Atom. molec. Phys.* **6** 436–49
Bransden B H, Coleman J P and Sullivan J 1972 *J. Phys.* B: *Atom. molec. Phys.* **5** 546–58
Burke P B and Webb T G 1970 *J. Phys.* B: *Atom. molec. Phys.* **3** L131–4
Flannery M R 1969a *Phys. Rev.* **183** 231–40
—— 1969b *Phys. Rev.* **183** 241–4
—— 1969c *J. Phys.* B: *Atom. molec. Phys.* **2** 913–22
Flannery M R and McCann K J 1973 *Phys. Rev.* A **8** 2915–21
Levy H 1969a *Phys. Rev.* **185** 7–15
—— 1969b *Phys. Rev.* **187** 136–42
Strand T G and Bonham R A 1964 *J. chem. Phys.* **40** 1686–91
Sullivan J, Coleman J P and Bransden B H 1972 *J. Phys.* B. *Atom. molec. Phys.* **5** 2061–5

APPENDIX V

ELASTIC AND 2s AND 2p INELASTIC SCATTERING OF ATOMIC HYDROGEN BY HELIUM-IONS

This appendix is a reprint of the proof of an article which will appear in the Journal of Physics B: Atom. Molec. Phys., 1974.

J. Phys. B: Atom. Molec. Phys., Vol. 7.

Elastic and 2s and 2p inelastic scattering of atomic hydrogen by helium-ions

M R Flannery and K J McCann

School of Physics, Georgia Institute of Technology, Atlanta, Georgia 30332, USA

Received 13 December 1973

Abstract. Differential cross sections are presented in the Born, Unitarized Born, two- and four-state treatments of the elastic and the 2s and 2p inelastic scattering of H(1s) by $He^+(1s)$, with impact speeds v_i in the range $0.5 \leqslant v_i \leqslant 3$ au. For elastic collisions, the Born approximation is successful only for large-angle scattering while for inelastic scattering it fails completely for large angles at all v_i, and for small angles at low v_i, when the effects of couplings to other close channels are important. Corresponding treatments are also carried out for H^+–H(1s) collisions, which represent the behavior of $He^+(1s)$–H(1s) collisions in the limit of high-impact-energies when the valence electron in $He^+(1s)$ completely screens its parent nucleus.

1. Introduction

Total cross sections for the excitation processes,

$$He^+(1s) + H(1s) \rightarrow He^+(1s) + H(2s \text{ or } 2p) \tag{1}$$

were previously determined (Flannery 1969) from a four state impact-parameter method, valid for the keV energy-range. Comparison with a corresponding treatment for incident protons revealed that He^+ in (1) behaved almost as a singly-charged structureless particle at high impact-energies.

A recent theory (Flannery and McCann 1973), which incorporated the multistate impact-parameter description for the internal electronic motions together with the eikonal approximation for the relative motion of the colliding species, was used to determine the differential cross sections as a function of scattering angle for H–H and H–He collisions (Flannery and McCann 1974a,b). In particular, this method provided elastic cross sections which are not calculable from the customary impact-parameter description of total cross sections (cf Bates 1961) alone.

In contrast to these neutral–neutral collisions, where the interactions are all short-range, the processes in (1) involve long-range ion-dipole interactions. In an effort to assess the relative influence of the 2p–2s, 2p–1s and other distortion couplings, we will present in this paper the differential cross sections in the Born, unitarized-Born, two-state and four-state treatments of the processes (1).

2. Theory

The basic expression for the amplitude for scattering into (θ, ϕ) in the center-of-mass

system is (Flannery and McCann 1973)

$$f_{if}(\theta, \phi) = -\frac{ik_i}{2\pi}\int \exp i(\boldsymbol{K}\cdot\boldsymbol{R} + m_{if}\Phi)\exp(i\varepsilon_{if}Z/\hbar v_i)\frac{\partial C_f(\rho, Z)}{\partial Z}\,d\boldsymbol{R} \tag{2}$$

where $\boldsymbol{k}_i$ is the initial relative momentum ($M_{AB}v_i$) directed along the polar axis, $\boldsymbol{K}$ is the momentum-change $\boldsymbol{k}_i - \boldsymbol{k}_f$ caused by the collision which also induces an $i \to f$ electronic transition. The nuclear separation of the colliding species with relative speed v_i, with reduced mass M_{AB}, is $\boldsymbol{R} = (R, \theta, \Phi) \equiv (\rho, \Phi, Z)$, and $\varepsilon_{if} = \varepsilon_i - \varepsilon_f$ and m_{if} are the resulting changes in the electronic energy and azimuthal quantum number respectively. The phase-independent transition amplitudes C_m satisfy the set of coupled differential equations,

$$\frac{\partial C_m(\rho, Z)}{\partial Z} = -\frac{i}{\hbar v_i}\sum_n C_n(\rho, Z)V_{mn}(\rho, Z)\exp(i\varepsilon_{mn}Z/\hbar v_i) \tag{3}$$

which are solved subject to the condition $C_m(\rho, -\infty) = \delta_{mi}$ where i labels the initial state of the collision system. The matrix elements coupling the various electronic states are

$$V_{jk}(\boldsymbol{R}) = \langle\Psi_j(\boldsymbol{r}_1, \boldsymbol{r}_2)|V(\boldsymbol{r}_1, \boldsymbol{r}_2, \boldsymbol{R})|\Psi_k(\boldsymbol{r}_1, \boldsymbol{r}_2)\rangle, \tag{4}$$

the instantaneous electrostatic interaction V averaged over the electronic wavefunctions Ψ_j which are eigenfunctions with eigenenergy ε_j of the Hamiltonian of the atomic systems at infinite nuclear separation. The basis set $\Psi_j(\boldsymbol{r}_1, \boldsymbol{r}_2)$ is taken as $\phi^1_{n_1 l_1 m}(\boldsymbol{r}_1)\phi^2_{n_2 l_2 m}(\boldsymbol{r}_2)$ where $\phi^Z_{nlm}(\boldsymbol{r})$ describe the hydrogenic system of charge Z (ie electron-exchange and electron-capture effects are explicitly excluded). The interactions appropriate for a four-state treatment of $H^+ + H$ and of $He^{++} + H$ are then already available (Flannery 1969) as analytical functions of R. With this knowledge, equations (3) can be solved by customary numerical procedures for the complex transition amplitudes C_m. Further progress is achieved by noting for heavy-particle collisions that K_z, the z-component of the momentum-change $\boldsymbol{K}$ is

$$K_z = k_i - k_f\cos\theta \approx k_i - k_f = \frac{\varepsilon_{fi}}{\hbar v_i}\left(1 + \frac{\varepsilon_{fi}}{2M_{AB}v_i^2} + \ldots\right). \tag{5}$$

thereby permitting simplification to (2). On performing the Φ-integration, (2) therefore reduces to

$$f_{if}(\theta, \phi) = -ik_i^{\Delta}e^{i\Delta\phi}\int_0^{\infty} J_{\Delta}(K'\rho)[C_f(\rho, \infty) - \delta_{if}]\rho\,d\rho \tag{6}$$

where J_{Δ} are Bessel functions of integral order $\Delta = m_{if}$, and $K'^2 = K^2 - K_z^2$.

The required differential and total cross sections are respectively

$$\sigma_{if}(\theta) = 2\pi\frac{k_f}{k_i}|f_{if}(\theta, \phi)|^2 \tag{7a}$$

which involves both the magnitude and relative phase of the transition amplitude C_f and

$$Q(v_i) = 2\pi\int_0^{\infty}|C_f(\rho, \infty) - \delta_{if}|^2\rho\,d\rho = \int_{-1}^{+1}\sigma_{if}(\theta)\,d(\cos\theta) \tag{7b}$$

which, for excitation, depends only on the magnitude of C_f.

The Born approximation follows by inserting $C_n(\rho, Z) = \delta_{ni}$ into the RHS of (3) and so (2) can be used directly to give

$$f_{ii}^{B}(\theta, \phi) = -\frac{1}{4\pi}\frac{2M_{AB}}{\hbar^2}\int V_{ii}(R)\exp(iK \cdot R)\,dR \tag{8}$$

which is the usual scattering amplitude, as derived from a Born-wave description. Moreover, a 'unitarized' Born approximation for elastic scattering follows by substituting $C_n = C_i\delta_{ni}$ in (3) to give

$$C_i(\rho, Z) = \exp\left(-\frac{i}{\hbar v_i}\int_{-\infty}^{Z} V_{ii}(\rho, Z)\,dZ\right) \tag{9}$$

which can also be used directly in (2), and which always conserves probability but ignores couplings to all excitation channels.

3. Results and discussion

By application of the preceding theory, differential cross sections have been computed for the processes

$$He^+(1s) + H(1s) \rightarrow He^+(1s) + H(1s, 2s, 2p_{0,\pm 1}) \tag{10}$$

in the incident velocity-range $0.5 \leqslant v_i \leqslant 3$ au. Corresponding treatments were also carried out for incident protons H^+.

3.1. Elastic scattering

For elastic scattering, the Born, Unitarized-Born and four-state differential cross sections, B, U and F, respectively, are displayed as computer-drawn graphs in figure 1 for various (hydrogen-impact) energies $E_i (\equiv 25 v_i^2$ keV). In general, U and F show closer agreement over the entire angular range than B which approaches agreement only for large v_i.

It is noted, for elastic scattering in the forward direction $\theta = 0$, that $\sigma^B(0)$ yields a non-zero value, which is constant for all impact energies E_i, and which is in marked contrast to the zero cross section exhibited for neutral-neutral collisions (cf. Flannery and McCann 1974a,b). This distinction arises from the fact that $\int_{-\infty}^{\infty} V_{ii}(R)\,dZ$ is identically zero for atom–atom collisions, (when electron-exchange is neglected in (4)), and is non-zero for ion-neutral collisions. The difference is also theoretically evident from examination of the Born amplitude (in au)

$$f_{ii}^{B}(\theta) = -\frac{2M_{AB}}{K^2}[Z_A - F_{ii}^{A}(K)][Z_B - F_{ii}^{B}(K)] \tag{11}$$

for scattering of a hydrogenic system B of charge Z_B by a similar system A of nuclear charge Z_A. As $\theta \rightarrow 0$ for elastic form factor F_{1s1s}^{A} for system A $\sim 1 - K^2/2Z_A^2$ with the result that $\sigma^B(0) = 0$, only for $Z_A = Z_B = 1$. When $Z_A = 1$ and $Z_B > 1$, then

$$\sigma^B(0) = 2\pi M_{AB}^2 (Z_B - 1)^2 a_0^2,$$

(ie increasing the reduced mass and increasing the projectile nuclear charge causes increased scattering in the forward direction).

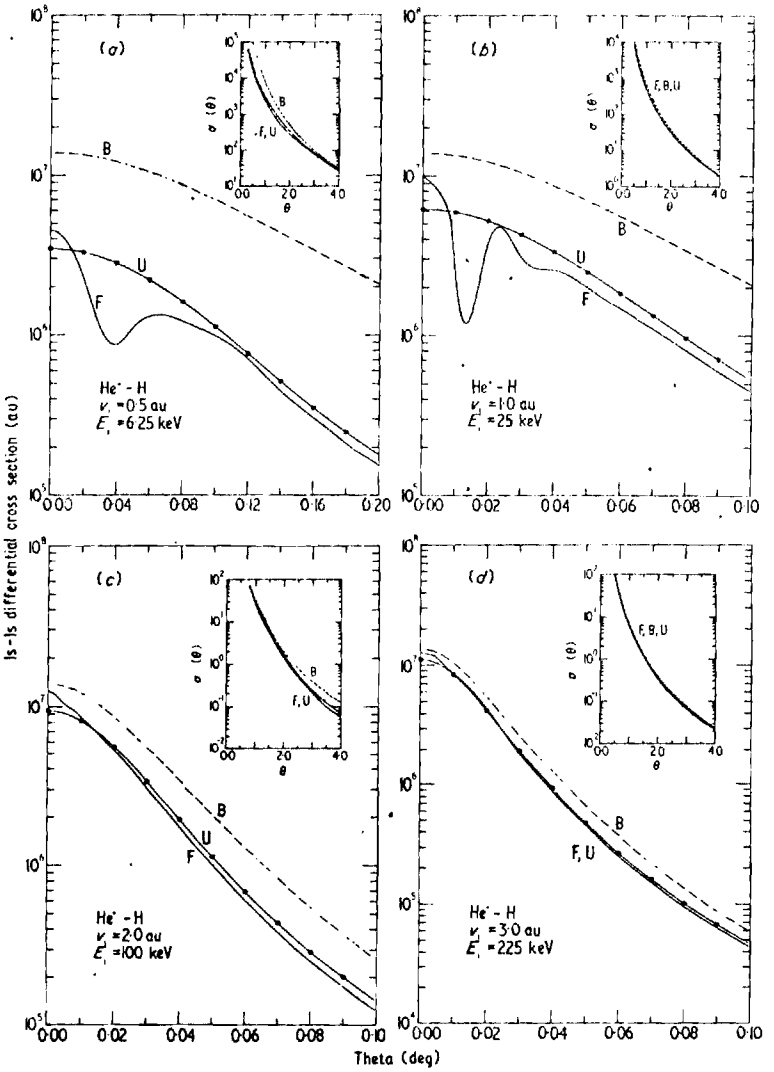

Figure 1. Differential cross sections for He^{+}–H(1s) elastic scattering at (*a*) 6·25 keV (*b*) 25 keV (*c*) 100 keV and (*d*) 225 keV incident H(1s) energy. B, Born approximation; U, Unitarized Born approximation; F, Four-state approximation

We also note, as the impact-energy is increased, that both $\sigma^{II}(0)$ and $\sigma^{I}(0)$ approaches this constant Born value, and the scattering is, not only becoming more concentrated in the forward direction, but is also becoming more intense.

At small and intermediate scattering angles the main difference (which becomes negligible at high E_i), between B, U and F can be attributed to the conservation of probability rather than to the coupling to other levels. The structure in F is presumably due to fact that as θ increases from zero, the decreasing $2p_0$ excitation cross section $\gg$ the increasing $2p_{+1}$ excitation cross section such that the contribution from the 2p channel to the elastic 1s channel initially decreases, until the increasing $2p_{\pm 1}$ excitation is large enough to cause an enhancement to the elastic scattering via the $2p_{\pm 1} - 1s$ coupling (see figure 4).

At large scattering angles ($\theta > 1°$), all the computed cross sections tend to the same Rutherford elastic scattering limit of $(8E^2 \sin 4\frac{1}{2}\theta)^{-1}$ where E is the kinetic energy $\frac{1}{2}M_{AB}v_i^2$ of relative motion. These large angles result from very close penetrating encounters which are dominated by the nuclear-nuclear interaction, and Born's approximation, while failing for strong interactions, nevertheless yields the exact differential cross section for the Coulombic interaction. This is the essential reason why Born's approximation is successful for large angle elastic scattering.

Comparison with the multistate treatment therefore reveals that for small angle scattering the unitarized Born description provides vast improvement over the customary Born Approximation, which describes only large-angle scattering adequately.

3.2. Inelastic scattering

In figures 2 and 3 are displayed the Born, two-state and four-state differential cross sections, B, T and F, respectively, for the 2p and 2s excitations at various impact speeds v_i. These sets of figures reveal, in general, that the Born approximation fails markedly for large-angle scattering. This expected result arises from the failure of Born's approximation to adequately describe the non-Coulombic close encounters that are responsible. In contrast with the elastic case, the nuclear–nuclear Coulombic interaction (for which the Born approximation yields the *exact* excitation probability) is ineffective for excitation.

We also observe by comparison, that the 2p–2s coupling in F increases the 2s-cross section more than it decreases the 2p-excitation, except for scattering in the forward direction when both excitations are enhanced. The structure in F for $v_i \approx 0{\cdot}5$ au at $\theta \sim 0{\cdot}04°$ may be attributed to the effect of the $2p_0$–$2p_{\pm 1}$ rotational coupling included in the four-state case, rather than the 2p–2s coupling. The rotational coupling is introduced to theoretically acknowledge the tendency of the atomic axis of quantization to follow the rotation of the internuclear line at low incident speeds, rather than remaining fixed in the Z-direction as it does at high incident speeds. This coupling therefore permits the model to assume molecular properties in that the molecular complex instantaneously formed becomes increasingly quantized along the internuclear line as v_i is reduced.

The effect of the individual $2p_0$ and $2p_{\pm 1}$ cross sections is examined further in figure 4, where 2-state and 4-state cross sections, T and F respectively are shown at $v_i = 0{\cdot}5$ au. In general, for scattering in the forward direction, the $2p_0$ cross section is maximum and the $2p_{\pm 1}$ excitations are negligible until larger angles are reached. The $2p_0$–$2p_{\pm 1}$, R^{-3} coupling introduces structure into the $2p_{\pm 1}$ cross section. This structure is then reproduced in the 2s-excitation via both $2p_{0,\pm 1}$–2s dipole R^{-2} couplings. Also this structure is reflected in the 2p cross section, the sum of the individual substate contributions.

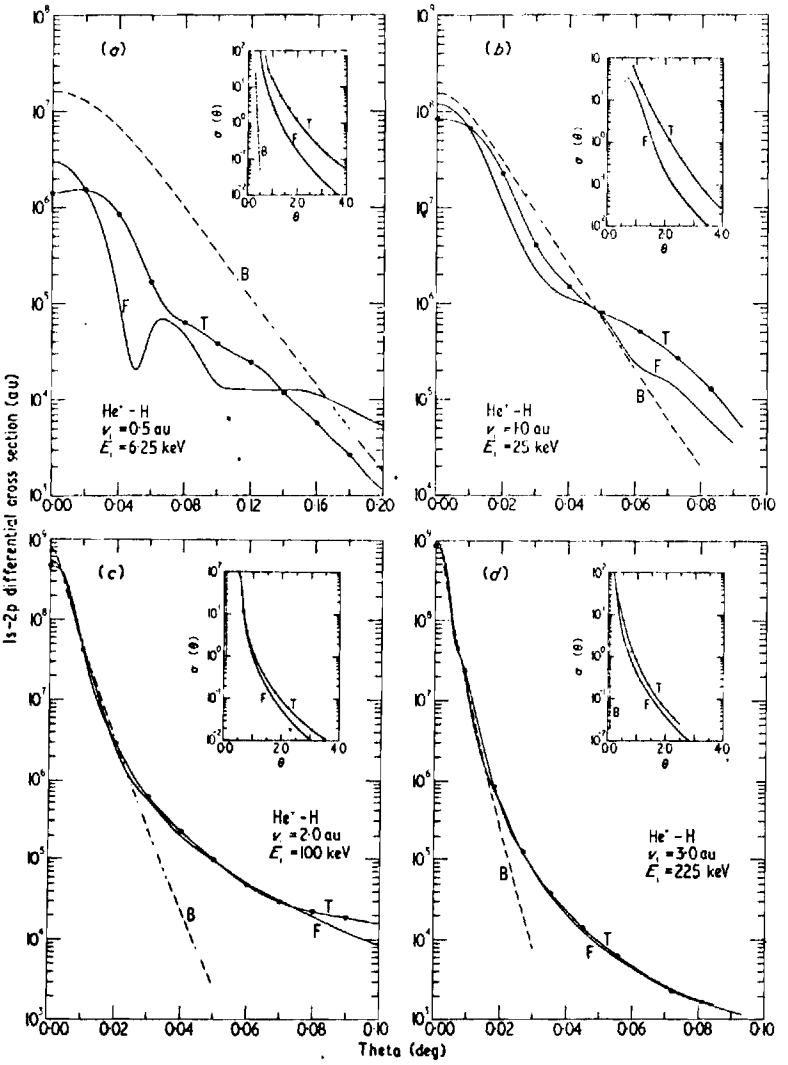

Figure 2. Differential cross sections for the 2p-excitation of atomic hydrogen by $He^+(1s)$ at (*a*) 6·25 keV, (*b*) 25 keV, (*c*) 100 keV and (*d*) 225 keV incident H(1s) energy. B, Born-approximation; T, Two-state approximation; F, Four-state approximation.

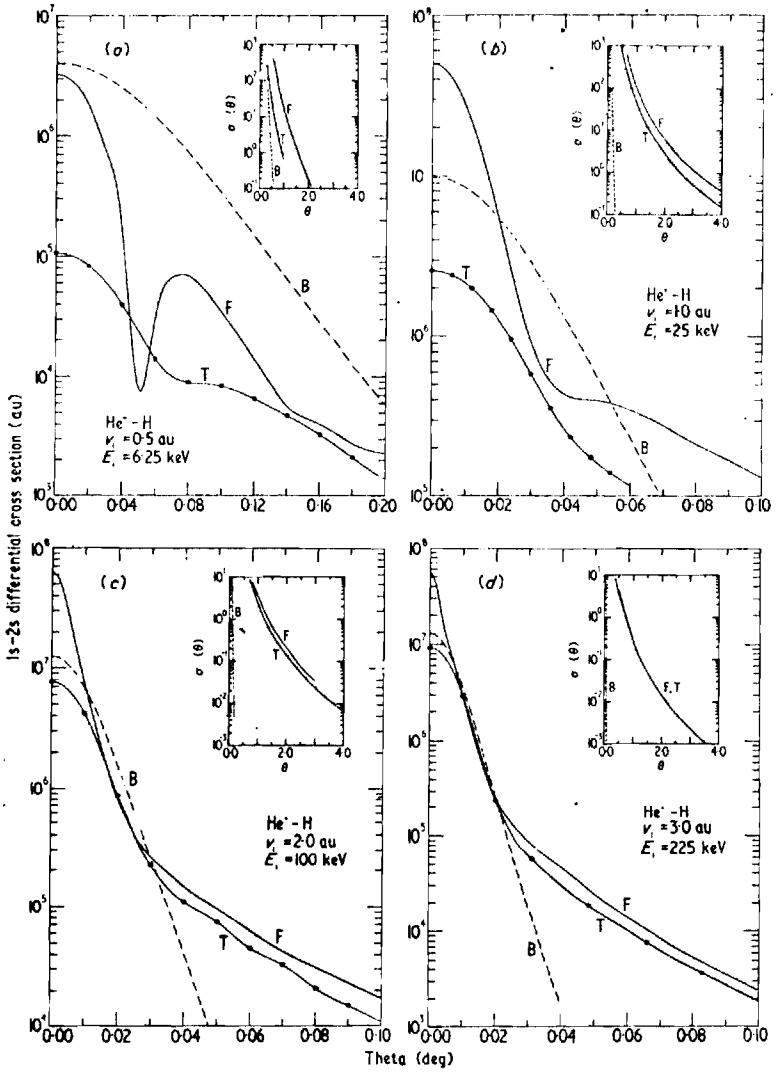

Figure 3. Differential cross sections for the 2s-excitation of atomic hydrogen by $He^+(1s)$ at (*a*) 6·25 keV, (*b*) 25 keV, (*c*) 100 keV and (*d*) 225 keV incident H(1s) energy. B, Born-approximation; T, Two-state approximation; F, Four-state approximation.

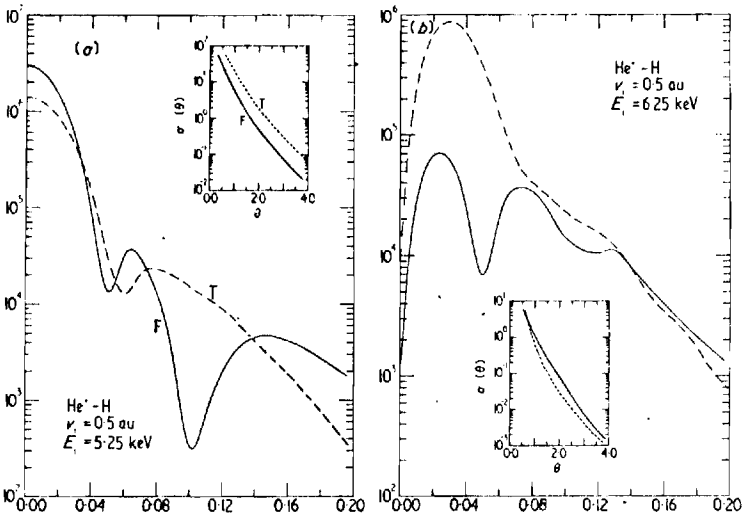

Figure 4. Differential cross sections for (*a*) $2p_0$ and (*b*) $2p_{\pm 1}$ excitations of atomic hydrogen by $He^+(1s)$ at 6·25 keV incident H(1s) energy. T, Two-state approximation; F, Four-state approximation.

Graphs for the substate excitations at $v_i = 1, 2$ and 3 au are available upon request, the only difference with figure 4 being the disappearance of the structure associated with the rotational coupling.

In conclusion, the Born approximation for excitation is inadequate for large angle scattering at all energies, and it fails for small angle scattering when coupling-effects become important at low impact energies.

3.3. H^+–H(1s) collisions

In an effort to examine the effectiveness of the screening of the helium nucleus by its orbital electron, corresponding calculations have been carried out for H^+–H(1s) elastic and inelastic collisions, with electron-capture channels excluded. Rather than presenting all the actual graphs (which are available upon request), it suffices to report that the general features already exhibited in figures 1–4 were preserved, although the differences between F, T, B and U were amplified, particularly at the lower impact energies (see figure for $v_i = 0{\cdot}5$ au). The cross sections were in general smaller, but did approach at high impact energies those for He^+–H(1s) *inelastic* collisions, only. The elastic cross sections were higher at $v_i = 0{\cdot}5$ and lower at $v_i = 3$ au.

3.4. Total cross sections

The total cross sections can be calculated either by integrating the differential cross section over all scattering angles, or by integrating the transition probabilities $|C_{fi}|^2$ over all impact-parameters, as in equation (7*b*). Table 1 displays the angular-integrated

Table 1. Four-state total cross sections (au) for (*a*) He^+–H and (*b*) H^+–H elastic and inelastic collisions

i–f	1s–1s		1s–2s		1s–2p$_0$		1s–2p$_{\pm1}$		1s–2p	
v_i	*a*	*b*	*a*	*b*	*a*	*b*	*a*	*b*	*a*	*b*
0·5	6·44^{0}†	7·42^{0}	4·29^{-1}	3·42^{-1}	2·86^{-1}	2·36^{-1}	9·08^{-2}	7·87^{-2}	3·77^{-1}	3·15^{-1}
1·0	3·55^{0}	3·30^{0}	2·12^{0}	1·92^{0}	2·12^{0}	1·95^{0}	1·41^{0}	1·28^{0}	3·53^{0}	3·23^{0}
2·0	1·83^{0}	1·42^{0}	6·25^{-1}	5·62^{-1}	1·51^{0}	1·45^{0}	1·89^{0}	1·08^{0}	3·40^{0}	3·25^{0}
3·0	1·80^{0}	7·32^{-1}	2·38^{-1}	2·13^{-1}	7·61^{-1}	7·49^{-1}	1·39^{0}	1·33^{0}	2·15^{0}	2·08^{0}

† The superscript gives the power of 10 by which the entry must be multiplied.

1.80°

1.08°

total cross sections for both incident He^+ and H^+ ions. These inelastic cross sections almost exactly agree with those calculated by p-integration. The elastic cross sections decrease monotonically with v_i and at $v_i = 1$ au are equal with those for the 2p-excitation which thereafter dominates the scattering for $v > 1$ au.

In summary, we have presented graphical displays of the behavior of the differential cross section for elastic and inelastic He^+–H scattering in the keV-energy region. The graphs demonstrate that the Born approximation is successful for elastic scattering only at large scattering angles when it tends to the (correct) limit of the Rutherford cross section. Elastic scattering of ground-state species is affected more by departures from probability conservation than from neglect of coupling to higher excited states, although these couplings do introduce structure for small-angle scattering at low impact energies.

For inelastic scattering the Born approximation fails both at large angles for all incident speeds v_i and at small angles for low $v_i < 1$ au. However, for high v_i, the contribution to the *total* cross section from the large angle scattering is very small in comparison to the contribution from the scattering concentrated in the forward direction, with the result that the Born approximation yields the correct high-energy limit. For low $v_i < 1$ au, a multistate description including 2p–2s and rotational coupling is essential.

Comparison with a corresponding treatment for H^+–H collisions demonstrates that the absence of an orbiting electron (with its repulsive effect) amplifies the general differences between B, U, T, and F for He^+–H collisions.

In the above multistate description of the ion-atom collisions, electron-capture channels have been explicitly neglected. The influence of these channels is expected to contribute only at low incident speeds $v_i < 1$ au. Here the actual effect of coupling of the excited direct channels in He^+–H(1s) collisions to the near-degenerate H^+–He(1s 2s) and H^+–He(1s 2p) levels is difficult to assess without resort to a much more elaborate eight-state treatment. Even with this modification, at these incident speeds, the validity of a truncated atomic basis expansion in the impact-parameter description is questionable.

References

Bates D R 1961 *Quantum Theory*, I. *Elements* (New York: Academic Press) pp 251–97

Flannery M R 1969 *J. Phys.* B: *Atom. molec. Phys.* **2** 1044–54

Flannery M R and K J McCann 1973 *Phys. Rev.* **8** 2915–21

Flannery M R and K J McCann 1974a *Phys. Rev.* (to be published)

Flannery M R and K J McCann 1974b *J. Phys.* B: *Atom. molec. Phys.* (accepted)

APPENDIX VI

ELASTIC AND THE 2 ^{1}S and 2 ^{1}P INELASTIC DIFFERENTIAL CROSS SECTIONS FOR PROTON-HELIUM SCATTERING

This appendix is a copy of the proofs of an article which will appear in the Journal of Physics B: Atom. Molec. Phys., 1974.

J. Phys. B: Atom. Molec. Phys., Vol. 7.

Elastic and the 2 ^{1}S and 2 ^{1}P inelastic differential cross sections for proton–helium scattering

M R Flannery and K J McCann
School of Physics, Georgia Institute of Technology, Atlanta, Georgia 30332, U.S.A.

Received 21 January 1974

Abstract. Differential cross sections for H^+–$He(1s^2)$ elastic and inelastic collisions in the keV-energy region are calculated using various approximate schemes

Although total excitation cross sections for H^+–$He(1s^2)$ collisions have already been reported (Flannery 1970, Begum *et al* 1973, Baye and Heenen 1973), knowledge of the corresponding differential cross sections $\sigma(\theta)$ as a function of scattering angle is absent. As a complement to the earlier work (Flannery 1970) in which the effect on total excitation cross sections of various approximations was assessed and in order to provide some theoretical input for experimental comparison as a test of the basic model, differential cross section $\sigma(\theta)$ are presented for the following processes

$$H^+ + He(1s^2) \rightarrow H^+ + He(1\,^1S, 2\,^1S, 2\,^1P). \tag{1}$$

The basic expression for $\sigma(\theta)$ in the CM-frame is (Flannery and McCann 1973)

$$\sigma(\theta) = \frac{k_i k_f}{2\pi} a_0^2 \left| \int \exp(i\boldsymbol{K}\cdot\boldsymbol{R} + i\Delta\Phi + \mathscr{E}_{if}Z/\hbar v_i)\frac{\partial C_f}{\partial Z}(\rho, Z)\,d\boldsymbol{R}\right|^2 \tag{2}$$

which, for heavy-particle collisions, reduces to

$$\sigma(\theta) = 2\pi a_0^2 k_i k_f \left| \int_0^\infty J_\Delta(K'\rho)[\underline{c}_f(\rho,\infty) - \delta_{if}]\rho\,d\rho\right|^2 \tag{6}$$

where k_i and k_f are the initial and final relative momenta of the colliding particles of reduced mass M_{AB}, $\mathscr{E}_{fi}$ is the internal energy change, and K' is the component of the momentum-change $\boldsymbol{K}$ along $\boldsymbol{\rho}$, the impact-parameter, which is perpendicular to the Z-direction of incidence. The Bessel functions J_Δ are of integral order $\Delta = m_i - m_f$, the change in azimuthal quantum number. The transition amplitudes $C_f(\rho,\infty)$, in general complex, are the solutions of a set of first-order coupled differential equations, thereby allowing the construction of various approximate schemes—Born, Unitarized-Born, full two- and four-state treatments B, U, T and F respectively, (cf Flannery and McCann 1974). The interaction potentials adopted in the calculation of $C_f(\rho,\infty)$ are those previously determined (Flannery 1970).

Illustrative results for the elastic and inelastic transitions (1) are displayed in the computer-drawn figures (1–3) for two representative incident speeds $v_i = 1$ and 2 au ($\equiv$25 keV and 100 keV incident H^+-energy). The figures show quite clearly the consequence of the various approximations to $\sigma(\theta)$, which is more sensitive to these variations

than is the total cross section. Since the figures provide a rather complete comparison, little discussion is necessary. However, some points of interest are of note.

The major improvement to Born's approximation B to elastic scattering is mainly achieved by the introduction of the Unitarized-Born approximation U which conserves probability. Further coupling with the $2\,^1S$ and $2\,^1P$ states is important only for small-angle scattering into a range which decreases with increasing ε_i. This effect is at first surprising since, for the distant encounters responsible for small θ, the interaction is weak indicating the validity of a first-order treatment like B or U. However, the actual interaction is not just the ordinary electrostatic interaction averaged over unperturbed ground-state helium wavefunctions,[9] but has an additional polarization contribution arising from the polarization-distortion of the unperturbed functions by the incident ion. The effect of that portion of the polarizability included in the $1\,^1S$–$2\,^1P$ dipole coupling is acknowledged via wavelength-distortion in the four-state treatment F and is exhibited essentially by the difference between U and F for small scattering angles. Also for small θ, B tends to

$$8\pi a_0^2 M_{AB}^2 \left[\lim_{K\to 0}\left\{\frac{Z-F(K)}{K}\right\}^2 = 0{\cdot}16\right],$$

a constant independent of impact-energy and determined by $F(K)$, the elastic form-factor for helium, at small momentum changes K. In the light of the preceding discussion, however, this constant is only meaningful for large impact-energies when the effect from polarization-distortion becomes considerably reduced. For large scattering angles, (or more correctly large K), figure 1 shows that F, U and B all tend to the same limit which is also given by the Rutherford cross section.

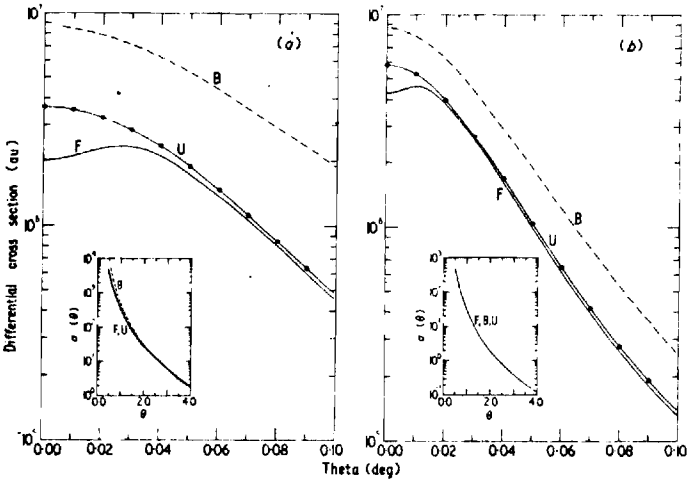

Figure 1. Differential cross sections for H^+–$He(1s^2)$ elastic scattering at (*a*) 25 keV and (*b*) 100 keV incident H^+ energy. B Born approximation, U Unitarized-Born approximation; F Four-state ($1\,^1S$, $2\,^1S$, $2\,^1P_{0,\pm1}$) approximation.

Figures 2 and 3 clearly demonstrate the failure of Born approximation to adequately describe the scattering at large angles at all energies. Also, for scattering in the forward direction, B, T and F differ markedly particularly at low energies. This difference can again be attributed to the misrepresentation of the actual static-interaction for the distant encounters mainly responsible for small θ. The difference is therefore smaller for the $2\,^1P$ excitation than for the $2\,^1S$ excitation, as indicated by the figures. In general, the $2\,^1P$--$2\,^1S$ coupling enhances the $2\,^1S$ excitation over the entire angular range at the expense of the $2\,^1P$ excitation which, however, is less affected.

Calculations at incident speeds $v_i = 0{\cdot}5$ au and 3 au have also been performed. The graphical results exhibit features similar to those described above and are available upon request. Also results for excitation of the $2\,^1P$ substates are available.

Finally, it is of interest to note the relationship of the above approximations with others in the literature. The Unitarized-Born treatment U for elastic scattering involves setting $C_n(\rho, Z) \simeq C_i(\rho, Z)\delta_{in}$ in the set of coupled differential equations (cf Flannery and McCann 1973) to give

$$C_i(\rho, Z) = \exp\left(-\frac{i}{\hbar v_i}\int_{-\infty}^{Z} V_{ii}[(\rho^2 + Z'^2)^{\frac{1}{2}}]\,dZ'\right) \tag{4}$$

where $V_{ii}(R)$ is the static interaction between the two atomic systems. Inserting (4) into (2), and by choosing the Z-path of integration along a straight line lying halfway between $\boldsymbol{k}_i$ and $\boldsymbol{k}_f$, parallel to the vector $(\boldsymbol{k}_i + \boldsymbol{k}_f)/|\boldsymbol{k}_i + \boldsymbol{k}_f|$ and perpendicular to ρ, then on completion of the Z- and Φ-integration we have for elastic scattering,

$$\sigma(\theta) = 2\pi k_i k_f a_0^2 \left|\int_0^\infty J_0(2k_i\rho \sin\tfrac{1}{2}\theta)\left[\exp\left(-\frac{i}{\hbar v_i}\int_{-\infty}^{\infty} V_{ii}[(\rho^2 + Z^2)^{1/2}]\,dZ\right) - 1\right]\rho\,d\rho\right|^2 \tag{5}$$

which is identical to the eikonal approximation for elastic scattering (cf Bransden 1970).

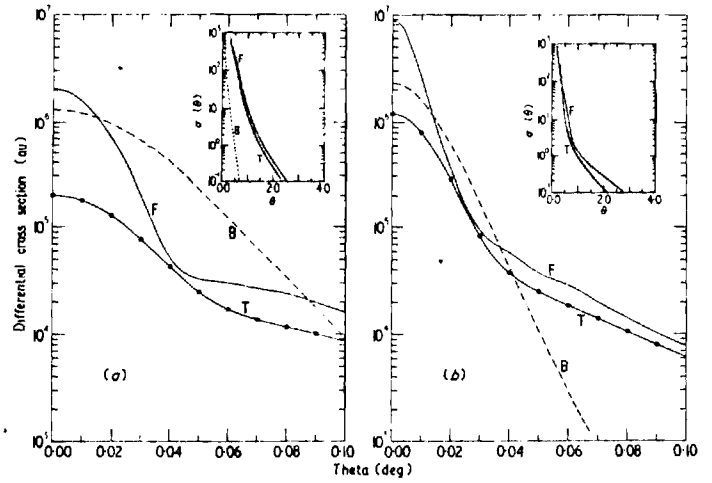

Figure 2. Differential cross sections for the $2\,^1S$-inelastic scattering at (*a*) 25 keV and (*b*) 100 keV incident H^+-energy. B Born approximation; T Two-state ($1\,^1S$, $2\,^1S$) approximation; F Four-state ($1\,^1S$, $2\,^1P_{0,\pm1}$, $2\,^1S$) approximation.

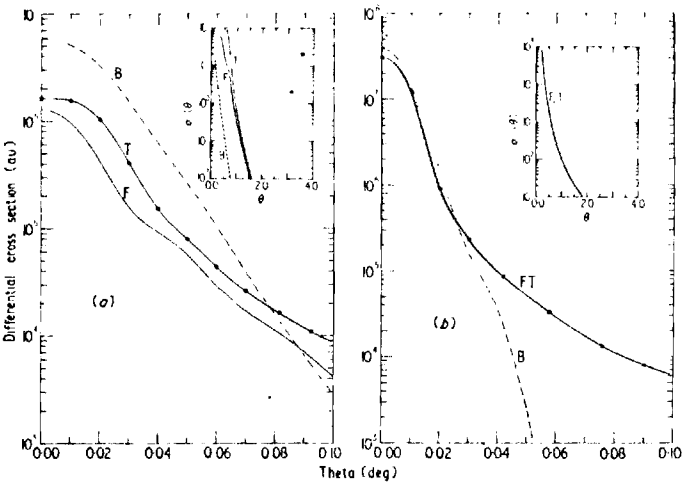

Figure 3. Differential cross sections for the $2\,^1$P-inelastic scattering at (*a*) 25 keV and (*b*) 100 keV incident H^+-energy. B Born approximation; T Two-state ($1\,^1S, 2\,^1P_{0,\pm1}$) approximation; F Four-state ($1\,^1S, 2\,^1S, 2\,^1P_{0,\pm1}$) approximation.

Glauber 1959) has already shown that the eikonal approximation to the elastic scattering amplitude satisfies the optical theorem thereby implying the conservation of probability. Equation (4) however demonstrates the conservation-property directly. The first-Born approximation follows from (4) by assuming V_{ii} is weak.

Moreover, according to the distortion approximation (cf Bates 1961) to the impact-parameter treatment for inelastic scattering,

$$C_f(\rho, Z) = \frac{i}{\hbar v_i}\int_{-\infty}^{Z} V_{fi}(\rho, Z)\left[\exp\frac{i}{\hbar v_i}\left(\mathscr{E}_{fi}Z + \int_{-\infty}^{Z}[V_{ff}(\rho, Z') - V_{ii}(\rho, Z')]\,dZ'\right)dZ\right] \qquad (6)$$

where $V_{fi}(\underset{\sim}{\rho})$ is the interaction coupling the initial and final states and V_{ff} is the static interaction in the final channel. Inserting (6) into (2) and proceeding as before, an expression similar to the eikonal distorted-wave expression derived by Chen *et al* (1972) for electron-atom collisions is obtained. In conclusion, the two- and the four-state treatments used here, being more accurate than the above methods, represent in effect, the multistate-eikonal treatment for elastic and inelastic atomic collisions.

References

Bates D R 1961 *Quantum Theory. I. Elements* (New York: Academic Press) p 259
Baye D and Heenen P H 1973 *J. Phys.* B: *Atom. molec. Phys.* **6** 1255–64
Begum S, Bransden B H and Coleman J 1973 *J. Phys.* B. *Atom. molec. Phys.* **6** 837–40
Bransden B H 1970 *Atomic Collisions Theory* (New York: Benjamin, Inc.) p 82
Chen J C Y, Joachain C J and Watson K M 1972 *Phys. Rev.* A, **5** 2460–74
Flannery M R 1970 *J. Phys.* B: *Atom. molec. Phys.* **3** 306–14
Flanney M R and McCann K J 1973 *Phys. Rev.* **8** 2915–21
—— 1974 *J. Phys.* B: *Atom. molec Phys.* **7**

APPENDIX VII

THE MULTISTATE EIKONAL TREATMENT OF ELECTRON-ATOM COLLISIONS

This appendix is a reprint of an article which appears in the Journal of Physics B: Atom. Molec. Phys., Volume 7, pages L223 to L227. The article is a brief report on the success of approximation B of Chapter III, which was the state of the present research at the time of submission.

J. Phys. B: Atom. Molec. Phys., Vol. 7, No. 7, 1974. Printed in Great Britain

LETTER TO THE EDITOR

The multistate eikonal treatment of electron–atom collisions

M R Flannery and K J McCann

School of Physics, Georgia Institute of Technology, Atlanta, Georgia 30332, USA

Received 18 February 1974

Abstract. The basic equation for the scattering amplitude as determined from a multistate eikonal description of electron–atom collisions is presented. The relationship with other semiclassical treatments is examined. Four-state eikonal calculations of the cross sections for elastic and the 2s and 2p excitations of H(1s) by electrons with incident energy E in the range $13{\cdot}6\,\text{eV} \leq E \leq 200\,\text{eV}$ are carried out, and are compared with other refined theoretical treatments and with experiment.

Recently, a variety of theoretical models have been proposed for elastic and inelastic electron–atom collisions at low and intermediate energies. These descriptions include the close-coupling expansion with its pseudo-state modifications (Burke and Webb 1970), a polarized orbital distorted-wave model of McDowell *et al* (1973), the Glauber approximation (Tai *et al* 1970), the impact-parameter approach (Bransden and Coleman 1972, Bransden *et al* 1972), the eikonal approximation of Byron (1971), and the distorted-wave eikonal theory of Chen *et al* (1972). The purpose of this letter is (*a*) to present a preliminary account of a new generalization of the eikonal method, (*b*) to illustrate its explicit relationship with other eikonal treatments and with the impact parameter approximation and (*c*) to present its comparison with experiment and various theories.

Flannery and McCann (1974, in preparation) have developed a multistate eikonal formulation of the stationary state description of a collision between an incident particle B with an atomic system (A + e). The treatment differs from previous approaches of Byron (1971) and of Bransden *et al* (1972) in that no additional assumptions, other than the eikonal approximation to the relative motion and a multistate expansion for the electronic motions, are made. Different speeds for various channels are acknowledged. The basic equation derived for the amplitude for scattering into $\hat{\boldsymbol{k}}_f(\theta, \phi)$ about the incident Z-direction $\hat{\boldsymbol{k}}_i$ is, in the centre-of-mass frame,

$$f_{fi}(\theta, \phi) = -\frac{1}{4\pi}\frac{2\mu}{\hbar^2}\int \exp(\mathrm{i}\boldsymbol{K}\cdot\boldsymbol{R})\,\mathrm{d}\boldsymbol{R}\sum_n B_n(\boldsymbol{\rho}, Z)V_{fn}(R)\exp \mathrm{i}(k_n - k_i)Z \qquad (1)$$

where k_n is the wavenumber of relative motion in each channel n, $\boldsymbol{K} = \boldsymbol{k}_i - \boldsymbol{k}_f$ is the momentum change caused by the collision, and V_{fn} is the interaction matrix element $\langle\phi_f(\boldsymbol{r})|\mathscr{V}(\boldsymbol{r}, \boldsymbol{R})|\phi_n(\boldsymbol{r})\rangle$ where $\phi_n(\boldsymbol{r})$ are the eigenstates describing the isolated systems with reduced mass μ. The electrostatic interaction between the B and (A + e) systems at separation $\boldsymbol{R} \equiv (R, \Theta, \Phi) \equiv (\rho, \Phi, Z)$, in spherical and cylindrical coordinate frames respectively, is $\mathscr{V}(\boldsymbol{R}, \boldsymbol{r})$. The coefficients B_n satisfy the set of coupled differential (phase Φ-dependent) equations,

$$\frac{\mathrm{i}\hbar^2 k_f}{\mu}\frac{\partial B_f}{\partial Z} = \sum_{n=1}^{N} B_n(\boldsymbol{\rho}, Z)V_{fn}(R)\exp \mathrm{i}(k_n - k_f)Z \qquad f = 1, 2, \ldots, N \qquad (2)$$

where N is the number of channels considered. It can be observed that (1), with $B_n = \delta_{ni}$ (where i is the initial state), reproduces the Born-wave amplitude. Also, after some algebraic manipulation, the distorted-wave Born formula of Chen *et al* (1972) is recovered from (1) and (2). Moreover, the expressions for the eikonal elastic scattering amplitude (cf Bransden 1970) follows by solving (2) with $B_n = B_i\delta_{ni}$ for B_i and by performing the Φ-integration in (1). The chief attributes of equations (1) and (2) above are that they account explicitly for different relative speeds in the various channels, and that they permit full inclusion of as many states (or pseudo-states) as desired. It is hoped that more complete details of the theory and its relationship with other theories will eventually be provided in a later paper.

The different exponents within the summation signs of (1) and (2) are significant. With the aid of (2), the scattering amplitude (1) reduces to

$$f_{if}(\theta, \phi) = -\frac{ik_f}{2\pi}\int \exp\{[K \cdot R-(k_i-k_f)Z]\}\frac{\partial B_f(\rho, Z)}{\partial Z}\,dR. \tag{3}$$

Since $\mathcal{V}$ is composed of central potentials, $V_{nm}(R) \equiv V_{nm}(R, \Theta)\exp(i\Delta\Phi)$ where $\Delta = M_m - M_n$, the integral change in the azimuthal quantum number M, and hence the substitution $C_n(\rho, Z) = B_n(\rho, Z)\exp(-i\Delta\Phi)$ yields a set of phase-independent equations for C_n similar to (2). The amplitude reduces on Φ-integration, to

$$f_{if}(\theta, \phi) = -ik_f i^{\Delta}\int_0^{\infty} J_{\Delta}(K'\rho)I(\rho, \theta)\rho\,d\rho \tag{4}$$

where K' is the XY-component $k_f \sin\theta$ of K, where J_Δ are Bessel functions of integral order Δ, and where the function

$$I(\rho, \theta) = \int_{-\infty}^{\infty} \exp(i\alpha Z)\frac{\partial C_f(\rho, Z)}{\partial Z}\,dZ \tag{5}$$

in which the difference between K_Z, the Z-component of the momentum change at angle θ, and the minimum momentum change $(k_i - k_f)$ in the collision is

$$\alpha(\theta) = k_f(1-\cos\theta). \tag{6}$$

We note, in the heavy-particle high-energy limit, when $\theta \approx 0$, that $\alpha \approx 0$ and hence

$$I(\rho, \theta) \approx I_\Delta(\rho) = (C_i(\rho, \infty) - \delta_{if}). \tag{7}$$

Thus the eikonal approximation of Byron (1971) is reproduced from (3) with (7) together with the further assumptions that the quantities k_f, and $(k_i - k_f)$ appearing explicitly in (3) are taken as k_i, and ϵ_{fi}/v_i respectively. If, in addition $k_f \sin\theta$ is approximated by $k_i \sin\theta \approx 2k_i \sin\frac{1}{2}\theta$ for small θ and large k_f, then the scattering amplitude based on the impact parameter description of Bransden and colleagues is recovered.

As a test of the present full eikonal model, calculations based on (1)–(6) have been performed for the processes

$$e + H(1s) \rightarrow e + H(1s, 2s, 2p_{0,\pm 1}) \tag{8}$$

in which the 1s, 2s, $2p_0$, $2p_{\pm 1}$ states of atomic hydrogen are closely coupled. The total elastic and inelastic cross sections $Q(nl)$ computed by direct integration of $(k_f/k_i)|f_{if}(\theta, \phi)|^2$ over all solid angles are displayed in the table and compared with other refined theoretical calculations (Burke and Webb 1970, Sullivan *et al* 1972, McDowell *et al* 1973), and with experimental data (Long *et al* 1968, Kauppila *et al* 1970) in figures

Table 1. Elastic and inelastic cross sections $Q(nl)\pi a_0^2$ for the processes $e + H(1s) \rightarrow e + H(nl)$, $nl = 1s, 2s, 2p_{0,\pm 1}$, at electron energy E_i (eV)

E_i (eV)	$Q(1s)$	$Q(2s)$	$Q(2p_0)$	$Q(2p_{\pm 1})$	$Q(2p)$
13.6	0.988	0.143	0.140	0.077	0.217
20	0.703	0.131	0.319	0.297	0.616
30	0.522	0.113	0.362	0.441	0.803
50	0.332	0.085	0.347	0.514	0.861
100	0.202	0.050	0.191	0.439	0.630
200	0.125	0.028	0.118	0.335	0.453

1 and 2. Note that the $2\,^2S$ measurements include the cascade contribution $0.23\,Q(3p)$ from the 3p level such that direct comparison is not possible until we perform similar multistate calculations for the 3p-excitation. Also, the experimental 2p-cross sections are normalized to our value of $0.453\,\pi a_0^2$ at 200 eV instead of the corresponding Born value of $0.485\,\pi a_0^2$, which is 7% higher.

The agreement for the 2p-excitation between the present treatment, the pseudo-state method and experiment is very good down to impact energies $E_i \sim 20$ eV, below which the effects of exchange and polarization distortion neglected in the present description become important. Also shown are cross sections computed from the standard four-state impact parameter prescription. The comparison of these results with those labelled S of Sullivan *et al* (1972) is then a direct measure of the effect arising from their inclusion of second-order potentials.

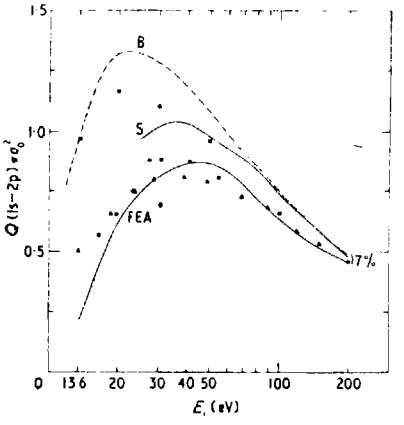

Figure 1. Total cross sections $Q(1s\text{-}2p)$ for $e + H(1s) \rightarrow e + H(2p)$ at electron energy E_i (eV). FEA four-state eikonal approximation (present treatment). ▲ experiment (Long *et al* 1968). ● pseudo-state (Burke and Webb 1970). ⊡ four-state impact-parameter treatment. S second-order potential method, four-channel approximation (Sullivan *et al* 1972). B Born approximation.

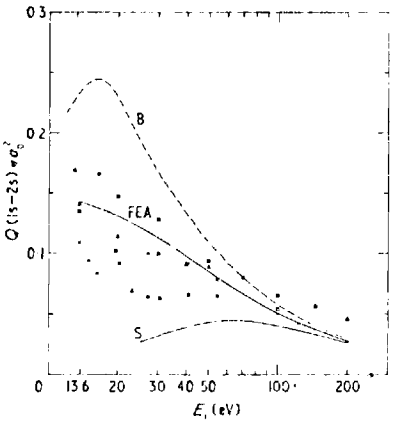

Figure 2. Total cross sections $Q(1s\text{-}2s)$ for $e + H(1s) \rightarrow e + H(2s)$ at electron energy E_i (eV). FEA four-state eikonal approximation (present treatment). ● pseudo-state (Burke and Webb 1970). × polarized-orbital distorted wave model (McDowell *et al* 1973). □ four-state impact-parameter treatment. S second-order potential method: four-channel approximation (Sullivan *et al* 1972). B Born approximation. ▲ $Q(1s\text{-}2s)+0{\cdot}23Q(1s\text{-}3p)$: experiment Kauppila *et al* 1970).

For the 2s-excitation, the agreement between the present results and the recent polarized-orbital distorted wave model of McDowell *et al* (1973) is encouraging. All the theoretical results show different variations with impact energy E_i below 40 eV. The experimental situation is somewhat obscured by the difficulty in obtaining direct account of the contributions arising from cascade, mainly from the 3p level. The large difference between the impact parameter cross sections indicates the sensitivity of the 2s-cross section to modification.

Finally, since the main object of this letter is to present the basic outline of the new treatment and to give some preliminary indication as to its success, it is our intention to eventually furnish a more complete theoretical description and a more detailed comparison (including differential cross sections, in particular) with other theoretical models.

Acknowledgment

This research was sponsored by the Air Force Aerospace Research Laboratories, Air Force Systems Command, United States Air Force, Contract F 33615-74-C-4003.

References

Bransden B H 1970 *Atomic Collisions Theory* (New York: Benjamin) p 82
Bransden B H and Coleman J P 1972 *J. Phys.* B: *Atom. molec. Phys.* **5** 537–45

Bransden B H, Coleman J P and Sullivan J 1972 *J. Phys. B: Atom. molec. Phys.* **5** 546–58
Burke P G and Webb T G 1970 *J. Phys. B. Atom. molec. Phys.* **3** L131–4
Byron F W 1971 *Phys. Rev.* **4** 1907–17
Chen J C Y, Joachain C J and Watson K M 1972 *Phys. Rev.* **5** 2460–74
Kauppila W E, Ott W R and Fite W L 1970 *Phys. Rev.* **141** 1099–108
Long R L, Cox D M and Smith S J 1968 *J. Res. Nat. Bur. Standards* **72** A 521–35
McDowell M R C, Morgan L A and Myerscough V P 1973 *J. Phys. B. Atom. molec. Phys.* **6** 1435–51
Sullivan J, Coleman J P and Bransden B H 1972 *J. Phys. B. Atom. molec. Phys.* **5** 2061–5
Tai H, Bassel R H, Gerjuoy E and Franco V 1970 *Phys. Rev.* **A 1** 1819–39

BIBLIOGRAPHY

Bates, D. R., Quantum Theory I. Elements (Academic Press, New York,1961)

Bates, D. R. and Griffing, G. W., Proc. Phys. Soc. (London) A216, 437 (1953)

Bates, D. R. and Holt, A. R., Proc. Roy. Soc. (London) A292, 168 (1966)

Bates, D. R. and Crothers, D. S. F., Proc. Roy. Soc. (London) A315, 465 (1970)

Bell, K. L., Kennedy, D. J., and Kingston, A. E., J. Phys. B: Atom. Molec. Phys. 2, 26 (1969)

Berrington, K. A., Bransden, B. H., and Coleman, J. P., J. Phys. B: Atom. Molec. Phys. 6, 436 (1973)

Bransden, B. H., Atomic Collision Theory (W. A. Benjamin, Inc., New York, 1970)

Bransden, B.H. and Coleman, J. P., J. Phys. B: Atom. Molec. Phys. 5, 537 (1972)

Bransden, B. H., Coleman, J. P., and Sullivan, J., J. Phys. B: Atom. Molec. Phys. 5, 546 (1972)

Burke, P. G., Ormonde, S., and Whittaker, W., Proc. Phys. Soc. (London) 92, 319 (1967)

Burke, P. G. and Webb, T. G., J. Phys. B: Atom. Molec. Phys. 5, 537 (1970)

Byron, F. W., Phys. Rev. 5, 1907 (1971)

Byron, F. W. and Joachain, C. J., Phys. Rev. 146, 1 (1966)

Chamberlain, G. E., Mielczarek, S. R., and Kuyatt, C. E., Phys. Rev. A 2, 1905 (1970)

Chen, J. C. Y. and Watson, K. M., Phys. Rev. A 5, 2460 (1972)

Cohen, M. and McEachran, R. P., Proc. Phys. Soc. (London) 92, 37 (1967)

Crooks, G. B. and Rudd, M. E., Thesis (Crooks), University of Nebraska, 1972

Crothers, D. S. F. and McEachran, R. P., J. Phys. B: Atom. Molec. Phys. 3, 976 (1970)

Donaldson, F. G., Hender, M. A., and McConkey, J. W., J. Phys. B: Atom. Molec. Phys. 6, 436 (1973)

Flannery, M. R., Phys. Rev. 183, 231 (1969a)

Flannery, M. R., J. Phys. B: Atom. Molec. Phys. 2, 1044 (1969b)

Flannery, M. R., J. Phys. B: Atom. Molec. Phys. 2, 913 (1969c)

Flannery, M. R., J. Phys. B: Atom. Molec. Phys. 3, 306 (1970a)

Flannery, M. R., Ann. Phys. (New York) 61, 465 (1970b)

Flannery, M. R., J. Phys. B: Atom. Molec. Phys. 3, 798 (1970c)

Flannery, M. R. and McCann, K. J., Phys. Rev. A 8, 2915 (1973)

Franco, V., Phys. Rev. Lett. 20, 709 (1968)

Glauber, R. J., Lectures in Theoretical Physics, ed. W. E. Brittin and L. G. Dunham (New York: Interscience) vol. 1, p. 369 (1959)

Goldberg, L. and Clogston, A. M., Phys. Rev. 56, 696 (1939)

Gradshteyn, I. S. and I. M. Ryzhik, Tables of Integrals, Series, and Products (Academic Press, New York, 1965)

Gryzinski, M., Phys. Rev. 115, 374 (1959)

Gryzinski, M., Phys. Rev. 138, 138,305,322,336 (1965)

Inokuti, M., Rev. Mod. Phys. 43, 297 (1971)

Jobe, J. E. and St. John, R. M., Phys. Rev. 164, 117 (1967)

Kauppila, W. E., Ott, W. R., and Fite, W. L., Phys. Rev. 141, 1099 (1970)

Lassetre, E. N., Skerbele, A., and Dillon, M. A., J. Chem. Phys. 52, 2797 (1970)

Long, R. L., Cox, D. M., and Smith, S. J., J. Res. Nat. Bur. Standards 72A, 521 (1968)

Mathur, K. C., Phys. Rev. A 9, 1200 (1974)

Merzbacher, E., Quantum Mechanics (John Wiley and Sons, Inc., 1961)

Miller, K. J., Mielczarek, S. R., Krauss, M., J. Chem. Phys. 51, 945 (1968)

Moiseiwitsch, B. L., and Smith, S. J., Rev. Mod. Phys. 40, 238 (1968)

Mott, N. F. and Massey, H. S. W., The Theory of Atomic Collisions (Clarendon Press, Oxford, England, 1965)

Moustafa-Moussa, H. R., de Heer, F. J., and Schulten, J., Physica 40, 517 (1969)

McDowell, M. R. C., Morgan, L. A., and Myerscough, V. P., J. Phys. B: Atom. Molec. Phys. 6, 1435 (1973)

McEachran, R. P. and Cohen, M., J. Phys. B: Atom. Molec. Phys. 2, 1271 (1969)

Percival, I. C. and Seaton, M. J., Phil. Trans. Roy. Soc. A (London) 251, 113 (1958)

Rice, J. K., Truhlar, D. G., Cartwright, D. C., and Trajmar, S., Phys. Rev. A 5, 205 (1972)

Simpson, J. A., Menendez, M. G., and Mielczarek, S. R., Phys. Rev. 150, 76 (1966)

Sullivan, J., Coleman, J. P., and Bransden, B. H., J. Phys. B: Atom. Molec. Phys. 5, 2061 (1972)

Tai, R. H., Gerjuoy, E., and Franco, V., Phys. Rev. A 1, 1819 (1970)

Teubner, P. J. O., Lloyd, C. R., and Weigold, E., J. Phys. B: Atom. Molec. Phys. 6, L134 (1973)

Thomas, L. H. Proc. Roy. Soc. (London) 114, 561 (1927)

Thomson, J. J., Phil. Mag. 23, 449 (1912)

Thomson, J. J., Phil. Mag. 47, 337 (1924)

Truhlar, D. G., Rice, J. K., Kuppermann, A., Trajmar, S., and Cartwright, D. C., Phys. Rev. A 5, 762 (1972)

van Eck, J. and de Jongh, J. P., Physica 47, 141 (1970)

Vriens, L., Case Studies in Atomic Collision Physics (E. W. McDaniel and M. R. C. McDowell, eds., North Holland, 1969) 1, 337

Vriens, L., Kuyatt, C. E., and Mielczarek, S. R., Phys. Rev. 165, 7 (1968)

Winters, K. H., Clark, C. D., Bransden, B. H., and Coleman, J. P., J. Phys. B: Atom. Molec. Phys. 6, L247 (1973)

VITA

I was born in Bronxville, N. Y. on December 21, 1947, the son of James and Vivian McCann. After an excellent upbringing by my parents I entered Georgia Tech in the fall of 1965, receiving a Bachelor of Science in physics in June 1969. I entered the physics graduate program at Georgia Tech in the fall of 1969, receiving a Master of Science in June, 1971 and a Doctor of Philosophy in August, 1974.